Charles University in Prague

Faculty of Science

Institute of Geochemistry, Mineralogy and Mineral Resources

Study programme: Geology

Branch of study: Geochemistry

Bc. Matúš Sadloň

Contamination of Peruvian drinking water by arsenic and boron – origin, properties and treatment

Kontaminace pitní vody arsenem a borem v Peru – původ, vlastnosti a řešení

Master´s thesis

Thesis supervisor: Mgr. Vojtěch Stejskal

Prague, 2020

Prohlášení:

Prohlašuji, že jsem závěrečnou práci zpracoval samostatně, a že jsem uvedl všechny použité informační zdroje a literaturu. Tato práce, ani její podstatná část, nebyla předložena k získání jiného nebo stejného akademického titulu.

V …… dne …….

Podpis:……..

Acknowledgements:

My sincere gratitude goes to the thesis supervisor Mgr. Vojtěch Stejskal for his expert, constructive and helpful guidance during the entire resolution of this thesis. Moreover, I would like to express my appreciation to the managing director of Photon Water Technology s.r.o. RNDr. Petr Kvapil, Ph.D. and other employees of Photon Water Technology s.r.o. for the chance to work on the company´s project in Peru within the framework of this master´s thesis. Last but not least, I wish to extend a huge thank you to my family and friends for their unwavering support during the past months of preparation of this thesis.

Summary in Czech

Nadlimitní koncentrace arsenu a boru ve vzorcích přírodních vod v provincii Tacna v jižním Peru souvisejí s aktivní vulkanickou činností v centrální části And, přičemž značnou roli hraje i v současnosti rozšířená těžební činnost v oblasti. Koncentrace arsenu i boru na pěti zkoumaných lokalitách výrazně převyšují maximální povolené limity obou prvků stanoveny Světovou zdravotnickou organizací (WHO) i peruánskou vyhláškou pro pitnou vodu, a tak způsobují zdravotní potíže místnímu obyvatelstvu, jehož kvalita života je tímto citelně ovlivněna. Vzhledem k odlehlosti zkoumané oblasti, ve které chybí potřebná infrastruktura, odborníci i finanční kapitál, společnost Photon Water Technology s.r.o. navrhla řešení pro odstranění arsenu a boru z místních vod založené na využití malých úpraven vody na principu kombinace reverzní osmózy s komerčním produktem Katalox Light® pro úpravu vody. Uvedený produkt umožňuje tvorbu alkalických podmínek nevyhnutných pro komplexaci boru do formy $B(OH)_4^-(aq)$, kterou je možno lépe odstranit v navrženém procesu úpravy vod. Reverzní osmóza dokáže odstranit arsen i bez zapojení produktu Katalox Light®, přičemž účinnost odstraňování arsenu závisí na chemickém složení vody na zkoumaných lokalitách. Laboratorní testy byly zaměřeny na potvrzení vhodnosti zapojení produktu Katalox Light® pro zvýšení míry odstranění boru v rámci navrženého dvoustupňového procesu úpravy vod v kombinaci s reverzní osmózou. Za použití produktu Katalox Light® byla dosažena účinnost odstranění boru 89 %, avšak při pH 11, což je příliš vysoká hodnota pro účely pitných vod. Snížení množství materiálu Katalox Light® (kolona o objemu 5 litrů namísto 31-litrové kolony používané v testování do listopadu 2019) nepřineslo očekávané zlepšení výsledků, když nejvyšší míra odstranění boru dosáhla pouze 50 % s jejím citelným poklesem při marginální změně pH. V kombinaci s reverzní osmózou vykazují oba zmíněné produkty potenciál pro odstranění boru z vod, avšak mnoho potíží ještě musí být překonáno s cílem dosáhnout účinnosti odstranění boru z vod a následné koncentraci boru v pitných vodách v souladu s nejvyššími přípustnými limity dle Světové zdravotnické organizace i peruánské vyhlášky pro pitnou vodu. Tyto potíže musí být v budoucnosti adresovány dalším výzkumem a testováním.

Klíčová slova: kontaminační geologie, arsen, bor, pitná voda, Peru

Summary in English

Excessive arsenic and boron concentrations determined in natural waters within the Department of Tacna in southern Peru are associated with active Andean volcanism, being further exacerbated by the ongoing mining activity in the area. Both arsenic and boron concentrations at five investigated sites significantly exceed the maximum permissible limits determined by the World Health Organisation and the Peruvian legislation for drinking water, thus affecting the health and wellbeing of the local population. Due to the remoteness of the area of interest, which lacks infrastructure, skilled human resources as well as capital, Photon Water Technology s.r.o. has come up with a solution based on the use of small water treatment plants operating on the principle of reverse osmosis in combination with a commercial remediation product Katalox Light®. This product enables the formation of alkaline conditions needed for proper complexation of boron into $B(OH)_4^-(aq)$, which is better remediated by the proposed technology. Reverse osmosis can remediate arsenic, although the efficiency of As removal depends on the chemical composition of natural waters at the investigated sites. Laboratory experiments have been focused to prove the viability of Katalox Light® for enhancing the rate of boron removal within the designed two-step remediation process. The usage of Katalox Light® led to the boron removal of 89%, albeit at pH 11, which is deemed unsuitable for drinking water purposes. Using a smaller column of Katalox Light® (containing an identical material, although with a filling volume of 5 litres instead of 31 litres column used prior to the testing in late November 2019) has not yielded satisfactory results as the highest boron removal was determined at 50% with a considerable slump in the efficiency of boron removal with a marginal decrease in pH only. The utilisation of Katalox Light® in combination with reverse osmosis shows promises in terms of boron remediation, though multiple issues concerning the compliance of this remediation technology with the WHO guidelines as well as the Peruvian legislation for drinking water must be addressed by further detailed studies.

Keywords: contamination geology, arsenic, boron, drinking water, Peru

CONTENT

LIST OF ABBREVIATIONS

AMD	Acid mine drainage
BAT	Best available technology
CVZ	Central Volcanic Zone of the Andes
DDW	Double-distilled water
Eh	Oxidation-reduction potential
FAO	Food and Agricultural Organisation of the United Nations
IARC	International Agency on Research on Cancer
INEI	National Institute of Statistics and Information of Peru
INIA	National Institute for Agricultural Development of Peru
NRC	National Research Council (USA)
PE	Polyethylene
PWT	Photon Water Technology s.r.o.
RO	Reverse osmosis
SENAMHI	National Service for Meteorology and Hydrology of Peru
TDS	Total dissolved solids
TOC	Total organic carbon
US EPA	United States Environmental Protection Agency
WHO	World Health Organisation

LIST OF FIGURES

LIST OF TABLES

1. INTRODUCTION

Nowadays, the availability of safe supplies of drinking water for humans is not common in many places around the globe. Both scarcity and inaccessibility of these supplies cause huge problems for millions of people living in such affected areas. The investigated sites within the Department of Tacna in southern Peru are located in a very remote, economically under-developed area with inadequate quality of life. In a considerably inhospitable climate with infrequent precipitation, long periods of drought and cold temperatures, the local population relies exclusively on natural waters flowing from the Andean Cordillera. Being situated on an active continental margin, the Andes are famous for their active volcanism and its features. The intensive volcanic activity and related phenomena are responsible for the naturally elevated concentrations of arsenic and boron in local rivers, exceeding both the World Health Organisation (WHO) guidelines as well as the Peruvian legislation for drinking water. When exposed to such excess concentrations of arsenic and boron, the health conditions of the local population deteriorate, and the overall life expectancy is significantly below the worldwide average.

Facing a difficult challenge, the local administration of the Department of Tacna together with the Peruvian Government asked for help within the framework of bilateral international cooperation between the Czech Republic and the Republic of Peru. By winning a grant funded by the Czech Development Agency, Photon Water Technology s.r.o. (PWT) has been able to successfully apply its experience and expertise in the field of water treatment technologies via the supply of small water treatment plants currently operating at five sites within the Department of Tacna (Candarave, Coracorani, Chipe, Ilabaya and Tarata). From the operation of these water treatment plants, it was observed that arsenic can be remediated in a one-step treatment process using reverse osmosis (RO), although this depends on the chemical composition of respective natural waters as proven by comprehensive laboratory analyses. Due to the small atomic size of boron, it was necessary to come up with a two-step treatment process using RO with a commercial water treatment product called Katalox Light® (also referred to as catalyst), which helps to create sufficiently alkaline conditions necessary for boron complexation prior to its treatment on a RO membrane.

The aim of PWT is to provide safe and environmentally friendly supply of potable water for local communities across various settlements within the Department of Tacna. The water

treatment methods designed to achieve such a supply should be easy to operate (so that the local technicians/experts will be able to handle the process themselves) with a low cost of operation, using predominantly local natural resources, except the supply of filtration materials for water treatment.

This thesis aims to support this cause by conducting necessary research on selected water treatment approaches. In the experimental part, the thesis focuses on the proof of the viability of a two-step treatment process using RO with Katalox Light® for boron removal under laboratory conditions through replication of the field treatment process (by a model preparation of a water tank solution in line with the chemical composition of Peruvian waters). Furthermore, the thesis deals with the evaluation of results related to the efficiency of this two-step treatment process under changing pH conditions as well as the analysis of possible adjustments needed for the successful long-term operation of this water treatment technology in Peru.

2. GEOGRAPHY AND CLIMATE

2.1. Geographical characteristics of the Department of Tacna

The Department of Tacna comprises the southernmost territory of the Republic of Peru. With an area of 16,076 km^2, it is bordered by the Pacific Ocean on the west, the Department of Moquegua on the north, the Department of Puno on the northeast, the La Paz Department in Bolivia on the east and the Arica-Panacota Region of Chile on the south. According to the 2017 population census carried out by the National Institute of Statistics and Information (INEI), this department is populated by 329,332 inhabitants with an average population density of 18 inhabitants per km^2. The Department of Tacna is administratively subdivided into 4 provinces (Tacna, Tarata, Candarave and Jorge Basadre) and 27 districts.

Similarly to the rest of Peruvian territory, climate factors crucially determine the overall socio-economic conditions across the Department of Tacna. Given its diverse geomorphology including widespread deserts as well as the Cordillera Occidental of the Andes and a part of the Altiplano Plateau, the territory of the Department of Tacna belongs to two major climatic zones – Costa (covering an area of 7,871.7 km^2) and Sierra (covering an area of 8,214.2 km^2; Dirección Regional de Salud Tacna, 2012). The coastal area is predominantly sandy with its relief locally altered by valleys, whereas the Sierra part of the territory is characterised by its rugged topography with low soil productivity, where agriculture is considerably dependant on precipitation (Dirección Regional de Salud Tacna, 2014).

Situated on the northern boundary of the Atacama Desert, which is well known for its hyperarid climate, the availability of water resources for agriculture and human consumption is considerably limited across the Department of Tacna. Furthermore, the scarcity of water resources among population is aggravated by the fact that 90% of inhabitants in the Department of Tacna live in the Caplina river basin, where the average flow is as low as 1.00 m^3/s (Dirección Regional de Salud Tacna, 2014). All the major rivers within the Department of Tacna originate in the Western Cordillera. The Locumba and Sama rivers are the longest rivers (178 and 168 km, respectively), being the only two rivers flowing into the Pacific Ocean within this territory (INEI, 2001). The Caplina River forms an endorheic basin together with its tributary Uchusama. The Maure River originates in the north-eastern part of the Department of Tacna, flowing into the neighbouring Puno Region and ending in the Lake Titicaca. The La Yarada aquifer provides underground water to the general water supply, allowing the irrigation of more than

6,000 hectares of agricultural land. However, signs of its depletion had been observed in certain areas (Dirección Regional de Salud Tacna, 2014).

According to the meteorological observations carried out by the National Service for Meteorology and Hydrology of Peru (SENAMHI), the average annual temperature in the Department of Tacna is 16.5 °C. The coldest months are July and August, while the warmest ones are January and February. During the winter months, fogs occur frequently in valleys as well as pampas and precipitation is scarce (Dirección Regional de Salud Tacna, 2014).

2.2. Peruvian climate

The climate of Peru is determined by its geographical position, since the country lies within the inner tropics at low latitude and near the Earth's equator. This implies that there are no major differences between the average winter and summer temperatures throughout the country, while also underlining a tropical rainy climate present in eastern Peru. The imposing presence of the Andes mountain range determines a variety of mountainous climates that range from the subtropical mountain climate to the cold alpine high mountain climate. Given such varying natural conditions in Peru, 28 out of 30 recognisable climatic provinces can be determined there according to the Köppen climate classification (Beck et al., 2018).

Contrary to other equatorial countries, Peru does not have an exclusively tropical climate. The influence of the Andes together with the cold Humboldt Current causes great climatic diversity within the Peruvian territory (INIA and FAO, 2009). The central and southern coast of the country has an arid or desert subtropical climate with an average temperature of 18 °C and annual rainfall of 150 mm due to the action of the cold Humboldt Current. On the other hand, the north coast has a semi-arid tropical climate, given its proximity to the tropical sea with an average temperature above 24 °C and rains during the summer. When the El Niño phenomenon occurs, the average temperature rises along the entire coast (with maximums greater than 30 °C) and the rains increase significantly in the north and central coast.

Major factors influencing the climatic conditions in Peru include:

a) Low latitude

Peru is classified as a tropical country given its location near the geographical equator. This characteristic represents the warm and humid climate of the Amazon, but also explains the presence of high temperature areas in the Andean region, for instance in the lower areas of Ayacucho or Tacna. Moreover, the low latitude influences the warm climate of the north coast as well as the high temperatures of the sea in its northern area and far from the coast.

b) Altitude of the Andean mountain range

Across the territory of Peru, it is possible to observe a variety of climates changing with an increase in altitude, e.g. from the temperate zones in Cajamarca to cold ones in Puno and Junín. The altitude of the Andean mountain range influences predominantly the climatic diversity of the Andean region, but also has an impact on the aridity of the coast via obstructing the passage of precipitation incoming from the east (Amazon basin) with tropical humid climate. Such conditions may lead to the occasional formation of waterspouts in Lake Titicaca, most recently observed in December 2016 (Diarro Correo, 2016). In the Andean Highlands, tornadoes can be registered, as observed on May 10, 2018 in Rinconada, Puno with a height of approximately 5,000 metres (La República, 2018).

c) The influence of sea currents

In the northern zone, the warm current of El Niño increases the temperature of the sea, thus leading to the warm and rainy climate of the north coast. To the contrary, the cold Humboldt (also known as Peruvian) Current enhances the coldness of the sea generated by the upwelling process, therefore causing the arid climate of the central-south coast.

2.3. Climate zones

Based on the above-mentioned climate characteristics and factors influencing the climate, three major climate zones are determined, covering the entire Peruvian territory (Ministry of Agriculture and Irrigation of Peru, 2015). In Spanish, these zones are called **Sierra** (i.e. mountain, equivalent to Alpine climate zone), **Selva** (i.e. tropical, Amazon climate zone) and **Costa** (coastal climate zone, comprising both the humid coastal conditions in the northern part as well as the arid coastal conditions in the central-southern part of Peru).

A) Sierra

The climate in this zone varies from warm temperate (Yunga Region), temperate (Quechua Region) and cold temperate (Puno Region) to glacial (Janca or Cordillera Region). In the Yunga Region, the weather is moderately warm and slightly humid in the altitudes from 1,000 to 2,000 meters above sea level. In the inter-Andean valleys of the eastern plain of the Andes (Yunga Fluvial), the climate is warm, moderate and dry with low rainfall, having abundant solar radiation throughout the year. The city of Chosica, 34 km from Lima, has a moderate warm or warm temperate climate, in Spanish defined as Yunga Marítima (Instituto Geográfico Nacional, 1989). During the summer, excessive rainfall leads to the occurrence of 'huaycos' (i.e. flash floods caused by torrential rainfall).

In the Quechua region, the temperature ranges between 15 °C and 0 °C at the altitudes greater than 2,000 to 3,000 meters above sea level. Predominant climate characteristics of this region include summer rains (January to March), low atmospheric humidity and prevailing winds from the southeast.

Cold temperate climate prevails in the Suni Region with altitudes ranging between 3,000 to 4,000 meters above sea level. In the Puno or Jalca Region, at altitudes of 4,000 to 5,000 meters above sea level, the climate is cold with low humidity.

The Janca or Cordillera Region is situated at altitudes greater than 5,000 meters above sea level. Its weather is classified as glacial with temperatures below 6 °C. The atmosphere is very dry with precipitation occurring exclusively as snowfall.

In general, the annual amount of precipitation in the mountains varies from 300 mm to 900 mm (Vidal, 1981).

B) Selva

This major climate zone is divided into two subgroups depending on the altitude – “High Forest” (*selva alta* in Spanish) and “Low Forest” (*selva baja* in Spanish); nevertheless, both of them are considered as tropical climate zones (Ministry of Agriculture and Irrigation of the Republic of Peru, 2015).

In the High Forest, the average annual temperature fluctuates between 22 and 26 °C. The annual precipitation in this area is abundant, ranging from 2,600 to 4,000 mm, although maximums may exceed 8,000 mm / year. The town of Quincemil (in Cusco Region) is the rainiest area in the country with the precipitation record of 8,965 mm in 1964.

In the Low Forest, temperatures are higher with the annual average of 31 °C; precipitation is exceeding 1,000 mm / year. The absence of horizontal movements of air masses or winds is typical for the area; however, strong convection currents occur, producing the ascent of air masses loaded with moisture (cumulus and nimbus clouds).

C) Costa

Two types of climate can be observed in the coastal region. In the area between the towns of Lambayeque and Tacna, subtropical climate dominates with average temperatures between 18 °C and 21 °C, having excessive atmospheric humidity that reaches 90 to 98%. Semitropical climate prevails in the area between the towns of Tumbes and Piura; high temperatures with an annual average of 24 °C can be observed with periodic summer rains and abundant humidity.

3. GEOLOGICAL CHARACTERISTICS

3.1. Andean geology and volcanism

Stretching across more than 7,500 km along the western margin of South America, the Andean mountain range constitutes one of the largest continuous mountain chains in the world. It is bordered by the Caribbean coast from the north, while Cape Horn constitutes its southernmost part. The geological evolution of the Andes is characterized by the subduction of Cocos and Nazca oceanic plates beneath the continental South American Plate at an average rate of 7-9 cm/year (Stern, 2004).

The first geological division of the Andes with respect to plate tectonics was carried out by Gansser in 1973. He divided the Andean Cordillera into Northern, Central and Southern segments according to the occurrence of metamorphic rocks and ophiolitic belts of Andean age. The Northern and Southern Andes are characterised by the presence of Jurassic and Cretaceous metamorphic rocks as well as various occurrences of oceanic crust obducted to the continental margin during the Andean times (Ramos, 2009). To the contrary, the subduction of oceanic crust is the principal mechanism of geological evolution of the Central Andes, where neither metamorphic nor ophiolitic rocks of Mesozoic and Cenozoic origin are documented (Ramos, 1999).

Considering Andean volcanism and its activity, four major volcanic zones can be distinguished – Northern, Central, Southern and Austral Volcanic Zone, which are further divided into smaller volcanic arc segments. Each of these zones underwent different tectonic evolution that contributed to the overall segmentation of the Andean Cordillera in terms of various pre-Andean basement ages, differences in magmas erupted within each segment, Mesozoic and Cenozoic geological activity, structural trends, crustal thickness and active tectonics (Stern, 2004). Recent active volcanoes within the Andean Cordillera are distributed in those areas, where the angle of subduction of the Nazca plate beneath the South American plate reaches 25° - 30° (Ecuador, southern Peru, northern and southern Chile). On the other hand, the regions of northern and central Peru as well as central Chile lack volcanic activity due to shallow angle of subduction of the Nazca plate to a depth of 100 km with no asthenospheric mantle between the plates (Pfiffner and Gonzalez, 2013).

In terms of the active volcanic belts, the most notable tectonic and geological events have occurred since the Late Oligocene, being related to the breakup of the Farallon plate

into the Cocos and Nazca plates at 27±2 Ma (Stern, 2004). This breakup caused a change from oblique to nearly orthogonal convergence between the Nazca and South American plates, reflected by changes in subduction geometry. Such changes comprise the acceleration of crustal shortening, uplift and thickening within the Northern Andes as well as the Northern Central Andes (Alemán and Ramos, 2000; Jaillard et al., 2000). These processes led to the formation of a broken foreland with basement uplifts and basins (Jordan et al., 1983; Ramos; 2009). To the contrary, the Southern Central and Southern Andes underwent the extension and crustal thinning within the same period (Jordan et al., 2001). Nevertheless, the magmatic activity increased along the entire Andean chain due to the increase in convergence rates (Stern, 2004).

With regards to the geological and volcanological divisions mentioned above, the area of interest within the Department of Tacna belongs to the Central Andes (specifically its Peruvian segment, known as the Northern Central Andes) and the Central Volcanic Zone (CVZ). Given that the geological evolution of the entire Andean mountain range is very complex (out of scope of this thesis), greater emphasis will be put on a comprehensive description of the geological evolution and characteristic features within the Northern Central Andes and the CVZ in this work.

The oldest geological record not only within the Department of Tacna, but also the entire Andean arc, is represented by the Paleoproterozoic igneous and metamorphic rocks of the Arequipa Massif, dated to 2.0 – 1.8 Ga, which constitute the basement of the northern part of the Central Volcanic Zone (Stern, 2004). In terms of stratigraphy, the Arequipa Massif belongs to the Coastal Belt of the Western Cordillera. The outcrops of crystalline basement within the Arequipa Massif consist of high-grade, partly migmatised gneisses and schists intruded by Early Palaeozoic granites (Schakelton et al., 1979; Pfiffner and Gonzalez, 2013). Concerning the origin of the Arequipa Massif, two major hypotheses prevail. Its Paleoproterozoic terranes could either be peri-Gondwanan, related to the Amazon craton (as determined by Tosdal, 1996) or a part of Laurentia (a Grenvillian province), thus indicating the allochtonous origin of the Arequipa Massif (Loewy et al., 2004). Analyses of Pb isotopic composition support the first hypothesis, which is further confirmed by the attachment of the parautochthonous Arequipa cratonic block to Amazonia during the breakup of Rodinia (associated with rifting) in Neoproterozoic times when the separation of Laurentia from Amazonia took place (Jaillard et al., 2000; Ramos, 2008).

The area below the CVZ in southern Peru has the highest crustal thickness within the entire Andes, reaching more than 70 km in depth below both the Western and Eastern Cordillera and approximately 60-65 km below the Altiplano and Puna plateaus (Beck et al., 1996; Schmitz et al., 1999; Swenson et al., 2000). This fact is well reflected in local morphology, where the average altitude exceeds 3,700 metres above sea level with multiple peaks reaching or exceeding an altitude of 6,000 metres above sea level. The crustal thickness decreases both eastwards of the Eastern Cordillera (to approximately 43-47 km) and northwards beyond the CVZ (recorded at 45 km) in northern Peru (Stern, 2004).

Various assumptions concerning the crustal thickness in the central Andes are documented by numerous studies. The most prevalent ones include crustal shortening (as explained in Isacks, 1988; Beck et al., 1996; Allmendinger et al., 1997 and Kley et al., 1999) and magmatic shortening (Tosdal et al., 1984; Schmitz et al., 1997). A combination of these two may be possible in some areas, with greater crustal shortening below the Eastern Cordillera and more significant magmatic underplating, lithospheric hydration or even lithospheric delamination proposed below the Western Cordillera (James and Sacks, 1999; Giese et al., 1999; Kay et al., 1999; Victor et al., 2004). In the Northern Central Andes, crustal thickening and uplift started during the "Incaic" tectonic event (dated to Eocene) as a reaction to an episode of rapid oblique convergence (Pardo-Casas and Molnar, 1987). Its further progression led to the formation of the very thick crust below this region (Kay et al., 1999; Jaillard et al., 2000).

When assessing magma genesis and types of magmatism within the Andean Cordillera, a comprehensive study by Thorpe (1984) concluded that the dehydration of the subducted oceanic lithosphere was the initial phase of Andean magmatism; this resulted in the addition of subducted components into the overlying mantle wedge and its melting. From this point of view, a similarity between the initial subcrustal stages of formation of Andean magmas and the magma generation processes in oceanic convergent plate boundary island arcs can be observed (Stern, 2004). The most notable examples supporting this hypothesis include tholeiitic and high-Al basalts from the volcanic front of the Central Southern Volcanic Zone with an approximate crustal thickness of 30 km. Both their isotope and trace-element ratios are similar to oceanic island arc basalts; therefore, it is suggested that these have not assimilated continental crust (Hickey-Vargas et al., 1986; 1989).

A different approach is represented by the participation of continental crust and/or subcontinental mantle lithosphere during the formation and evolution of magmas in Central and Northern Southern Volcanic Zones. This is underlined by variable isotopic composition

of volcanic rocks from Central and Northern Southern Volcanic Zones and those originated within the Central Southern Volcanic Zone and oceanic island arcs (Stern, 2004). The above-mentioned participation could occur due to multiple reasons, for instance through the interaction of magmas derived in the subarc asthenospheric mantle wedge with continental lithosphere (Stern et al., 1990; Stern and Kilian, 1996; Hickey-Vargas et al., 2002), by intra-crustal assimilation (MASH or AFC processes; James, 1984; Davidson et al., 1991) and/or due to source region contamination of subarc mantle by subducted continental components (Stern et al., 1984; Stern, 1988; Stern and Skewes, 1995).

In the CVZ, dominant rock types include andesites, dacites and rhyolites; basaltic andesites and basalts occur marginally. Magmas within the CVZ are characterised by elevated $^{87}Sr/^{86}Sr$ and $d^{18}O$ values (James, 1984), while having lower $^{143}Nd/^{144}Nd$ values than magmas of the Southern Volcanic Zone (Davidson et al., 1990). Together with considerably different Pb isotopic compositions (as presented by Barreiro and Clark, 1984; Wörner et al., 1992; Aitcheson et al., 1995), these data indicate a greater share of continental crust incorporated within the CVZ than the Southern Volcanic Zone magmas (Davidson et al., 1991; Francis and Hawkesworth, 1994; Lindsay et al., 2001; Schmitt et al., 2001, 2002).

The process of crustal contamination of CVZ magmas is explained by the combination of intra-crustal assimilation combined with crystallization of these magmas and/or crustal anatexis (Schneider, 1987; Davidson and de Silva, 1995). This is indicated by correlated variations of Sr, Nd and O isotopes with increasing SiO_2 content (Francis et al., 1985; Feeley and Davidson, 1994) as well as regional correlations of Pb isotopic compositions and the Andean basement age (Wörner et al., 1992, 1994; Aitcheson et al., 1995). Partial melting is thought to affect the crustal structure, as interpreted by geophysical studies (Schmitz et al., 1997). The extent of crustal contamination of CVZ magmas has increased since prior to the Miocene to Recent; this is indicated by temporal variations in CVZ magmas and supported by the fact that the crustal thickness increased up to 70 km within this period (Miller and Harris, 1989; Trumbull et al., 1999; Lucassen et al., 2001).

3.2. Regional geology and stratigraphy of the Department of Tacna

In southern Peru and adjacent territories, crustal deformation of the South American Plate led to the formation of four major geomorphological units – the Western and Eastern

Cordillera flank the intermontane plateaus of Altiplano and Puna. The western coastal side of the Western Cordillera is famous for the presence of a chain of plutons known as the Coastal Batholith, which has been considered as a model intrusion in order to understand the emplacement of large plutons in the crust (Pfiffner and Gonzalez, 2013). The oldest plutonic sequences are dated to Early Palaeozoic and Carboniferous, being associated to the evolution of the Proto-Andean margin on the edge of the Amazon craton (Chew et al., 2008).

The stratigraphy of the rocks occurring within the Department of Tacna ranges from Proterozoic to Cenozoic. Proterozoic rocks constitute the crystalline basement within the Peruvian territory. Such rocks include a complex of igneous and metamorphic rocks with a prevalence of granitic bodies; basic and ultrabasic bodies are less present.

Palaeozoic sequences of both marine and continental origin have a discontinuous and limited extension within the Department of Tacna. Resting discordantly on the metamorphic complex, these include the Devonian Cabanillas Group composed of siltstones, sandstones and fetid limestones (Bedoya et al., 2007).

The beginning of the Andean cycle and its development during the Mesozoic led to the deposition of sedimentary filling in a marginal geosynclinal basin on the South American continent. The Mesozoic sequences are constituted by Jurassic and Cretaceous rocks deposited in a marine environment. Among the Jurassic rocks, the volcanic rocks of the coastal platform stand out, being the dominant rock type in the feet of mountain ranges.

Early Jurassic rocks are represented by sedimentary volcanic sequences known as the Chocolate Formation. This formation is followed by the Lower and Upper Guaneros Formations; these are sedimentary volcanic sequences dated to Late Jurassic. The Lower Guaneros Formation is composed of fossiliferous, agglomerated sandstones and arkoses, while porphyric andesite and agglomerates are the principal rock types of the Upper Guaneros Formation. Other important Late Jurassic formations include the Labra Formation (composed of quartz sandstones and dark grey siltstones) as well as the Gramadal Formation, where the prevalent rock types include dark shales, sandstones and quartz sandstones (Bedoya et al., 2007).

The Early Cretaceous rocks are preserved mostly on the feet of the Western Cordillera, including predominantly whitish grey quartzites that occur in the upper part of Yura Group in the Hualhuani Formation. Concerning the Late Cretaceous rocks, their most notable occurrence is represented by the Toquepala Group, outcropping as sedimentary volcanic

sequences preserved on the feet of the Western Cordillera. In terms of lithology, the Toquepala Group is composed of agglomerates, pyroclastics, reddish brown and grey to greenish lavas of andesitic, trachytic and rhyolitic composition with intercalations of clastic sediments such as sandstones, limestones and conglomerates. The stratigraphical division of the Toquepala Group includes the Matalaque Formation (comprised of porphyric andesites), the Paralaque Formation (made up of lithic welded tuff) and the Quellaveco Formation (composed of crystallolytic tuffs, breccias, porphyric dacites and andesites (Bedoya et al., 2007).

In southern Peru, Cenozoic rocks are represented by marine sequences occurring in coastal area and continental sequences present in the Cordillera area. In terms of lithology, these comprise molassic sediments, volcanoclastic rocks, andesites, dacites, rhyodacites and rhyolites. Episodic eruptions lasted from Oligocene to Recent and nowadays cover wide areas of the Western Cordillera and the Altiplano Plateau.

Cenozoic in the Western Cordillera is documented by the Tacaza Group consisting of volcanic sequences, being dated to ca 17-30 Ma (Miocene-Oligocene). Its lithology is variable, comprising breccias, tuffs and andesitic lavas. Strongly folded and inclined, the layers of the Tacaza Group do not allow a precise interpretation of volcanic activity in that period due to subsequent later volcanism within this area (Bedoya et al., 2007). Stratigraphic division of the Tacaza Group includes the Lower Tarata Formation (made up of volcanoclastic rocks and blocks) and the Upper Tarata Formation (composed of siltstones, porphyric dacites, pyroclastics and limestones). Another Cenozoic geological entity is the Huylacollo Formation, lithologically constituted of tuffs, tuffitic sands and beige rhyodacitic ignimbrites.

In high altitudes of the Western Cordillera, the Maure Formation can be traced above the rocks belonging to the Tacaza Group. Having variable lithology, the Maure Formation includes intercalations of breccias, sandstones, conglomerates, tuffs and siltstones. Its dark-coloured breccias are of volcanic origin, while conglomerates have a rounded to subangular shape. Both sandstones and tuffitic sandstones are coarse to fine-grained, dominantly white-to-greenish grey in colour. Thin layers of brown siltstones indicate the movement and deposition of constituent rocks by torrents in a lacustrine environment (Bedoya et al., 2007).

The Late Paleogene Upper Moquegua Formation rests discordantly on Mesozoic sequences. Dominant rock types of this formation include polymorphic conglomerates intercalated

with sandstone lenses and reworked tuffs. Within the Miocene-Pliocene series, ignimbrite sequences of the Huaylillas Formation are the most notable, being dated to 17-22 Ma. Its rocks well reflect explosive volcanic eruptions in that period, as documented by a number of pyroclastic flows and fine ashes documented on multiple hills within the Department of Tacna (Bedoya et al., 2007). Lying discordantly on the Huaylillas Formation, the frequently outcropping Millo Formation comprises polymorphic conglomerates intercalated with reworked tuffs.

Positioned in angular discordance to the bottom Maure Formation, the Sencca Group represents approximately 100 metres thick pyroclastic sequences outcropping along the Peru-Chile border. Dominant rock types within the Sencca Group include crystallolytic lapilli tuffs with plagioclase, biotite and quartz. To the northeast of Pachía, the Proterozoic Basal de la Costa Complex is composed of gneisses, granulites and shales.

The uppermost part of the Western Cordillera contains volcanic rocks belonging to the Barroso Group, forming a series of volcanoes aligned in the form of an arc trending from NW-SE with a length of ca 500 kilometres. Having otherwise intact morphology, it hosts a number of craters with diameters of several hundred meters wide, such as Tutupaca and Yucamani. In general, its lithology consists of lavas and pyroclastics originated during effusive and explosive volcanic episodes (tuffs, tuffitic blocks, ignimbrites and lapilli). The composition of lavas varies from andesitic to trachyandesitic and basaltic-andesitic (Bedoya et al., 2007). They have greenish grey colour and fluid texture with vesicles indicating the orientation of the flow.

Quaternary geologic features within the Department of Tacna comprise younger volcanic rocks in the uppermost parts of the Western Cordillera as well as materials deposited on the slopes of the valleys. Lithologically, these are made up of trachyandesitic lavas, basaltic andesites and pyroclastics (lapilli, ashes and breccias). Sedimentary deposits of Pleistocene age contain river, lacustrine and glacial sediments with silt, sand and conglomerate content (Bedoya et al., 2007).

3.3. Mining

The mining industry in Peru has a long historical tradition. According to the data provided by the Ministry of Energy and Mines of Peru in 2014, Peru ranked 3rd among

the world producers of silver, copper, zinc and tin, 4th among the world producers of molybdenum and lead and 6th among the world producers of gold. Despite the recent slump in mineral prices, the mining sector still has an especially important share in the Peruvian economy at 12.35% on average between 2010-2014, with total mining exports at $20.5 billion in 2014 (Molina et al., 2016). Unfortunately, such revenue is not used effectively, mainly due to the incompetence of regional and/or national authorities. In many cases, these pursue their own financial interests and collaboration with mining enterprises in the first place, thus contributing to the long-term neglected resolution of various problems that local communities encounter. The most tangible problems include the availability of water and its contamination, affecting the entire agricultural sector (the worst effects being observed in arid and mountainous areas), leading to stagnation and/or decrease of living standard and life expectancy within these territories (Arellano-Yanguas, 2011; Hart and Paucar-Caceres, 2014). Escalation of social unrests occurs frequently, as indicated by 140 environmental and social conflicts that occurred from 2012-2014 across the whole Peru (Molina et al., 2016).

In the Department of Tacna, mining operation further exacerbates the insufficiency of water resources, primarily related to its arid climatic conditions (see Chapter 2.1.). The gradual progression of exploration for mining purposes and subsequent extraction processes lead to land degradation and erosion associated with considerable changes in local topography. Other adverse effects of mining include the alteration of both groundwater and surface water flow, excessive use of water resources in the mining process and most notably, the contamination of water by a variety of metals and metalloids caused by the absence of water treatment mechanisms. Major mines within this region encompass the Pucamarca mine (extracting gold and silver) and the Toquepala porphyry copper deposit (including two additional known deposits, Cuajone and Quellaveco), in addition to the mining exploration zones in Ticato, Province of Tarata (Fernández Prado et al., 2013; Mining Data Online, 2020).

4. ARSENIC

4.1. Physico-chemical properties of arsenic

Arsenic is situated within Group VA of the periodic table with an atomic number of 33. The most stable and only non-radioactive isotope of arsenic is ^{75}As; besides; other 11 unstable and radioactive isotopes are documented (^{68}As to ^{79}As). The stable form of arsenic [As(0)] has five valence electrons available for participation in chemical bonding, having an empty p orbital available for electron occupation (Flora, 2015).

Four redox states of arsenic can be determined: 0, -3, +3 and +5. Elemental arsenic [As(0)] shares equally its three electrons with other three surrounding arsenic atoms in a trigonal pyramidal structure, thus appearing as a brittle grey metal (Flora, 2015). The oxidation state of -3 for arsenic is achieved by addition of three electrons to the p orbital (which initially has 3 electrons) during chemical bonding. Under natural conditions, the oxidation states of +3 and +5 for arsenic are the most common ones. The oxidation state of +3 is associated with the bonding of three As electrons to a non-metal, usually sulphur or oxygen. Even stronger bonding of arsenic to these non-metals, when all five electrons of 4s and 4p orbitals are more associated with the non-metal, causes the oxidation state of +5 for arsenic in this type of chemical bonding (Flora, 2015).

The atomic weight of arsenic at 74.921 g/mol marks arsenic as heavier than manganese, nickel and iron as well as lighter than lead, gold or silver. Another significant physico-chemical property of arsenic is electronegativity, which is estimated at 2.18 according to Pauling scale. This is reflected by the cationic character of arsenic in its +3 and +5 oxidation states. Both oxidation states of arsenic may react with methyl group to form organic species, out of which the most common include monomethylarsonic acid (MMA) and dimethylarsonic acid (DMA; Flora, 2015). Under ambient conditions, however, organic species occur far less often than inorganic species of arsenic. In terms of toxicity, trivalent arsenic species (arsenites) are more toxic than pentavalent ones (arsenates). Also, inorganic species are more toxic than organic ones (Flora, 2015).

Other important physico-chemical characteristics as well as atomic data for arsenic are listed in Table 1.

Tab. 1: Selected physical and chemical properties of arsenic and its atomic data (based on Haynes ed., 2015 and Coursey et al., 2015):

State at 20°C	Solid
Electron configuration	$[Ar]3d^{10}4s^24p^3$
Melting point	1087 K
Boiling point	889 K
Density	5.75 g/cm^3
Atomic radius (non-bonded)	1.85 Å
Covalent radius	1.20 Å
Electron affinity	77.574 kJ/mol

4.2. Reactivity of arsenic

Both the oxidation and reduction of arsenic are dependent on redox potential and pH conditions. Trivalent (arsenite) and pentavalent (arsenate) species of arsenic are the most occurring ones within natural water bodies. The presence of arsenate oxyanions in waters depends on pH – at pH lower than 6.9, $H_2AsO_4^-$ is the most prevalent form, while at pH greater than 6.9, $HAsO_4^{2-}$ is far more represented (Flora, 2015). The neutral trivalent arsenic species (HAs_3O_3) occurs under reducing conditions at pH lower than 9.2. These species dissociate to form anions under high pH conditions only (Flora, 2015).

Multiple natural processes, for instance weathering of rocks, geothermal, hydrothermal and biological activities as well as a variety of anthropogenic activities (the most notable include mining, combustion of fossil fuels and use of arsenical pesticides, herbicides and crop desiccants) influence the mobilization of arsenic in the environment (Flora, 2015). In terms of human exposure to arsenic, the presence of arsenic in drinking water and groundwater represents the most significant concern; other exposure pathways include diet and inhalation.

Due to the extensive mining activity within the Department of Tacna, the major source of anthropogenically-related arsenic contamination is represented by acid mine drainage (AMD) effluents; besides arsenic, these have elevated concentrations of other heavy metals like Pb, Cd, Ni as well as Zn and Fe (Flora, 2015). The occurrence of arsenic in AMD is of a great concern due to its high mobility downstream when not treated immediately after ore excavation. Especially, gold deposits are known for very high concentrations of arsenic in their AMD effluents (Savage et al., 2000). The physical weathering of arsenopyrite and/or As-bearing pyrite is accelerated by grinding up the ore and subsequent oxidation of these minerals:

$$FeAsS + 13Fe^{3+} + 8H_2O \leftrightarrow 14\ Fe^{2+} + SO_4^{2-} + 13H^+ + H_3AsO_4$$

Within the pH range of 6.5 to 8.5, which is typically determined in groundwater, both arsenite and arsenate oxyanions are readily formed; moreover, these are mobile in this pH range (Flora, 2015). The mobility of arsenic over a wide range of redox conditions makes arsenic a unique example among all oxyanion-forming elements. Arsenic speciation in aqueous systems is controlled predominantly by pH and Eh. Under moderately reducing conditions (+300 mV at pH 4 to -200 mV at pH 9), arsenite oxyanions become stable, while arsenate oxyanions are stable under oxidising conditions in aqueous solutions (Nordstrom and Archer, 2003; Flora, 2015). Moreover, redox-dependent mobilisation of arsenic expressed by the As(V)/As(III) ratio is a reliable redox indicator in groundwater systems (Yan et al., 2000; Flora, 2015). Under acidic conditions (at pH 5), the rate of As(III) oxidation is slow, whereas this rate accelerates under alkaline conditions (in the pH range of 8 – 12.5). The oxidation of As(III) is not influenced by the concentration of dissolved oxygen, although it is controlled by surface reactions (e.g. photochemical oxidation) as well as reduction caused by the presence of titanium-containing particles (Scott and Morgan, 1995; Flora, 2015).

When addressing excessive concentrations of arsenic in aqueous systems, adsorption and desorption behaviour of arsenic on mineral systems plays a key role in this process. In solution, arsenic occurs in the form of sulphides (e.g. AsS, As_2S_3) in the presence of reduced sulphur; these sulphides precipitate under reducing conditions (Flora, 2015). Furthermore, temperature affects the form of arsenic species in hydrothermal waters (for instance in those from shallow-water islands). Trivalent arsenic (as H_3AsO_3) is the most

occurring form in the pH range of 5-7, whereas the $HAs_2O_4^-$ arsenic species is the most prevailing form in deep-water systems under high pressure and temperatures (Flora, 2015). In sulphide-rich hydrothermal systems, the occurrence of thio-arsenic species is possible, as documented in geothermal waters of the Yellowstone National Park (Planer-Friedrich et al., 2010).

4.3. Geogenic sources of arsenic

Arsenic represents the 20th most abundant element in Earth´s crust with its average concentration ranging between 1.5 and 2 ppm. Overall, arsenic can be found in approximately 320 inorganic compounds and 5 categories of arsenic minerals – elemental arsenic, arsenosulphides, arsenites, arsenides and arsenates (Flora, 2015). Arsenosulphides and arsenides are typically observed in metamorphic and igneous rocks as well as anoxic hydrothermal ore deposits. Once arsenosulphdes and arsenides react with oxygen and/or water, both arsenates and arsenites are rapidly formed. The most notable arsenosulphides include arsenopyrite (FeAsS), realgar (AsS/As_4S_4) and orpiment (As_2S_3); their occurrence is closely associated with hydrothermal and magmatic ore deposits. Moreover, arsenic occurrence is documented in sulphide-bearing mineral deposits, particularly in those with gold mineralisation (Flora, 2015).

Three major categories of arsenic mobilisation and remobilisation processes can be distinguished. The first one includes the oxidation of sulphides in mineralised areas close to sulphide ore deposits and hydrothermal deposits. Secondly, the formation of secondary As minerals (mostly metal hydroxyoxides) takes place through the action of various geological processes, particularly sulphide oxidation, leaching/dissolution of rocks and minerals and subsequent precipitation of secondary minerals; these processes are controlled by local hydrochemical conditions (redox and pH) on sediment particles in sedimentary aquifers (Bundschuh et al., 2012). Arsenic remobilisation from oxyhydroxides and metal oxides is associated either with the dissolution of metal oxyhydroxides under significantly acid conditions or with As desorption from metal oxyhydroxides under alkaline (pH > 8) and oxidising conditions (Bundschuh et al., 2012).

The distribution of arsenic and its release into the environment is mostly related to the oxidation of arsenopyrite and As-bearing pyrite. The formation of arsenopyrite takes

place under reductive conditions at high temperatures, mostly in areas close to buried plant roots or various nuclei of decomposing organic matter (Flora, 2015). Iron oxides and traces of arsenic are readily created after the oxidation of pyrite under aerobic conditions. Upon the reaction of arsenopyrite with oxygen and/or water, arsenic oxidises rapidly into As^{2+}, As^{3+}, As^{5+} and a precipitate – either scorodite ($FeAsO_4 \cdot 2H_2O$) or amorphous Fe(III) oxide (Williams, 2001).

The proportion of arsenic in sulphide minerals differs significantly (arsenic can be a dominant mineral-forming element as well as an impurity). Mineral weathering of arsenic is rather slow, although the rate of arsenic release may be increased by mining-related actions like grinding, crushing and pulverisation (Flora, 2015). Various other sulphides may be formed upon the reaction of arsenosulphides with transition metals such as Ni, Cu and Co (Nordstrom, 2002).

Three major sources of geogenic arsenic contamination can be distinguished – hydrothermal activity, ore deposits and Cenozoic sediments. Minor sources are related to coal formation and coal combustion. The Latin American arsenic-contaminated areas are located within the circum-Pacific region, being associated with the volcanic activity at the eastern flank of the Pacific Ring of Fire (Masuda, 2018). The sources of arsenic contamination include the dispersion of volcanic ash from numerous eruptions as well as the formation of sulphide deposits across the Andean Cordillera. Moreover, more than 100 aquifers along river basins in Latin America suffer from elevated concentrations of arsenic, exceeding the maximum recommended limit of 10 µg/l (WHO, 2006) for arsenic in drinking water by several orders of magnitude (Bundschuh et al., 2012).

The excessive concentrations of arsenic in areas with intensive volcanic activity reflect the fact that arsenic is a volatile component of magma; arsenic-containing minerals are highly soluble in water. Concentrations of arsenic as well as other volatile elements associated with geothermal fluids are controlled by the type of host rock, water chemistry, temperature, boiling and mixing properties and proportion of volcanic gases and vapour in thermal waters (Ellis and Mahon, 1977; Yokoyama et al., 1993; Aiuppa et al., 2006; Morales-Simfors et al., 2020). During the ascent of geothermal fluids and volcanic gases containing As, multiple geochemical processes influence the speciation of arsenic in these media. Such geochemical processes are controlled by thermodynamic conditions (temperature and pressure), redox processes (oxidation/reduction), biotic and abiotic processes, methylation and As-S cycling (Wang et al., 2018).

Four principal zones of geothermal systems with elevated As concentrations can be distinguished; all of these occur along the boundaries of active tectonic plates. These zones are determined as: a) zones of active volcanism, b) continental collision zones, c) continental rift systems associated with active volcanism and d) continental rift zones with active volcanism (Morales-Simfors et al., 2020). In the case of Latin American countries, the origin of arsenic contamination is related to the first example, given the ongoing volcanic activity within the CVZ of the Andes.

Alike the transport pathway of boron, the decomposition of arsenic-containing materials is closely related to the very high mobility of arsenic in various geological media during active tectonic and volcanic activity. Especially, this decomposition is significant in areas with arc magmatism and subsequent hydrothermal activity in combination with high erosion rates and downstream transport to sedimentary basins (Masuda, 2018). A major enhancement in values of arsenic concentrations is observed in arc magmas (ca 10 ppm) as well as in the depositions of surface sediments (up to 20 ppm) and marine sediments (14 ppm), as shown in Figure 1.

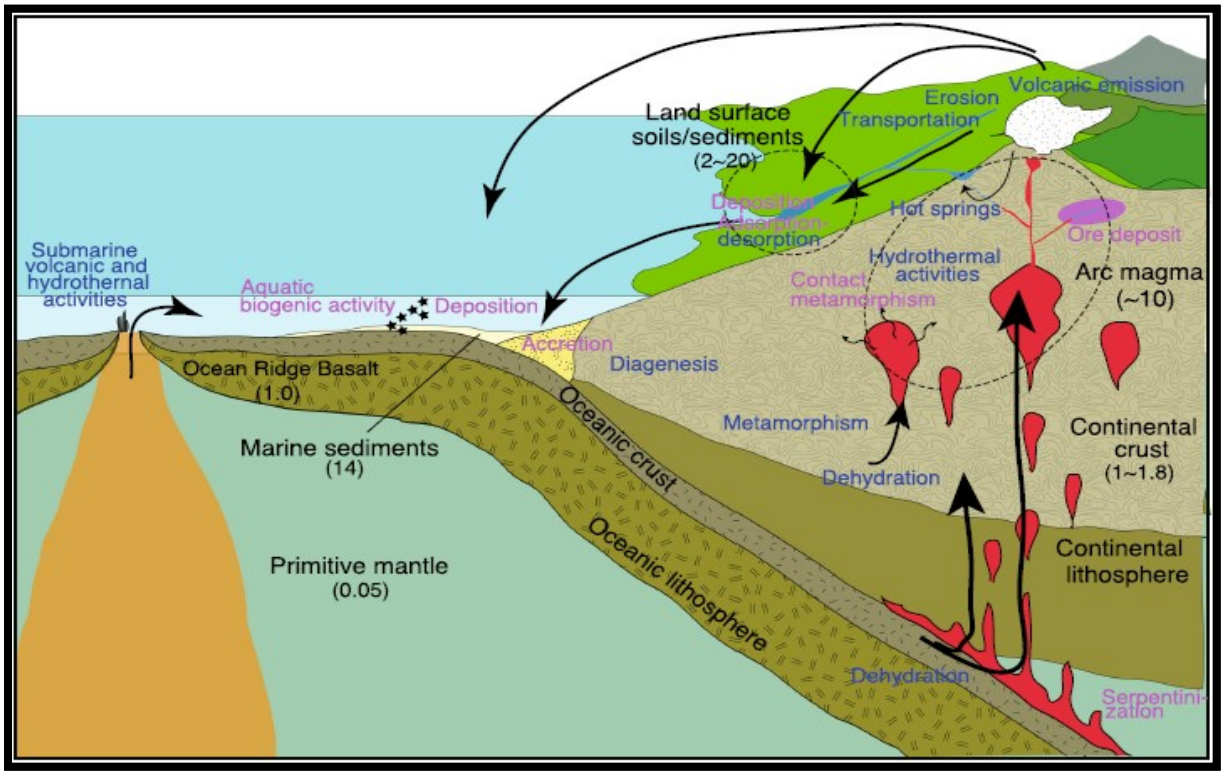

Fig. 1: A schematic illustration depicting the geogenic cycle of arsenic in areas with active tectonic and volcanic activity. Blue- and purple-denoted processes indicate mechanisms of arsenic fixation and release, respectively. Numbers in parentheses determine arsenic concentrations within respective geological media. Adapted from Masuda (2018).

The second main source of natural arsenic contamination includes ore deposits. For instance, the release of arsenic from As-bearing marcasite (dated to 5 Ma) in a hydrothermal ore deposit in New Zealand caused excessive arsenic concentrations in groundwater, reaching more than 100 µg/l (Craw et al., 2000). Even though the extent of natural arsenic contamination around ore bodies is determined adequately, the anthropogenic materials/products associated with mining (such as sludge and tailings) cause the rapid progress of arsenic contamination into surrounding soils and water bodies. After excavation, ore bodies and the subsequent long-term chemical weathering form sediments with elevated As concentrations that later represent numerous point sources of potential arsenic contamination (Masuda, 2018).

Cenozoic sediments represent the third major source of natural arsenic contamination. In comparison with the average As concentration in surrounding soils and sediments, the values of As concentrations in contaminated groundwater are not very high; this is documented by a case of a Holocene aquifer in Bangladesh, where the total arsenic concentrations in bulk aquifer sediments range between 5 and 16 mg/kg, whereas less than 1 mg/l of As has been detected in groundwater (Seddique et al., 2011). Therefore, it can be assumed that the contamination of groundwater is mainly influenced by the chemical form of arsenic host phase and the extent of changes driving the release of arsenic from the aquifer sediments into the aquatic environment, whereas the initial concentration of As in the sediments is less important (Masuda, 2018). The dissolution of arsenic in Cenozoic aquifers is related to reducing conditions in groundwater; the major phases strongly adsorbing arsenic include iron oxides/hydroxyoxides (Nickson et al., 2000; van Geen et al., 2004). The highest stability of iron oxides/hydroxyoxides is achieved under weakly acid to alkaline (pH > 4) and oxic (positive Eh) conditions. To the contrary, the greatest rate of arsenic release due to decomposition and/or desorption from these substances can be observed under alkaline and reducing conditions (van Geen et al., 2006).

5. BORON

5.1. Physico-chemical characteristics of boron

With an atomic number of 5, boron is found within Group IIIA of the periodic table. Contrary to other Group IIIA elements, it is very difficult for boron to complete its valence shell, given it has only three valence electrons. Thus, boron is considered as "electron deficient" as three single bonds still leave boron with just six electrons in its valence shell (boron therefore lacks two electrons to complete a full valence shell). The so-called "three centre-bonds" composed of a boron atom linked to two hydrogen atoms compensate this deficiency; three centre-bonds contain only one pair of electrons, while extending over three nuclei (Brady and Humiston, 1978; Parks and Edwards, 2005).

Two stable isotopes of boron are found in nature – ^{10}B and ^{11}B. The ^{11}B isotope occurs approximately fourfold more than the ^{10}B isotope, leading to the relative atomic mass of 10.81 g/mol (Power and Woods, 1997). The boron isotope ratio of waters is sometimes used for determination of water sources. Different water sources have slightly different isotope ratios and upon their mixing, the resultant isotope ratio represents a proportional change between the two original ratios (Davidson and Bassett, 1993; Vengosh et al., 1994).

Under ambient conditions, essentially all boron is present in +3 oxidation state. However, boron cannot be found in the form of B^{3+} cation due to its rapid reactivity with oxygen (Holleman and Wiberg, 2001). Due to its small size and high ionic potential, boron can form covalent bonds only (Brady and Humiston, 1978). Usually, boron has a coordination number of +3, for instance in boric acid and its salts as well as in boron trifluoride (BF_3). A coordination number of +4 for boron is observed in the tetrafluoroborate anion (BF_4^-); in this compound, boron achieves a full valence shell (Holleman and Wiberg, 2001).

Other important physical and chemical properties of boron together with its atomic data are presented in Table 2.

Tab. 2: Selected physical and chemical properties of boron and its atomic data (based on Haynes ed., 2015 and Coursey et al., 2015):

State at 20°C	Solid
Electron configuration	$1s^2 2s^2 2p^1$
Melting point	2370 K
Boiling point	4273 K
Density	2.34 g/cm^3
Atomic radius (non-bonded)	1.92 **Å**
Covalent radius	0.84 **Å**
Electron affinity	26.989 kJ/mol
Electronegativity (Pauling scale)	2.04

In aqueous solutions, boron is mostly present in the form of boric acid (H_3BO_3), which behaves as a weak Lewis acid (Power and Woods, 1997). Boric acid accepts hydroxide ion from water, while releasing hydrogen proton into solution as shown by the following equilibrium equation (K_a = 5.8 x 10^{-10}; pK_a = 9.24 at 25°C as presented in Dean, 1987):

$$H_3BO_3 + H_2O \rightleftharpoons B(OH)_4^- + H^+$$

At 25°C, 5.5 g of boric acid dissolves per 100 g solution in water; the solubility of boric acid increases with temperature (Waggott, 1969). Only the mononuclear species H_3BO_3 and $B(OH)_4^-$ are present at concentrations below 0.02 M (216 mg/l as B; Parks and Edwards, 2005).

5.2. Reactivity of boron

When assessing the reactivity of boron under ambient conditions, sorption represents the most important process of boron fixation. Various mineral and solid surfaces are capable to adsorb boron, forming labile bonds. A weak adsorption of boron onto illite and kaolinite clay

as well as onto sewage sludge was detected by Banerji (1969); a maximum sorption density of 31 mg B per 1 g of these sorbents was recorded in this study. Sorption reactions have an important control role concerning the concentration of boron in soils (Evans and Sparks, 1983; Goldberg et al., 1993). A maximum sorption density of ca 0.047 mg B per 1 g of soil was detected by Gupta et al. (1985). Moreover, boron can form inner-sphere complexes with various minerals, for instance iron and aluminium hydroxides, kaolinite and allophane. To the contrary, calcite and quartz are unsuitable for boron adsorption from solution (Su and Suarez, 1995).

Accessible interlayers in 2:1 phyllosilicates have a specific role in boron adsorption. The major species capable to adsorb boron include freshly precipitated aluminium hydroxide [$Al(OH)_3$] and related hydroxyaluminium materials, as reported in a study by Hatcher et al. (1967). The Fe and/or Al species occurring as interlayer materials, impurities and coatings affecting the access of boron to interlayer positions have a crucial role in terms of achieving maximum boron retention (Parks and Edwards, 2005). Minerals with no aluminium or iron present (such as tremolite, enstatite and diopside) are also capable to adsorb significant quantities of boron. This fact indicates that the magnesium-hydroxide coatings could represent active sorption sites (Parks and Edwards, 2005). A study by Rhoades et al. (1970) found out that magnesium hydroxide [$Mg(OH)_2$] can adsorb large quantities of boron from solution and most importantly, this ability does not diminish in time.

Depending on the form of $CaCO_3$ as well as the concentrations of Mg and NaCl, co-precipitation of boron with either aragonite or calcite is possible; the co-precipitation is easier in the case of aragonite. The formation of aragonite is favoured in the presence of magnesium (Parks and Edwards, 2005). With increasing NaCl concentration, boron co-precipitation decreases in aragonite, while increasing in calcite (Kitano et al., 1978).

Concerning other physical and chemical processes, including complex formation, precipitation and volatilization, their importance in terms of boron reactivity is less significant. Very little or no information is available regarding the complexes of boron with environmentally important cations, for instance Al^{3+}, Fe^{3+}, Fe^{2+}, Ca^{2+}, Mg^{2+}, K^{+}, Na^{+}, Cu^{+} and Cu^{2+} (Parks and Edwards, 2005). Boron buffers are frequently used in metal complexation studies involving solids containing Al^{3+}, Fe^{3+}, Fe^{2+}, Ca^{2+}, Mg^{2+}, K^{+}, Na^{+}, Cu^{+} and Cu^{2+}. For these solids, no solubility products can be readily found due to insignificance of complexation (Parks and Edwards, 2005). However, a study by Lapp and Cooper (1976) has determined the solubility of calcium borate at ca 600 mg/l.

Despite the insignificant volatilization of boron at ambient temperatures, boric acid may co-evaporate with seawater moisture to form borate aerosols in the atmosphere (Argust, 1998). The amount of boron in the distillate is a function of concentration in the feed; the distillate can contain up to 25-30% of the borate (in mg/l) originally present in the feed water (Wong, 1984; Park and Edwards, 2005). Also, significantly high values of boron concentrations can be recorded in a steam phase in equilibrium with water (Ellis and Mahon, 1977).

5.3. Geogenic sources of boron

The very high mobility of boron in aqueous fluids enables it to be easily transported across various types of geological media. Moreover, boron is well-known for its incompatible behaviour in most magmatic processes, which makes it an especially useful tracer for mass transfer in subduction settings (Morris et al., 1990; Bebout et al., 1999). A characteristic B-isotope composition is observed within the upper altered oceanic crust; this considerably differs from other major source reservoirs associated with magma genesis at arcs (including subducted sediments, continental crust and mantle peridotite; Rosner et al., 2003).

At most subduction settings, it is generally accepted that primary arc magmas originate from partial melting of the asthenospheric mantle wedge; its solidus temperature is decreased by an influx of hydrous fluids released from the subducting slab (Gill, 1981; Tatsumi and Eggins, 1995). Slab-derived fluids play a key role in the transport of fluid-mobile elements into the mantle wedge; such subduction components represent a marker distinguishing most arc magmas from other mantle-derived as well as MORB magmas (Hawkesworth et al., 1993; Pearce and Peate, 1995). Temperatures at the slab-mantle interface range between 300 to 1250 °C as determined by thermal models of subduction zones in a study by Peacock (1996). However, the temperatures in majority of subduction settings are insufficient to initiate melting in the subducting slab. This is also true for the Central Andean subduction zone, given the Eocene age of the subducting Nazca Plate, the low subduction angle (ranging from 20° to 30°) as well as the relatively rapid convergence rate (Rosner et al., 2003). The data presented in a geophysical model for the Central Andean subduction zone after the ANCORP Working Group (1999) predicted a temperature of 400°C at the slab-mantle interface below the volcanic front. Therefore, it is assumed that hydrous fluids enable the transport of slab-derived

components into the mantle under the Central Volcanic Zone (Rosner et al., 2003) and as mentioned above, boron is one of the most mobile components in this process.

When assessing the release of boron and other fluid-mobile elements from the subducting slab, it is necessary to consider whether dehydration is rather a continuous process driven by sliding reactions or if it is associated to breakdown of hydrous phases within narrow P-T intervals (Rosner et al., 2003). A study by Kerrick and Connolly (2001) showed that the rate of devolatilization is dependent on the thermal structure of subduction zones. Progressive dehydration of metabasalt over the interval of subduction depth (88 to 152 km below the arc as presented in a study by Rosner et al., 2003) is expected for the Central Andean setting given its low to intermediate temperature conditions. Therefore, slab-derived boron should be incorporated to the mantle wedge across the entire area of their interaction (Rosner et al., 2003).

With an average concentration of 10 ppm in continental crust and 4-5 ppm in seawater, boron is considered as a rare element in the nature. Major accumulations having significant concentrations of boron are found in borate deposits across the globe. The most notable borate deposits are associated with Cenozoic volcanic activity in orogenic belts. These deposits are located close to convergent plate margins with characteristic andesitic-rhyolitic magmas and considerable hydrothermal activity, in close basins present in arid or semiarid climates and predominantly in non-marine evaporitic environments, as depicted in Figure 2 (Helvacı, 2017). Besides South American deposits, other major commercial deposits supplying worldwide consumption of borates are situated in Turkey (the region of Anatolia), United States and China; all of these include non-marine evaporites associated with volcanic activity (Watanabe, 1964; Ozol, 1977; Kistler and Helvacı, 1994; Helvacı, 2015). These regions constitute four main metallogenic borate provinces recognized at a global scale (Helvacı, 2017).

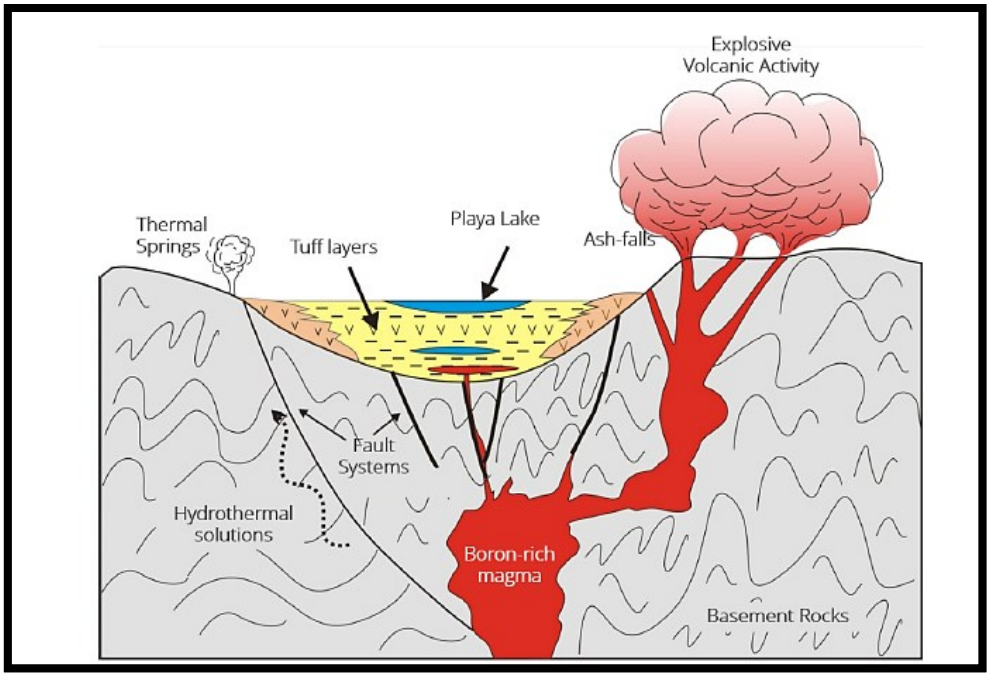

Fig. 2: Formation of borate deposits in arid basins filled with products of volcanic activity as occurring in Turkey (Anatolia). This region exhibits similar features of Neogene volcanism to the South American borate deposits. Adapted from Helvaci (2015, 2017).

Three major groups of borate deposits are determined with respect to their formation under various geological conditions. The first group includes skarn deposits (mostly in Eastern Europe and Asia) associated with intrusives, containing iron oxides and silicates. These deposits were prospected in well-preserved fold belts in which limy sediments are in close contact with potassic to alkaline volcanics (Helvacı, 2017). The second group is comprised of magnesium oxide group hosted by marine evaporitic sediments; together with borates associated with iron ores, these borates are considered as low-grade (Helvaci, 2017). The most important as well as the most exploited group of borate deposits encompass a sodium- and calcium borate- hydrates group. Such borates are formed in a playa-like environment where boron accumulates during episodes of explosive volcanic activity, when the basin is filled with andesitic to rhyolitic volcanics as well as direct ash fall. Moreover, these deposits are affected by thermal springs close to the area of volcanism, hydrothermal solutions along graben-margin faults (Helvacı, 2017). These deposits are situated in areas with arid to semiarid climatic conditions with lake water pH ranging between 8.5 and 12. A schematic illustration of all major groups of borate deposits is presented in Figure 3.

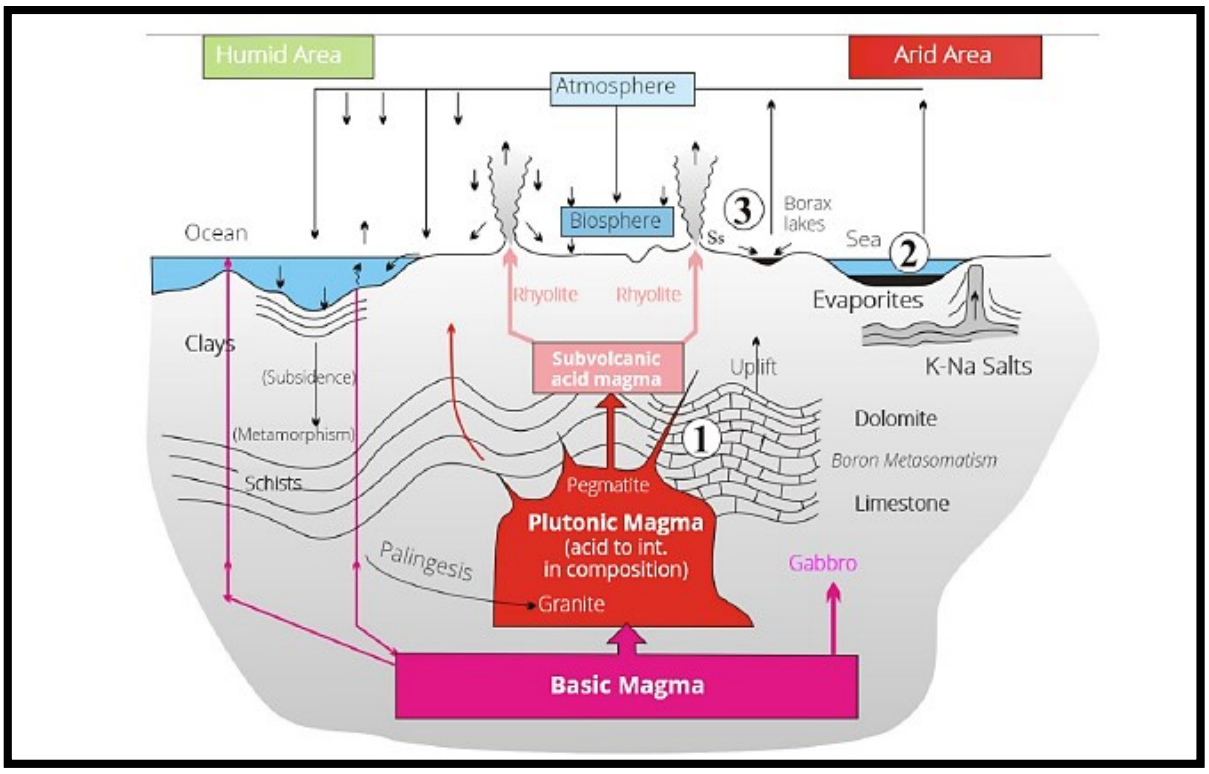

Fig. 3: A schematic illustration showing the major group of borate deposits and geological processes of their formation. Modified after Watanabe (1964), adapted from Helvacı (2017).

The South American borate deposits are located within a region known as the "Central Andean Boratífera Province", which stretches from the southernmost Peru (territories belonging to the departments of Arequipa and Tacna) across northern and north-eastern Chile, south-western and southern Bolivia to northern and north-western Argentina. In this region, the greatest resources available for exploitation are found in Argentina (600 mil ton) and Chile (570 mil ton); Peruvian deposits contain 290 mil ton of borates (Millas, 2020). The basins located within the Central Andean Boratífera Province are of volcanic and tectonic origin, being dated within the Middle Cenozoic – Quaternary age interval. In some basins, their specific characteristics include the development of lacustrine systems with both fresh and saline waters; in terminal stages; these have evolved into evaporitic basins known as salars (Millas, 2020). Salars are usually situated in lower parts of arid basins, being in an asymmetrical position within them. The formation of salars is related to the breakdown of the balance between the waters inflowing into the basins and the evapotranspiration as well as the evaporation process (Millas, 2020). Despite salars may vary in time and space, their common characteristics involve

the presence of both detrital and chemical components originated from Cenozoic volcanic activity (Garcés, 2000). Associated features of this activity in arid basins include weathering and erosion processes, leaching of volcanic rocks as well as the direct volcanic activity through the geothermal gradient, contribution of thermal sources and the falls of pyroclastic materials into the basins (Millas, 2020).

The presence and activity of geothermal fields represent another important source of boron. The brines of geothermal fields have an elevated content of salts, including borates (Millas, 2020). Due to a high geothermal gradient, the local volcanic activity supplies considerable amount of leached transport ions to the basins (Munk et al., 2016; Warren, 2016). In total, over 220,000 g/l of TDS (total dissolved solids) can be present in brines; this value exceeds tenfold the usual value of TDS in thermal waters and hundredfold the usual value of TDS in meteoric waters (Millas, 2020). Besides major cations and anions (Na^{+}, $Ca^{2+,}$ Li^{+}, Mg^{2+}, Cl^{-}, SO_4^{2-}, BO_3^{3-} and CO_3^{2-}), the brines are known to have significant concentrations of Hg, As and Sb as well as trace elements, such as Cs and Rb (Risacher et al., 2003; Risacher and Fritz, 2009; Munk et al., 2016, 2018). In total, volcanic and volcanoclastic rocks (mainly ignimbrites) constitute almost 90% of rocks in which borate deposits are formed (Garcés and Chong, 1993).

6. TOXICITY PROPERTIES

6.1. Toxicity of boron

Human exposure to boron and boron-containing solutions involves ingestion (diet) and intake from drinking water. The entire boron intake is almost completely absorbed by gastrointestinal and respiratory systems, where boron is present in body fluids and tissues either as boric acid (H_3BO_3) or $B(OH)_4^-$ anion (in smaller quantities; Bakirdere et al., 2010). The WHO estimates that the average boron intake is 1.2 mg/day through diet, 0.2-0.6 mg/day via drinking water and 0.44 µg/day through inhalation (WHO, 1998). However, in areas with extensive volcanic activity and/or vast borate deposits in arid environment with little or no water treatment facilities in operation, the average boron intake is considerably greater; this is also the case of the Department of Tacna in Peru, where boron concentrations in drinking water far exceed the guideline value of 0.5 mg/l determined by the WHO (WHO, 2009).

Long-term exposure to elevated intakes of boron may lead to reproductive and developmental toxicities (Fail et al., 1998). Lethal doses of boron are estimated at 3,000-6,000 mg/l for infants and 15,000-20,000 mg/l for adults (Bakirdere et al., 2010). However, risk assessments indicate that common intake of boron from diet and drinking water (even in the areas mentioned above) does not present a significant risk for human health, even though sodium borates and boric acid have low acute toxicity. Although certain sodium borates cause eye irritation in animals, no adverse ocular effects in humans had been observed during 50 years of occupational exposure (European Centre for Ecotoxicology and Toxicology of Chemicals, 1995).

Experimental studies have proven adverse effects such as anorexia, bone disorders, weight loss and testicular atrophy in mice after these had been exposed to a boron dose of 80 mg/kg/day (Price et al., 1996; Korkmaz et al., 2007). The most concerning adverse effect related to boron exposure in mice, rats and rabbits was foetal toxicity associated with high prenatal mortality, reduced foetal body weight, malformations of eyes, axial skeleton and dysfunctions of cardiovascular and central nervous system (Bakirdere et al., 2010). Fortunately for humans, no such concerns have been proven in a toxicological study by Şaylı et al. (2001), which analysed the boron exposure to humans in six different areas of the western Anatolia in Turkey, an area known for the occurrence of vast borate deposits and excessive boron concentrations (up to 29 mg/l) in drinking water.

6.2. Toxicity of arsenic

Ever since the beginning of human civilisation, arsenic has been considered as one of the most dangerous poisons as well as lethal weapons in hands of those who possessed it. Nowadays, inorganic arsenic is determined among the most toxic elements, being present in Group A of the US Environmental Protection Agency classification and Group I of the International Agency on Research on Cancer classification (IARC, 2004; US EPA, 2016). Common ways of arsenic exposure to humans include diet, drinking water and inhalation, particularly in industrial areas (air pollution) of developed countries as well as areas of active tectonic and volcanic activity (air with elevated concentrations of volcanic emissions). The health hazards stemming from long-term exposure to excessive amounts of arsenic are thus related mainly to developing countries and their remote areas (such is the case of the Andean region in Latin America besides other examples like India, Bangladesh etc.). In these areas, a lack of water treatment facilities combined with insufficient and often very inaccessible healthcare facilities leads to numerous health risks affecting the quality of life of the local population, which is often unaware of these risks due to a lack of their knowledge and/or neglection of the problem by their authorities. Overall, it is estimated that 200 million people across the globe suffer from health problems associated with exposure to excessive arsenic concentrations in drinking water (NRC, 2001; Ravenscroft et al., 2009; Khairul et al., 2017).

Inorganic species (trivalent and pentavalent) of arsenic are the most prevalent in surface waters within the Department of Tacna. The toxicity of trivalent arsenic is higher than in the case of pentavalent arsenic; moreover, trivalent arsenic is estimated to be 25-60 times more mobile than pentavalent arsenic (Dutré and Vanecasteele, 1995). Furthermore, the lower rate of pentavalent arsenic toxicity is associated with its smaller accumulation potential in comparison to trivalent arsenic species (Styblo et al., 2000; Mass et al., 2001; Hirano et al., 2003). The assessment of arsenic toxicity also depends on the rate of metabolism and accumulation in human and animal tissues. In general, the toxicity pattern of As is described as follows: $AsH_3 > As^{3+} > As^{5+} >$ RAs-X (Flora, 2015).

Long-term exposure to excessive arsenic concentrations in drinking water is reflected by both acute and chronic symptoms. The symptoms of acute arsenic poisoning include abdominal pain, severe diarrhoea, nausea and vomiting. On the other hand, chronic symptoms of arsenic poisoning associated with the accumulation of As in vital organs are related to the development of diabetes mellitus, hypertension, ischemic heart disease, atherosclerosis, nephrotoxicity,

hepatotoxicity and multiple types of cancer (lung, bladder and skin cancer; Khairul et al., 2017). Undoubtedly, all such diseases have a detrimental impact on the quality of life of the local population as well as on the average life expectancy, which was determined in the range of 60.4-65.1 years across the four provinces constituting the Department of Tacna in 2016, way below the global average life expectancy of 72.0 years determined by the WHO (Atencio et al., 2017).

7. BORON REMEDIATION METHODS

Various methods have been developed for boron remediation with regards to the origin and extent of respective boron contamination in affected areas. The efficiency of remediation methods is assessed and eventually confirmed by satisfying the limit of boron concentration lower than 0.5 mg/l in drinking water recognised by the WHO (WHO, 2009). National limits may vary, especially in areas known for significantly high boron concentrations (e.g. Latin American countries, Turkey, Canada and others).

Overall, boron remediation methods encompass both biological and physico-chemical approaches. These methods display variable ability to successfully reduce boron contamination, having been modified and/or combined to create multi-step processes of boron remediation. When contemplating about the most suitable boron remediation method for a given case, the following aspects must be taken into consideration:

- the source and extent of boron contamination (natural and/or anthropogenic) and initial boron concentration,
- the characteristics of a contaminated area (in terms of local geology, groundwater flow and the exposure of humans and wildlife to this contamination),
- determination of the purpose of boron remediation (i.e. whether the output water will serve as a source of drinking or irrigation water),
- the assessment of desired output water production (in litres per hour) and maintenance of such a supply
- and the available financial resources associated with the preparation of remediation technology and its operation (both in short and long term).

7.1. Biological boron remediation methods

7.1.1. Phytoremediation

This remediation method represents an approach traditionally used for areas with extensive boron contamination in soils. Its principle lies in plating tolerant species suitable

for taking up and accumulation of significant B quantities in the upper part, which can be harvested and disposed in suitable places afterwards. After such species are harvested, they are disposed primarily in boron-deficient soils. At low concentrations, boron is an essential micronutrient, having an important role in cell walls of higher plants, where the cross-links of B-binding molecules provide stability to the cell wall matrix (O´Neil et al., 2004; Tassi et al., 2011). Phytoremediation is a low-cost and environmentally sound technology, capable of reducing boron contamination in both soils and soil leachates. Its disadvantages are associated with the availability of tolerant species, which can accumulate lower amounts of boron in comparison with other physico-chemical methods. Also, relying exclusively on bioaccumulation of these species makes the entire process considerably time-consuming.

7.1.2. Constructed wetlands

This remediation approach includes the creation of a wetland, in which tolerant species are planted; these can absorb boron through their roots and accumulate it in their cell wall structures. Usually, constructed wetlands are designed to remediate various heavy metals and metalloids thanks to their specific microenvironment. When set up properly with no significant changes occurring within their environment (e.g. no new source of contamination, sufficient water level in the wetland and proper growth of plants), constructed wetlands can reduce considerable amount of boron in the long term with minimal maintenance needed over time. However, it is advised to conduct continuous and regular monitoring of biological and physico-chemical properties within the wetland and to react immediately once any adverse change may occur.

7.2. Physico-chemical boron remediation methods

7.2.1. Membrane filtration of boron

This remediation technique consists of multi-step processing of boron species concerning their complexation into complexes of a bigger size, followed by their subsequent membrane filtration leading to their elimination from drinking water. In aquatic environment, boron is presented mostly in the form of boric acid (H_3BO_3), which is a waxy solid soluble in water (55 g/l at 25°C; Tu et al., 2010). Given the small molecular weight of boric acid

(at 61.831 g/mol), the same assumption concerning its size is widely expressed, thus underlining the need to perform complexation processes before the membrane filtration of boron can take place.

The most well-known boron complexation process includes the utilisation of chemical compounds containing several hydroxyl groups (e.g. mannitol), whose reaction with boric acid and/or boric compounds leads to the formation of complexes (Geffen et al., 2006; Tu et al. 2010). Acidity of borate solutions and boric acid is enhanced through the process of complexation. The formation of cyclic borate esters is the fundamental cause of increase in acidity, as can be seen in Figure 4.

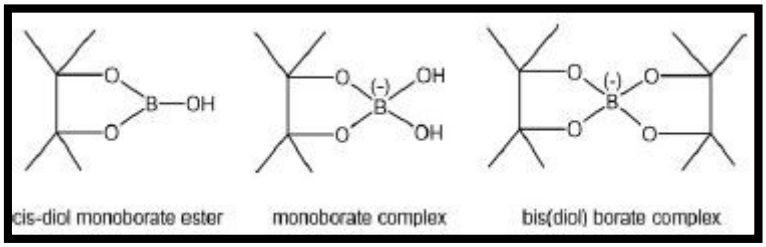

Fig. 4: Illustrational drawings showing the structures of neutral cis-diol monoborate ester (left), monoborate complex (central) and bis(diol) borate complex (right). Adapted from Power & Woods (1997) and Tu et al. (2010).

The type of diol used significantly influences the overall stability of the borate complex. A stable complex is formed when OH- groups in the diol used are oriented as such they accurately match the structural parameters necessary for a tetrahedrally coordinated boron. The highest stability has been observed in the esters formed with cis-diols on a furanoid ring, although these are rarely found in nature, being limited to rebose and apiose (Tu et al., 2010).

The mechanism of reverse osmosis desalination represents the most important method in terms of boron membrane remediation. Reverse osmosis seawater desalination plants commonly involve two or more passes (the first pass has a natural pH of 6-7), while aiming to decrease the boron concentration by alkalinisation up to pH 11 at the second pass according to the WHO guidelines for drinking water (set below 0.5 mg/l). The actual number of passes can vary with respect to the characteristics of feed water and product water standards (Greenlee et al., 2009). At the first pass, high-pressure seawater RO membranes are used to significantly reduce the amount of TDS; therefore, high TDS rejection is no longer necessary

(Tu et al., 2010). Consequently, low-pressure brackish RO membranes can be utilised for energy saving, while allowing higher recovery as well in the second pass.

The utilisation and development of reverse osmosis desalination techniques are primarily concentrated to developed countries in arid environments with infrequent precipitation and insufficient freshwater resources. Since the beginning of this century, Israel is considered as a global leader in construction, development as well as research on reverse osmosis techniques supplying significant quantities of freshwater for its population. The biggest and oldest desalination plant in Israel is situated in Ashkelon, being in full operation since 2005. In contrast to then conventional arrangement of desalination mechanisms characterised by several identical outsized trains (common in small-scale RO plants), the construction of Ashkelon plant represented a breakthrough, being the first desalination plant having a three-centre model used for desalination. Such a model involves high-pressure pumps, energy recovery devices and membranes aiming to work independently with the highest efficiency during the desalination process (Water Technology, unknown date).

The whole complex is composed of North and South plant sections working independently, each producing 50 million m^3 of desalinated water per year. Both sections have their own pumping centre, which comprises 3 + 1 large 5.5 MW pumps operating at high pressure as well as 105 pressure vessels contained in 16 RO banks and a common feed ring. Overall, the entire facility consists of 40,000 membrane elements using optimised boron removal and multi-stage RO processes (Water Technology, unknown date).

Filtration is carried out in two stages, beginning with gravity filters involving quartz, gravel, anthracite media and sand. The high efficiency of filtration is supported by a distribution system designed to decrease clogging as well as the preferential channel formation.

Besides that, the challenge of boron removal represented a huge task when constructing the plant and designing the devices involved in this process. After a thorough consideration of all necessary aspects such as the adjustment to feed water temperature fluctuations, continuous low-pressure operation, high pH tolerance, cost-effectiveness, minimal membrane fouling and reliable performance, the relevant Israeli authorities decided to select FilmTec elements for the RO operation. Before the desalinated water enters the national supply system, it is re-mineralised through post-treatment with lime (Water Technology, unknown date).

Certain innovative approaches have been adopted concerning the development of reverse osmosis desalination plants. One of those involve a design known as split parting system (firstly

introduced in Eilat, Israel), whose primary target is to reduce the over-print of the second stage (Glueckstern and Priel, 2003; Nadav et al., 2005). The principle of this technique can be explained by the collection of permeate from both ends of the membrane vessels within the first part. Only the permeate produced from the concentrate end with higher boron concentration is fed into the second pass; the permeate produced from the feed end with lower boron concentration and salinity is used for blending (Tu et al., 2010). The efficiency of boron rejection is inversely proportional to the split ratio. According to a study by Glueckstern and Priel (2003), the overall boron rejection decreased from 91% to 87% with a simultaneous increase in the split ratio (from 28% to 80%, respectively). Boron is successfully removed once pH of permeate of the first pass is increased up to pH 10 before the next pass is fed (Tu et al., 2010). Due to the precipitation of sparingly soluble salts occurring at such high pH, it is advised to use an anti-scalant (in appropriate quantities) to the second pass feed, aiming to mitigate the effects of scaling. Another obstacle stemming from the utilisation of a multi-pass configuration is represented by an increased cost of operation associated with a low overall system recovery (Tu et al., 2010).

The possibility of combining reverse osmosis with ion exchange resins to enhance membrane filtration of boron has also been broadly researched (Bansal, 1980; Redondo et al., 2003). Such a configuration involving a boron-selective ion exchange resin in the process of membrane filtration helps to remove boron from the first pass RO permeate, thus decreasing the boron concentration way below 0.1 mg/l, clearly satisfying the required limits for boron concentration in drinking water (Kabay et al., 2008). A considerable problem originating from the use of this technology results in the need for treatment and disposal of the regeneration solutions (Kabay et al., 2007; Bryjak et al., 2009). Treatment of the regeneration solutions may be carried out via electrodialysis and reverse osmosis, as demonstrated in an experiment by Melnik et al. (1999). Nevertheless, further research concerning the efficiency of boron removal and operational costs needs to be done before such technique could be used on an industrial scale.

Besides common practice in terms of boron removal (particularly through the multi-step reverse osmosis (RO) process), current studies have focused on the possibility of boron remediation through high boron rejection RO membranes via coupling of a coating layer (additives) with a denser membrane active skin layer (thus having greater boron rejection). The primary purpose of the chemical coating layer (either containing one or a group of chemicals) is to enhance the membrane affinity with water (also known as hydrophilicity), which therefore

compensates the increase in membrane resistance induced by an active skin layer of greater density (Taniguchi et al., 2004; Tu et al., 2010). An experiment carried out by Comstock (2009) utilised the coating of polyhexamethylene biguanide to a seawater reverse osmosis membrane, resulting in progress of boron rejection from 92.7% to 97.6%. The ultimate advantage of this technique lies in the possible use of single-stage membrane system in RO seawater desalination plants, which could save operational cost as well as capital in terms of seawater desalination via RO processes. On the other hand, it is needed to carry out further research investigating the stability of the coating layer before this method could be utilised far greater in industry (Tu et al., 2010).

7.2.2. Electrocoagulation

The mechanism of this remediation method is represented by the in-situ application of a coagulant, while the sacrificial anode corrodes simultaneously because of the fixed current density. At the same time, the gradual accumulation of hydrogen at the cathode enables the removal of a pollutant by flotation (Yilmaz et al., 2007).

At the start of the electrocoagulation process, metallic hydroxide flocs are formed in the water by electrodissolution of soluble anodes, which are composed of aluminium or iron (Koparal, 2002). The coagulants, which are necessary for successful completion of electrocoagulation and subsequent precipitation, are delivered into the system through electrodes in the reactor (Yildiz et al., 2007).

The fundamental principle of electrocoagulation concerns the influence of electric charges on the stability of colloids, suspensions and emulsions. Thus, if further electric charges are applied to the charged particles via convenient electrodes, the neutralization of the surface charge of particles occurs and these particles merge into separable, larger agglomerates (Öğütveren & Koparal, 1997; Yilmaz et al., 2007). Careful selection of material used for this process has considerable importance as the electrode assembly represents the principal tool in the treatment facility. Iron and aluminium are predominantly used as electrode materials due to their proven effectiveness, instant availability and low cost of operation (Chen et al., 2000).

Three major mechanisms illustrate the electrocoagulation process. The first step involves the formation of a coagulant by the sacrificial oxidation of anode. The destabilisation of pollutants and particulate suspension is included in the second step. In the end, the breaking

of emulsions and aggregation of destabilised phases take place, leading to the formation of a floc (Îrdemez et al., 2006; Yilmaz et al., 2007; Babu et al., 2007, Isa et al., 2014).

The chemistry of the aqueous medium and its conductivity influence significantly the process of electrocoagulation. Moreover, other factors including particle size, pH and concentrations of chemical constituents affect the electrocoagulation process as well. The following reactions occur if aluminium is selected as electrode material:

1) At the cathode: $3H_2O + 3e^- \rightarrow 3/2\ H_2(g) + 3OH^-(aq)$
2) At the anode: $Al(s) \rightarrow Al^{3+}(aq) + 3e^-$
3) In the solution: $Al^{3+}(aq) + 3H_2O \rightarrow Al(OH)_3(s) + 3H^+(aq)$

The precipitated aluminium hydroxide in the solution appears in the form of sweep flocs having large surface area, which increases its adsorption capacity and thus helps to remove boron from solution. Flotation and/or sedimentation are used in the first place in order to separate the formed flocs from an aqueous medium (Isa et al., 2014).

However, the flocs are formed predominantly under slightly to moderately alkaline conditions (up to pH 9), which are reached by the utilisation of soluble anodes, where the process of electrolysis leads to the formation of amorphous aluminium hydroxide (Wided et al., 2014). Furthermore, such conditions are enhanced by increasing OH^- concentration caused by the evolution of H_2 at the cathode.

When the pH of the treated water exceeds 9.0, electrocoagulation mechanism can neutralise it to a certain extent through several reactions. The purge of CO_2 associated with the evolution of O_2 and H_2 occurs under acidic conditions (Wided et al., 2014). The alkaline conditions are further increased by the formation of aluminium hydroxide; however, once it is formed close to the anode, hydrogen cations are released, thus enhancing the decrease in pH.

The efficiency of electrocoagulation process is considerably pH dependent as well. A study by Wided et al. (2014) has confirmed the results previously published that mark the highest performance of electrocoagulation in terms of boron removal at pH 8.0. Moreover, it was observed that such pH presents the best conditions for boron removal, regardless of its concentrations (Wided et al., 2014). Moving to more alkaline conditions, the performance of electrocoagulation deteriorates due to the prevalence of $Al(OH)_4^-(aq)$, which is a dissolving form unsuitable for the formation of flocs.

At the same time, the exact knowledge of borate species present in a solution is necessary to achieve the highest efficiency of electrocoagulation process (see Figure 5). When pH exceeds 9.0, borate ions are predominant in the $B(OH)_4^-$ (aq) form. To the contrary, the $B(OH)_3$ form is mostly present in solution under pH conditions below 9.0. The amount of boron removed from the solution was the greatest at pH 8.0, which is closely related to the highest formation of aluminium hydroxide under such pH.

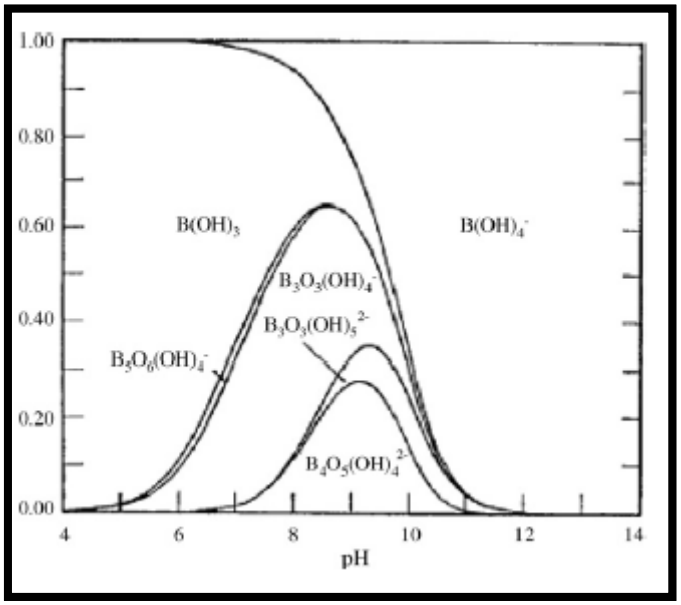

Fig. 5: A graphical illustration showing the speciation of borate ions upon pH in an aqueous solution. Adapted from Yilmaz et al. (2007).

The primary advantages of using electrocoagulation for boron removal include a relatively low cost of operation, high particulate removal efficiency, a compact treatment facility and the possible perspective of total automation (Vasudevan et al., 2012).

7.2.3. Chemical coagulation

The principle of chemical coagulation in terms of boron removal is similar to the mechanism of electrocoagulation – coagulant is added into solution in order to enhance flocculation, thus concentrating boron particles in flocs, which can be subsequently removed from the solution via flotation. Two major steps constitute the process of chemical coagulation. Electrokinetic (or perikinetic) coagulation deals with reduction of the zeta potential by colloids

or ions of opposite charge to a level below the van der Waal´s forces (Yilmaz et al., 2007). Orthokinetic coagulation represents the aggregation of micelles, leading to the formation of clums agglomerating the colloidal particles (Yilmaz et al., 2007).

The zeta potential is also reduced by the decrease in the effective distance of the double layer as well as the particle charge, which is caused by the addition of high-valence cations. The cations neutralise the negative charge on the colloids during the dissolution of a coagulant. This phase is characterised by a significant impact of rapid mixing (Yilmaz et al., 2007). Consequently, microflocs are formed, while the adsorption of hydrogen cations enables them to retain a positive charge in the acid range. A hydrous oxide floc is formed on the surface of colloids as a result of flocculation. Those colloids, which cannot be adsorbed initially, are later removed by enmeshment in the floc (Eckenfelder, unknown date).

The entire mechanism of the chemical coagulation process can be described by the following four stages (according to Yilmaz et al., 2007):

a) Addition of the chemical to the wastewater.

b) Flash (rapid) mixing necessary for homogeneous distribution of the chemical within the wastewater.

c) Slow mixing, which enhance flocculation (creation of the insoluble solid precipitate).

d) Filtration, decanting or settling in order to take away the flocculated immobile particles.

In combination with sedimentation, chemical coagulation is well-known as a reliable technology for the remediation of wastewater containing high concentrations of suspended solids. Research and practical measurements in several studies (Al-Malack et al., 1999; Aguilar et al., 2002; Holt et al., 2002; Al-Mutairi et al., 2004) have proven the suitability of chemical coagulation in terms of reducing the pollution load, generating a sufficient water recovery. Inorganic metal salts, notably aluminium and ferric sulphates as well as chlorides, are the most frequently used as coagulants in remediation of wastewater.

Two key mechanisms explain their mode of action. The first one concerns the charge neutralization of negatively charged colloids by cationic hydrolysis products. The so-called sweep flocculation represents the second mechanism, being composed of an amorphous hydroxide precipitate resulting from the incorporation of impurities (Yilmaz et al., 2007).

The most striking difference between electrocoagulation and chemical coagulation can be seen in terms of their efficiency. A study by Yilmaz et al. (2007) found out that the utilisation of electrocoagulation as the remediation method helped remove 94% of boron from wastewater, whereas chemical coagulation succeeded to remove 24% of boron only. The major reason defining such a contrasting difference is the rapid influence of high current density on the treatment rate, where the applied current is a far better performing mechanism for boron removal. This is also underlined by the fundamental physical separation processes, where settling is the most important removal stage in the case of chemical coagulation; this is considerably outperformed by the effect of high current density in the case of electrocoagulation, explained by the relationship between reaction kinetics and thermodynamic equilibrium in terms of pollutant removal from wastewater (Yilmaz et al., 2007).

7.2.4. Boron retention by fly ash

During the combustion of coal, most of the boron released into the environment because of decomposition of the organic matter is bounded into iron and calcium oxides as well as silicate (mullite) in the newly formed fly ash. Therefore, there exist two phases of boron within fly ash – the mineralogically-bound and the leachable component of boron.

The pH conditions play a crucial role in terms of boron removal by an interaction with fly ash. A number of studies (Cox et al., 1978; James et al., 1982; Hollis et al., 1988; Nathan et al., 1999; Sheps-Pelleg & Cohen, 2001; Jones, 2005) proved that a significant proportion of boron is leached from fly ash under low pH conditions. Moreover, pH has considerable influence upon the overall chemical composition. This is underlined by the leaching of calcium and chlorine into the residual solution under low pH conditions, while magnesium content is unaffected when compared to its proportions in seawater.

A study by Polat et al. (2004) changed the perception of utilising double-distilled water (DDW) for the leaching of boron only as the authors decided to use seawater instead, which leads to a different composition of the resulting effluent. To give a detail account of seawater impact, the authors created a comprehensive mass-balance of the solutes regarding both the leachate from fly ash as well as the solution. The obtained results showed that balance can only be reached by acid extraction from the fly ash; on the contrary, DDW leaching failed to extract the amount of solutes needed to balance the proportions of B, Mg and Ca. Given the confirmed

role of acid extraction for complete removal of boron, it was also found out that dissolution processes take place besides the adsorption ones.

In addition to the balance of ions, the inverse relationships between calcium enrichment and magnesium depletion indicate that the reaction of Mg-rich seawater with Ca-abundant fly ash leads to the precipitation of Mg-hydroxides. Also, this works conversely when the co-precipitation of Mg-hydroxides enhances the dissolution of Ca-oxides, releasing Ca into the solution. Furthermore, it was observed that the ratios of Ca/Mg in acid leachates and CaO/MgO in the bulk ash samples were similar, confirming the hypothesis that the principal mechanism controlling the chemistry of seawater with regards to the interaction with fly ash is dissolution and precipitation of Mg- and Ca-oxides, respectively.

A study by Rhoades et al. (1968) found out that magnesium hydroxide has a sufficient capacity for boron fixation. The dependence of boron removal of pH conditions was related to the suggestion that the hydroxyl groups in the coordination sphere act as bridging ligands between the surface of Al and Fe oxides and the form of adsorbed boron (predominantly $B(OH)_4^-$.The principle of boron co-precipitation and accumulation in magnesium hydroxide was also documented in a study by Petric et al. (1998), where magnesium hydroxide was formed as a precipitate from the reaction of seawater with dolomite lime. Given the determined ratios of MgO in coal and fly ash (according to the study by Polat et al., 2004), it can be assumed that this principle also works for coal and fly ash. The precipitation of magnesium hydroxide is influenced by various factors, including high-pH conditions, release of oxides from fly ash and the supply of Mg from seawater (Polat et al., 2004).

The mechanism of boron co-precipitation with magnesium hydroxide can be explained by the creation of ion-borate species during the reaction of fly ash with seawater. The dominant boron precipitate resulting from the evaporation of seawater is magnesium borate, which is further converted into boracite mineral (Valyashko, 1970; Aksenova et al., 1989).

7.2.5. Ion exchange of boron with basic exchangers

This remediation method works on the principle of Donnan dialysis, which is a process based on the counter-diffusion of two or more ions across an ion exchange membrane, aiming to separate such diffusing ions. Cation exchange membranes have been used predominantly

in various separation processes and experiments; anion exchange membranes are less frequently used (Davis, 2010). The diffusion of ions in opposite directions through the membrane takes place until equilibrium is reached. Given that these membranes are mostly impermeable to anions, equivalent amounts of counter-diffusing ions must be present in this process in order to maintain electroneutrality. In practice, Donnan dialysis is frequently used for pollution control, water softening and deionization of a process stream. The deionization process, also known as neutralization dialysis, combines Donnan dialysis across both anion and cation exchange membranes with hydroxide anions and hydrogen cations for the cations and anions of a salt (Davis, 2010).

The chemistry of aqueous borate solutions is rather complex, consisting of a series of polyborate anionic species in addition to monomeric borates and boric acid, which is subjected to hydration before ionization (Cengeloglu et al., 2002). Boron concentration, temperature and pH influence the creation of various borate groups and their structure. The formation of polynuclear borates is enhanced either by increasing boron concentration or by decreasing temperature.

An experiment conducted by Ayyildiz & Kaya (2004) demonstrated the dependence of boron transport on ionic charges and hydratized radius of ions, concurrently with an increase in the occupied volume. Increasing ionic charges make the transport of boron through membranes far more difficult, this is explained by an increase in charge/radius ratio. The comparison of hydrated radii stated that sulphate ions have the biggest hydratized radius, while HCO_3^- and Cl^- ions have smaller hydratized radius in such descending order. Due to its stronger ionic charge, the transport of sulphate ions was observed to be lower compared to HCO_3^- and Cl^- ions. Furthermore, it was detected that the transport of HCO_3^- ion was faster than Cl^- because of its greater hydratized radius (Ayyildiz & Kaya, 2004).

Furthermore, this study also concentrated on the influence of boron transport by species presented in the receiving phase. In these experiments, such species were the same both in the feed phase and the receiving phase, given the driving force of borate ion instead of other anions. The presence of sulphate ions in the receiving phase was found out to cause the decrease in boron transport. This is caused by the greater ion charge as well as hydratized radius of sulphate ions in comparison with the other ions. The transport of boron is less allowed once the hydratized sulphate ion plugged pores of the membrane. The most efficient boron transport was detected when HCO_3^- ions were present in both the feed phase and the receiving phase, given their lower ions rate compared to Cl^- and SO_4^{2-} ions. This resulted in more frequent

transport of HCO_3^- ions from the receiving phase to the feed phase; to the contrary, borate ions were passed into the receiving phase instead of HCO_3^- ions.

The addition of SO_4^{2-} and HCO_3^- ions to the feed phase, while Cl^- ions passed to the feed phase, led to the transport of borate ions to the receiving phase. However, borate ions were accompanied by SO_4^{2-} and HCO_3^- ions when passing through the membrane (Ayyildiz & Kaya, 2004).

Besides Donnan dialysis, electrolysis represents another mechanism of boron removal via ion exchange. The electrolysis involves the mutual action of cation-exchange membranes and anion-exchange membranes, which are emplaced alternately, being exposed to an external electric field (see Figure 6). Given the perpendicular position of electric field lines with respect to the membrane, both the anions and cations are moving along the field lines in opposite directions (Dydo & Turek, 2012). The movement takes place from the so-called diluate compartment into the concentrate compartment. Cations move across cation exchange membranes, while anions pass through anion exchange membranes. The rates of cations moving across anion exchange membranes as well as anions passing through cation exchange membranes are very small, thus considered negligible in most cases (Dydo & Turek, 2012). The alternative feeding of diluate and concentrate compartment causes the diluate solution to become ion-depleted, while ion-enrichment occurs in concentrate solution as the electrodialysis progresses. The entire process leads to an efficient removal of ionic salts from the diluate. Electric potential gradient represents the principal force for electrodialysis desalination.

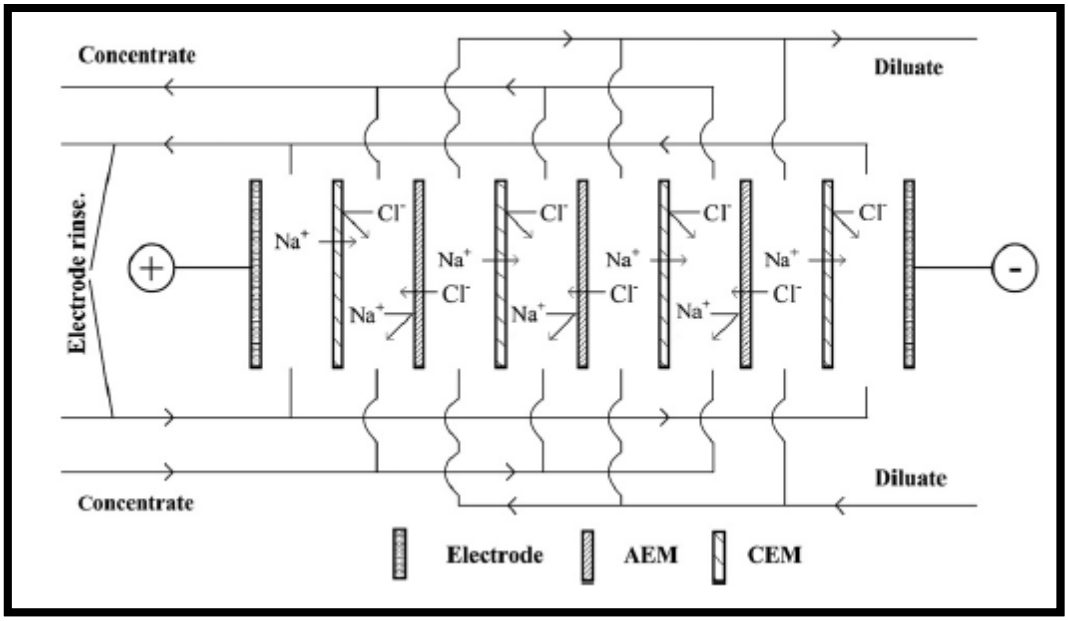

Fig. 6: A scheme illustrating electrodialysis separation of ionic species. Adapted from Dydo & Turek (2012).

7.2.6. Boron-specific resins

The usage of boron-specific resins represents another method for sufficient boron remediation from waters. Recent studies have proven their efficiency in the removal of mononuclear boron species (i.e. boric acid (H_3BO_3) and borate ion ($B(OH)_4^-$), which are mostly found at dissolved boron concentrations lower than 216 mg/l (Sasaki et al., 2013). Such resins are composed of macroporous polystyrene matrices having active N-methyl-glucamine groups. In practice, the presence of two vicinal hydroxyls in the N-methyl-glucamine group enables the formation of a stable complex by the sorption of borates and boric acid on the resin (Kabay et al., 2010; Darwish et al., 2015). The tertiary amine of the N-methyl-glucamine group has a crucial role in terms of neutralization of the proton originated from the formation of tetraborate complex in order to reduce a probable decrease in pH, which could lead to boron liberating hydrolysis (Jacob, 2007; Darwish et al., 2015). Due to its proven efficiency in terms of boron removal, Amberlite IRA 743 resin is one of the most scientifically and commercially used boron-specific resin nowadays with a capacity of 0.7 eq/l (Simonnot et al., 2000; Sasaki et al., 2013). In a study by Kabay et al. (2006), several other boron-specific resins were used for boron remediation from wastewater of geothermal plants, including Diaion CRB 01, Diaion CRB 02,

Purolite SRB (1) and Purolite SRB (2). This investigation underlined the efficiency and appropriate usage of these resins particularly at small-scale water treatment facilities.

Nevertheless, the ion exchange kinetics concerning this remediation technique is highly influenced by diffusion resistance in resin particles. The utilisation of smaller resin particles having larger total surface area in comparison with greater particles of the same mass leads to a decrease in diffusion resistance (Yilmaz-Ipek et al., 2011). An increase in the ion-exchange process rate is achieved by the larger total surface area of fine resin particles (Blahušiak and Schlosser, 2009; Darwish et al., 2015).

8. ARSENIC REMEDIATION METHODS

The mechanism of arsenic remediation from waters strongly depends on chemical composition of As-contaminated water. The oxidation of As(III) into As(V) seems to be crucial for a successful resolution of arsenic contamination, given the fact that As(III) species are reported as the primary source of As contamination from a wide range of case studies.

In general, inorganic species of arsenic are more toxic. Trivalent arsenic, which prevails in reduced redox environment, is more toxic and less stable than pentavalent arsenic (Singh et al., 2015).

Figure 7 shows the distribution of arsenic species under various redox conditions. As can be seen in this Figure, trivalent arsenic species prevail across the full range of pH, having slightly positive (or close to zero) values of oxidation-reduction potential (Eh) under acidic conditions and negative values of Eh under alkaline conditions. Pentavalent arsenic species are predominant under acidic conditions, while showing high values of Eh. Other species of As include hexavalent and heptavalent forms, both occurring exclusively under alkaline conditions in the form of anions. Native arsenic is present across the full range of pH, although in a narrow range of Eh values decreasing from the most acidic to the most alkaline conditions.

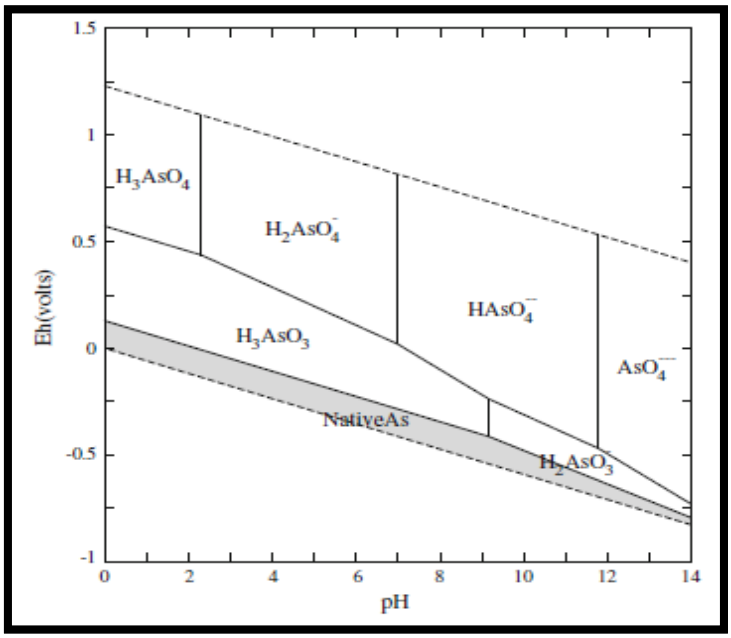

Fig. 7: Eh-pH diagram of arsenic species at 25°C and 1 bar. The sum of arsenic species was set at 10^{-6} M. The area marked in grey represents the occurrence of As solid phase.

Dashed lines (upper and lower) determine the field of stability for arsenic species. Adapted from Lu and Zhu (2011).

The remediation of arsenic from contaminated waters is a complex topic and hundreds of studies have dealt with this issue using a wide range of biological as well as physico-chemical remediation approaches. Their description would go beyond the scope of this thesis. Given the field operation of small water treatment plants based on RO, remediation methods of arsenic related to the application of membrane technology will be comprehensively enlisted further.

8.1. Membrane remediation of arsenic

Correspondingly to the membrane remediation of boron from waters, the application of a membrane capable of preventing arsenic molecules from entering the solution after filtration is the principal mechanism driving this remediation process. The movement of constituents across the membrane is influenced by pressure difference between the two sides of the membrane; furthermore, the movement is also dependent on the concentration of a particular constituent in the feed water, feed water flow rate, temperature and chemical properties of the feed water (for instance dissolved organic carbon, pH, nature of constituents etc.), electrical potential of the membrane and the size of the membrane (US EPA, 2000a).

In general, pressure-driven membrane filtration is divided into the following categories according to the pore size: microfiltration (membrane pore size 0.1-10 μm), ultrafiltration (0.01-0.1 μm), nanofiltration (0.001-0.01 μm) and reverse osmosis (~0.0001 μm). Physical sieving is the principal method for removal of constituents from the feed water in the case of microfiltration and ultrafiltration, while chemical diffusion is the principle by which the particles are removed from the feed water in the case of nanofiltration and reverse osmosis (Brandhuber & Amy, 1998; US EPA, 2000a). Under high pressure conditions (present in nanofiltration and reverse osmosis), the retention of feed water constituents covers a wider range that could not be achieved during microfiltration and ultrafiltration, given both processes operate under low pressure conditions (US EPA, 2000a; Sarkar & Paul, 2016). Therefore, these two techniques are not considered as suitable for remediation of arsenic from the feed water, because their capacity is constrained only to the removal of particulate and colloidal arsenic compounds (Choong et al., 2007).

Within membrane processes, it has been observed that the rejection of arsenic species occurs in the form of adsorption, filtration and electrostatic repulsion. Nevertheless, the size of arsenic species does not necessary lead to their rejection in every case; several observations have confirmed the rejection of arsenic species having smaller size than the membrane pores caused by physical straining (US EPA, 2000a; Sarkar & Paul, 2016).

Given the wide range of physical and chemical conditions at the sites affected by arsenic contamination, numerous solid, liquid and hybrid membranes have been utilised for remediation of arsenic species. For instance, these comprise nanofiltration membranes, microporous ceramic membranes, ion-exchange membranes, hybrid zero-valent iron membranes and hydrogen-based membranes in addition to a variety of liquid membranes. Therefore, it is necessary to consider carefully all the aspects concerning arsenic contamination at a respective site prior to the application of a suitable type of the membrane for successful remediation.

8.1.1. Nanofiltration membranes

Arsenic remediation by nanofiltration membranes is particularly reliable due to its low energy demands, thus being a feasible option for developing countries suffering from power shortages. Aiming to achieve the maximum arsenic contamination level of 10 µg/l (WHO, 2006), the extensive usage of nanofiltration membranes as a means of arsenic removal represents a method compliant with the above-mentioned level thanks to its enhanced recovery and greater selectivity at much lower operating pressure. Moreover, divalent oxyanion $(HAsO_4)^{2-}$ is the predominant form of residual arsenic after water pretreatment, which leads to the assumption that the greater efficiency of arsenic remediation is achieved by negatively charged nanofiltration membranes (Nguyen C.M. et al., 2009). Maintaining constant negative charge on membranes is essential for repelling of oxyanions, which helps to restrict further movement of arsenic species through the filter membrane. This mechanism is known as Donnan exclusion.

The great advantage of nanofiltration membranes is characterized by a considerable retention capacity for both multivalent and monovalent ions, where the efficiency of removal is greater for multivalent ions. When investigating the ion specific capacity of nanofiltration membranes, the most suitable way is the evaluation of separation mechanism and the measurement

of removal efficiency (Nguyen C.M. et al., 2009). The rejection performance is assessed by model individual salts, e.g. NaCl, $CaCl_2$ and Na_2SO_4.

Under aqueous conditions, the bulk diffusivity of a solute depends on its radius and molecular weight (together also known as hydrated radius). During the transport of a solute through a confined pore matrix (being analogous to the one present in nanofiltration membrane), the steric effect at the membrane-bulk interface is thought to cause the rejection of a solute (Nguyen C.M. et al., 2009). In addition, convection through the membrane and steric-hindered diffusion also cause the rejection of a solute (Bowen & Mukhtar, 1996; Bowen et al., 1997). On the other hand, it is necessary to consider the electric interaction of a solute with the charged nanofiltration membrane, because this interaction also influences the mobility of a solute through an electrically charged nanofiltration membrane (Bowen & Mukhtar, 1996; Bowen et al., 1997). Consequently, the most suitable method for the assessment of mobility of a solute through the nanofiltration membrane is rejection of the solute by the nanofiltration membrane.

8.1.2. Porous ceramic membranes

The remediation of arsenic species via porous ceramic membranes is based on adsorption and ultrafiltration processes occurring at very high temperatures, which is of great importance thanks to the inert ceramic character of the membrane. Such high thermal resistance provides significant corrosion resistance (being utilised under extreme conditions), considerable mechanical strength and a prolonged service life (Pagana et al., 2008). Another advantage of this remediation approach is represented by high water fluxes obtained at low operating pressures thanks to the porous character of sharply distributed nanosized pores (Brinker and Sherer, 1990; Pagana et al., 2008).

The structure of ceramic membranes can be described as an asymmetric four-layer system. The first layer has a support function, whereas the third layer represents a microfiltration layer (pore sizes varying between 100 and 200 nm according to the firing temperature). The second layer has a pore size up to 500 nm and in principle bridges the gap between the microfiltration layer and the microporous support (Pagana et al., 2008). The preparation of the fourth layer involves a dip coating technique from colloidal boehmite suspensions of nanoparticle size subjected to synthesis by alkoxide hydrolysis further followed by peptization taking place under acidic conditions (Pagana et al., 2008). The final structure of γ-Al_2O_3 is formed by

the slip-casting procedure and subsequent drying and calcination at 600°C (Kikkinedes et al., 2003; Kikkinedes et al., 2004).

In terms of pentavalent arsenic species removal, the combination of adsorption-ultrafiltration processes in series based on Fe_2O_3 adsorbent nanoparticles (at a concentration of 0.2 wt.%) was reported to be successful in reducing the As(V) concentration from 1 mg/l to 10 μg/l, which meets the requirements for drinking water (Zaspalis et al., 2007).

8.1.3. Ion-exchange membranes

Ion-exchange membranes were utilised for remediation of arsenate species from waters in several studies, primarily thanks to their ease of handling, reuse of anion-exchangers and low cost of operation. The most common ion-exchange media include activated carbons, polymeric resins, biologic materials and mineral oxides (An et al., 2010; Donia et al., 2011; Issa et al., 2011; Urbano et al., 2012; Pessoa-Lopes et al., 2016). However, the remediation process can be complicated by interferences related to the presence of accompanying anions whose concentrations in waters are greater in comparison to arsenic-containing species. For strong base anion exchangers, the following selectivity order has been observed: $SO_4^{2-} > HAsO_4^{2-} > Cl^- > H_2AsO_4^- > HCO_3^- > OH^-$ (US EPA, 2000b; Pessoa-Lopes et al., 2016).

Given the common concentrations of several μg/l for arsenic-containing species in waters, conventional strong ion-exchange resins face difficulties to meet the required limit for As at 10 μg/l due to their strong affinity for sulphate in sulphate-abundant waters (concentrations exceeding 1000 mg/l). This problem can be addressed by a frequent regeneration before reuse, leading to the production of considerable volumes of brines (An et al., 2010; Saha and Sarkar, 2012; Awual et al., 2012; Pessoa-Lopes et al., 2016).

In contrast to the conventional ion exchange treatment via resin saturation, where secondary pollution of the treated water could take place after the breakthrough of target pollutant has occurred, the integration of Donnan dialysis with precipitation of target ionic pollutants involved in an ion-exchange membrane process can lead to their selective removal, thus minimizing the risk of secondary pollution of the treated water. Considerable advantages of this approach include lower energy demands and easy operation, which outweigh the relatively slow kinetics in comparison to electrodialysis; therefore, ion-exchange membrane

processes are suitable for rural applications in developing countries (Oehmen et al., 2011; Pessoa-Lopes et al., 2016).

A study conducted by Velizarov (2013) confirmed the dependence of Donnan dialysis performance on the type of anion-exchange membrane, particularly used under batch operating conditions. Several factors influence the removal of ions by Donnan dialysis, for instance nature and concentration of accompanying ions, pH as well as concentration and composition of the receiving solution (Hichour et al., 1999). When evaluating the efficiency and performance of the ion-exchange process, three receiving solutions (NaCl, Na_2SO_4 and $FeSO_4$) have been tested (Pessoa-Lopes et al., 2016).

8.1.4. Hybrid zero-valent iron membranes

Individual application of zero-valent iron for remediation purposes is based on the adsorption of metal/metalloid ions onto the surface of zero-valent iron that can remove such ions, leading to their elimination from waters. When assessing the efficiency of zero-valent iron remediation processes, the most important properties are large surface area, high in-situ reactivity and extremely small particle size. This mechanism is successful for both As(V) and As(III) removal; the application of zero-valent iron filings (either in-situ or ex-situ) and its reaction with arsenate enables the production and subsequent precipitation of ferrous iron (Lackovic et al., 2000), while arsenite species are subjected to adsorption onto pyrite and/or co-precipitation during their removal from waters (Nguyen V.T. et al., 2009).

The utilisation of nanoscale zero-valent iron particles (10 to 100 nm in size) in remediation processes has been found out useful in terms of enhancing the kinetics of As(III) adsorption process onto the zero-valent iron surface, occurring in minutes under pseudo first order rate expression. In comparison to micron size zero-valent iron, the observed reaction rate constants in this experiment were 1000x greater at 0.07-1.3/min. (Kanel et al., 2005; Nguyen V.T. et al., 2009).

Given the valuable properties of nanoscale zero-valent iron in terms of arsenic remediation combined with high rejection rates for both As(III) and As(V) in membrane remediation, several studies have recently aimed to integrate these techniques into a hybrid technology enhancing the removal of arsenic species from waters. Previously, the addition of nanoparticles of various metals, metal and/or metallic oxides onto the membrane surface had

been reported to increase the efficiency of remediation. For instance, nanoparticles of TiO_2, ZrO_2, Al_2O_3 and silver have been found out to be improving the properties of polysulfone membranes, including greater permeability, higher tensile strength and larger selectivity of certain components while showing decrease in fouling and far better performance across wider temperature and pH range (Davies & Etris, 1997; Elimelech et al., 1997; Mills & Le Hunte, 1997; Bottino et al., 2002; Yan et al., 2006; Ng et al., 2013).

Increased mechanical robustness is the primary advantage stemming from the addition of zero-valent iron onto the polysulfone membrane matrix; this is significantly important in terms of durability of the hybrid remediation system. In a study by Georgiou et al. (2015), this mechanism and setting of the hybrid system enabled the remediation process to be repeated four times with negligible (lower than 1%) decreases in arsenic rejection rates between subsequent steps of the process.

The principle of hybrid zero-valent iron - polysulfone membrane is based on the observation that prevailing As(III) species in natural waters (notably in the $H_3AsO_3(aq)$ form) are adsorbed by neutral surface sites on adsorbing materials (Manning & Goldberg, 1997; Manning et al., 1998; Daikopoulos et al., 2014; Georgiou et al., 2015). Within the hybrid membrane system, polysulfone represents an electron-rich bed (having strong reducing properties) acting as a base for hosting zero-valent iron particles. This setting is considerably important as a precaution against the oxidative attack of oxygen on the zero-valent iron; such attack is the major cause of the formation of a Fe-oxide layer around the zero-valent iron core (Fu et al., 2014; Georgiou et al., 2015).

Another hybrid system used in remediation of arsenic species involves the combination of zero-valent iron with microfiltration or nanofiltration. A study by Nguyen V.T. et al. (2009) proved that the addition of zero-valent iron even at a concentration as low as 0.1 g/l onto the membrane surface significantly increased the amount of As(III) and As(V) reduced. In the case of microfiltration, only 37% of trivalent arsenic and 40% of As(V) were reduced by microfiltration itself, while after the addition of zero-valent iron the newly-formed hybrid system was successful to remove 84% of As(III) and 90% of As(V). When analysing the efficiency of nanofiltration within the same study, the authors observed that nanofiltration alone was able to remove 57% of As(III) and 81% of As(V). Again, the addition of zero-valent iron at a concentration of 0.1 g/l raised the rejection rates to 86% for As(III) and 97% for As(V), respectively.

Such considerable rejection rates for both arsenite and arsenate species can be contributed to several factors. Firstly, the high arsenic adsorption onto the zero-valent iron before the separation of arsenic species by membranes is important for achieving greater rejection rates compared to other remediation methods. Moreover, the removal efficiency is enhanced by the distribution of nanoscale zero-valent iron on the membrane surface, causing retardation in transport of arsenic species across the membrane (Nguyen V.T. et al., 2009).

When comparing the deployment of microfiltration and nanofiltration in the hybrid remediation system, substantial differences in energy demand are observed, where the hybrid microfiltration – zero-valent iron system can operate at a pressure of 10 kPa. Furthermore, the utilisation of microfiltration can generate larger quantities of treated water. Therefore, the operating cost is far greater when using the hybrid nanofiltration – zero-valent iron system (Nguyen V.T. et al., 2009).

8.1.5. Reverse osmosis

Together with nanofiltration, the remediation of arsenic species via reverse osmosis is reported as one of the most successful remediation methods concerning arsenic elimination from waters. Usually, RO requires a substantial amount of energy for its operation, thus being expensive for potential industrial use in developing countries. Trying to address this issue, research has aimed to lessen the energy demand of RO, making it more feasible for broader use in these countries, especially in rural areas with limited or no supply of electricity. For instance, a bicycle passing system has been developed for the transport of fluids across the reverse osmosis and nanofiltration membranes (Oh et al., 2000).

Numerous studies have utilised a wide range of membranes and experimental setups to achieve lower energy demands in the reverse osmosis process (Oh et al., 2000; Kosutic et al., 2005; Saitúa et al., 2005; Uddin et al., 2007; Akin et al., 2011; Fang & Deng, 2014; Chang et al., 2014). In general, the outputs of these studies can be summarized into the following statements (as enlisted in Abejón et al., 2015):

a) a more efficient removal of arsenic is achieved under high pressure, high pH and low temperature

b) the removal of arsenate is reduced with increasing ionic strength

c) the rejection of As(V) is more complete in comparison to As(III), given that As(V) occurs predominantly in an anionic form $(HAsO_4)^{2-}$, while As(III) is largely present in a neutral molecular form (H_3AsO_3) with complicated rejection in waters

d) reverse osmosis does not require a pre-oxidation step concerning the oxidation of arsenite into arsenate in contrast to nanofiltration, where such oxidation is needed to obtain drinking water due to low removal of arsenic

The use of oxidising agents (e.g. chlorine) has been suggested for increasing arsenic rejection rates in waters predominantly containing trivalent arsenic. However, care must be taken when applying this approach as the oxidant could damage the membrane (Abejón et al., 2015). Particular microorganisms can transform the arsenic oxidation state with no addition of an oxidant, thus representing a possible remediation method involving the combination of membrane processes with biooxidation (Shih, 2005).

8.1.6. Liquid membranes and membrane contractors

These remediation techniques for removal of arsenic species represent a relatively new field of research, having been broadly studied during the past decade, although not being used on an industrial scale. The operation of membrane contractors is described by the action of microporous hydrophobic membranes, which form barriers between phases (Marino & Figoli, 2015). Therefore, they enable the one-step removal of volatile compounds as well as water vapour from aqueous solutions with no need to conduct a pre-oxidation step (Bey et al., 2010; Criscouli et al., 2010; Figoli et al., 2011).

In general, the structure of a liquid membrane consists of a thin membrane containing an organic phase dividing two aqueous solutions; the structure is applicable as well in reverse configuration (Marino & Figoli, 2015). Continuously operating membrane systems and liquid-liquid extraction are the principal forces affecting the transport. The solution-diffusion mechanism represents the key principle of mass transfer process across the liquid membrane. During the solution diffusion through the membrane, separation occurs due to the action of electric/chemical gradient. Application of electric impulses and utilisation of chemical compounds and/or specific carriers are essential for improving the selectivity and efficiency of the separation process (Marino & Figoli, 2015).

Based on the configuration model, three types of liquid membrane processes are distinguished: bulk liquid membranes, supported (immobilized) liquid membranes and emulsion liquid membranes (Figoli et al., 2001; Figoli, 2010).

In bulk liquid membranes, a bulk liquid phase separates aqueous (feed) and acceptor phases. These membranes are characterised by a simple design suitable for conducting liquid membrane operations. To the contrary, their most notable disadvantage is small membrane surface, which prevents its wider usage on an industrial scale (Ajwani et al., 2012).

Emulsion liquid membranes are composed of an internal stripping phase (in an aqueous form) stabilised by oil soluble surfactants with dispersed droplets of 1-10 μm in size inside an oil phase (Marino & Figoli, 2015). The water/oil emulsion created is further subjected to dispersion in the form of globules of ca 0.1 – 2 mm in size within another aqueous solution that represents the donor phase. Primary advantages include greater surface area, achieving higher transport rates across the membrane (Marino & Figoli, 2015).

Supported (immobilized) liquid membranes involve the use of a polymeric, ceramic or porous membrane supporting the organic phase, while separating the receptor aqueous solution from the donor phase. The organic / carrier phase fully fills the pores of the solid membrane due to the action of capillarity, forming a heterogeneous solid-liquid membrane with relatively high stability (Marino & Figoli, 2015). Given the occurrence of the solid support, this set-up is well known for its considerable mechanical resistance. Hydrophobic solid membranes boost the rejection of aqueous phases and enhance wetting by the organic solution (Marino & Figoli, 2015). Frequently utilised operational systems within supported (immobilized) liquid membranes include hollow fibres, spiral wound modules and thin flat sheet supports (Kocherginsky & Yang, 2007).

Schematic illustrations of all above-listed liquid membrane configurations are present in Figure 8.

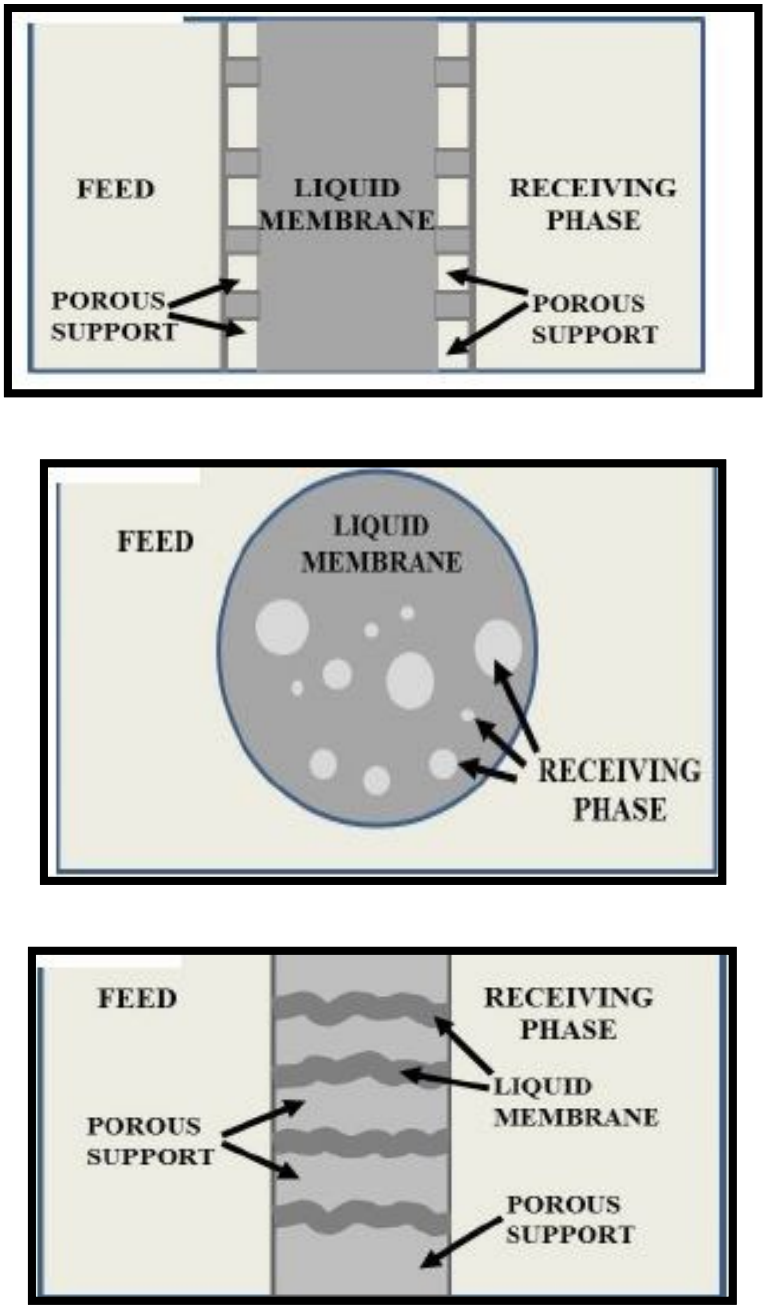

Fig. 8: Schematic illustrations showing the composition of bulk liquid membranes (top), emulsion liquid membranes (centre) and supported (immobilized) liquid membranes (bottom). Adapted from Marino & Figoli (2015).

When assessing the remediation of arsenic species by liquid membranes, one of their most valuable assets is the integration of arsenic ion extraction and stripping processes into a one step, whereas conventional approaches (e.g. solvent extraction) perform ion extraction and stripping in two separate phases. One-step conduction of these processes enables to use

the maximum driving force during the remediation of toxic chemicals, obtaining higher efficiency for arsenic removal as well as better clean-up (Marino & Figoli, 2015). Recently, huge attention has been paid to the development and use of a hydrophobic microporous hollow fibre supported liquid membrane, where organic elements are fixed within the membrane pores that allow diffusion of the target component across the membrane, while it simultaneously prevents the diffusion of other components (Molinari et al., 2009; Zhao et al., 2010; Ahmad et al., 2011).

A hydrophobic microporous hollow fibre supported liquid membrane usually consists of a feed phase, liquid membrane and stripping solution (see Figure 9). In general, the target component is present in the feed phase, from which it is transported across the membrane during diffusion and consequently moved into the stripping phase. The combination of mass transfer across the membrane with a solvent extraction involved in such liquid membrane configuration is particularly useful for remediation of arsenic species, notably for its continuous flow operation and large surface area to volume ratio (Marino & Figoli, 2015).

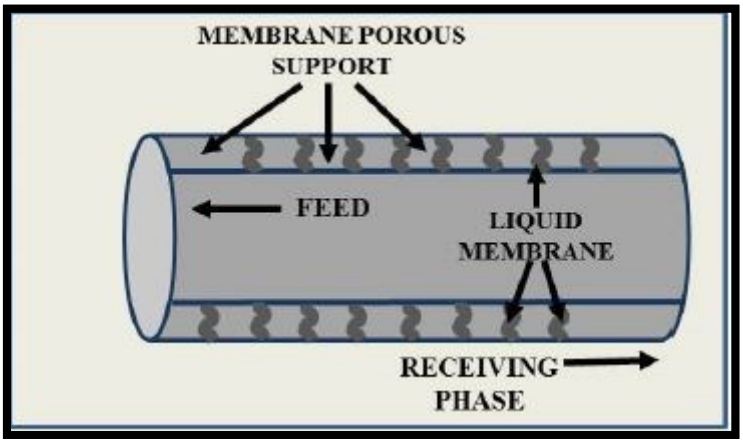

Fig. 9: A schematic illustration of a hydrophobic microporous hollow fibre supported liquid membrane system. Adapted from Marino & Figoli (2015).

8.1.7. Hydrogen-based membranes

This remediation approach for arsenic species is quite unconventional comparing to other remediation methods, which are based on the oxidation of trivalent arsenic into pentavalent arsenic that is consequently subjected to the remediation process. Conversely, the principle of hydrogen-based membranes is the bio-reduction of As(V) into As(III) occurring

on the hydrogen-based membrane biofilm reactor (Chung et al., 2006). The hydrogen-based membrane biofilm reactor represents a configuration suitable for the microbial reduction of oxidised contaminants by hydrogen in a water- or wastewater-treatment setting (Rittmann et al., 2004).

Different electron donors can be applied for the bioremediation of arsenate species. Various studies have utilised organic electron donors such as ethanol, lactate, pyruvate, acetate and butyrate (Oremland et al., 1994; Dowdle et al., 1996, Macy et al., 1996; Blum et al., 1998; Harrington et al., 1998; Stolz & Oremland, 1999; Stolz et al., 1999). Besides hydrogen, sulphide represents another commonly used inorganic electron donor enhancing the bio-reduction process (Hoeft et al., 2004; Liu et al., 2004). The main advantages of hydrogen in terms of supporting the bio-reduction of As(V) into As(III) include its non-toxic nature, no bacterial re-growth and low purchase price (Lee and Rittmann, 2000; Nerenberg et al., 2002; Rittmann et al., 2004).

9. EXPERIMENTAL PART

9.1. General information

All rounds of laboratory experiments were carried out at the headquarters of Photon Water Technology s.r.o., situated on Generála Svobody 25/108, 460 01 Liberec XII – Staré Pavlovice, the Czech Republic. The primary aim of these experiments was to determine the efficiency of a two-step water treatment process consisting of a combination of a reverse osmosis (RO) unit with a commercial product called Katalox Light® produced by WatchWater GmbH from Germany. The efficiency of this setup determined at a laboratory scale is crucial for its potential field application across various sites within the Department of Tacna in southern Peru, in line with the project "Drinking water treatment plants for small and medium-sized municipalities in Peru", having been resolved by Photon Water Technology s.r.o. since 2018.

Primarily, it is necessary to consider the most striking difference between laboratory and natural waters, which includes the variable concentration of arsenic and boron in respective waters as well as occurrence of different cations and anions influencing the overall chemical composition of these waters. In the case of Peruvian waters, boron occurrence is of geogenic origin related to the ongoing volcanic activity within the CVZ of the Andes. According to a comprehensive survey on the quality of waters within the Department of Tacna, which was carried out by the provincial health and epidemiological authorities in 2018, 42 out of 73 investigated sites had arsenic concentrations exceeding both the WHO as well as Peruvian maximum permissible limit of As in drinking water at 10 µg/l, while 28 cases of boron concentrations exceeding the Peruvian maximum permissible of limit of boron in drinking water at 1.5 mg/l were reported. With regards to the maximum permissible limit of boron determined by the World Health Organisation at 0.5 mg/l, additional seven sites had boron concentrations greater than this limit, i.e. 35 out of 73 sites across the Department of Tacna had boron concentrations exceeding the maximum permissible limit according to the WHO guidelines for drinking water. The tap water used for laboratory experiments has no geogenic-related occurrence of arsenic and boron, hence it was necessary to use commercially available arsenic trioxide (As_4O_6) and borax decahydrate ($Na_2B_4O_7 \cdot 10H_2O$) as sources of these elements to be remediated using the proposed technology.

From the already conducted rounds of laboratory testing of arsenic and boron removal efficiency of deployed water treatment plants in Peru since 2018, it is clear that these are capable of remediating arsenic below the maximum permissible limit of arsenic in drinking water set by the WHO at 10 µg/l. This fact has a crucial implications for the local population, which therefore has an access to a safe, arsenic-free supply of drinking water improving its health conditions as well as standard of living. Laboratory tests related to arsenic removal using the proposed technology were carried out within the scope of a project funded by the Czech Development Agency in 2018, prior to the beginning of resolution of this thesis.

In the case of boron, however, the already deployed technology has not been proven to be capable of removing boron neither below the maximum permissible limit determined by the WHO at 0.5 mg/l nor below the maximum permissible limit of 1.5 mg/l stated by the Ministry of Health of Peru (Ministerio de Salud del Perú, 2011). Therefore, the experimental part of this master´s thesis focuses solely on the improvements in boron removal techniques as to comply with both of the aforementioned limits of boron in drinking water.

9.2. Field operation of the technology

Given the remoteness of sites within the Department of Tacna in southern Peru, the operation of the proposed technology aims to be carried out using affordable and durable materials capable of withstanding various adverse factors (low temperatures, dry climate, difficult accessibility, poor engineering networks, minimum stores and/or services available in the area etc.). Preferably, the materials used should be of local provenance in order to minimise the operating costs. Furthermore, the handling of these materials should be easy to understand for the local population and trained personnel as such they should be able to carry out real-time service and necessary repairments concerning the safe and continuous operation of the technology. In terms of more advanced disruptions in operation, PWT experts are ready to provide important knowledge and guidelines as to ensure the continuous provision of drinking water supplies for local communities using this technology. Both the experience and expertise of PWT have proven invaluable since the very beginning of operation of the proposed technology in Peru, particularly in terms of its ecological soundness and flexibility of operation in such difficult circumstances.

In the majority of cases, the water treatment plants currently in operation are located in public places (e.g. schools, health centres and squares), where the water treatment plants are connected to the public electricity grid. Within the Department of Tacna, there are five water treatment plants currently in operation; these are deployed in the municipalities of Candarave, Coracorani, Chipe, Ilabaya and Tarata (see Figure 10).

Fig. 10: A map showing the position of investigated sites within the Department of Tacna in Peru. Adapted from Water for Peru (2020).

At one site, a trial unit has been put into operation where solar panels are deployed as the source of electricity needed for a continuous operation of the proposed technology. In this case, associated on-site construction works had been carried out prior to the start of operation of this unit. Thanks to the local dry weather with infrequent precipitation, solar panels are considered as the best available technology (BAT) supplying enough electricity for operation of the proposed technology, notably at remote sites and in sparsely populated settlements.

9.3. Materials and laboratory setup of the technology

The proposed treatment technology consists of multiple objects deployed in series. Their appropriate installation enables a continuous operation of the technology over time, although permanent supervision is needed as to immediately conduct any necessary actions addressing potential disruptions in operation of the technology. When operating smoothly, the proposed technology represents an affordable option for arsenic and boron removal from waters.

Besides the differences in chemical composition of treated water between the Peruvian waters and the tap water used in laboratory experiments, another major contrast among these two treatment set-ups includes the deployment of a 12V lead-acid battery accumulator instead of solar panels as a source of electricity for operation of the proposed technology. Concerning other parts constituting the setup of the proposed technology, these are present in both versions (i.e. field and laboratory) of the technology and are comprehensively described below. The entire treatment apparatus is depicted in Figure 11.

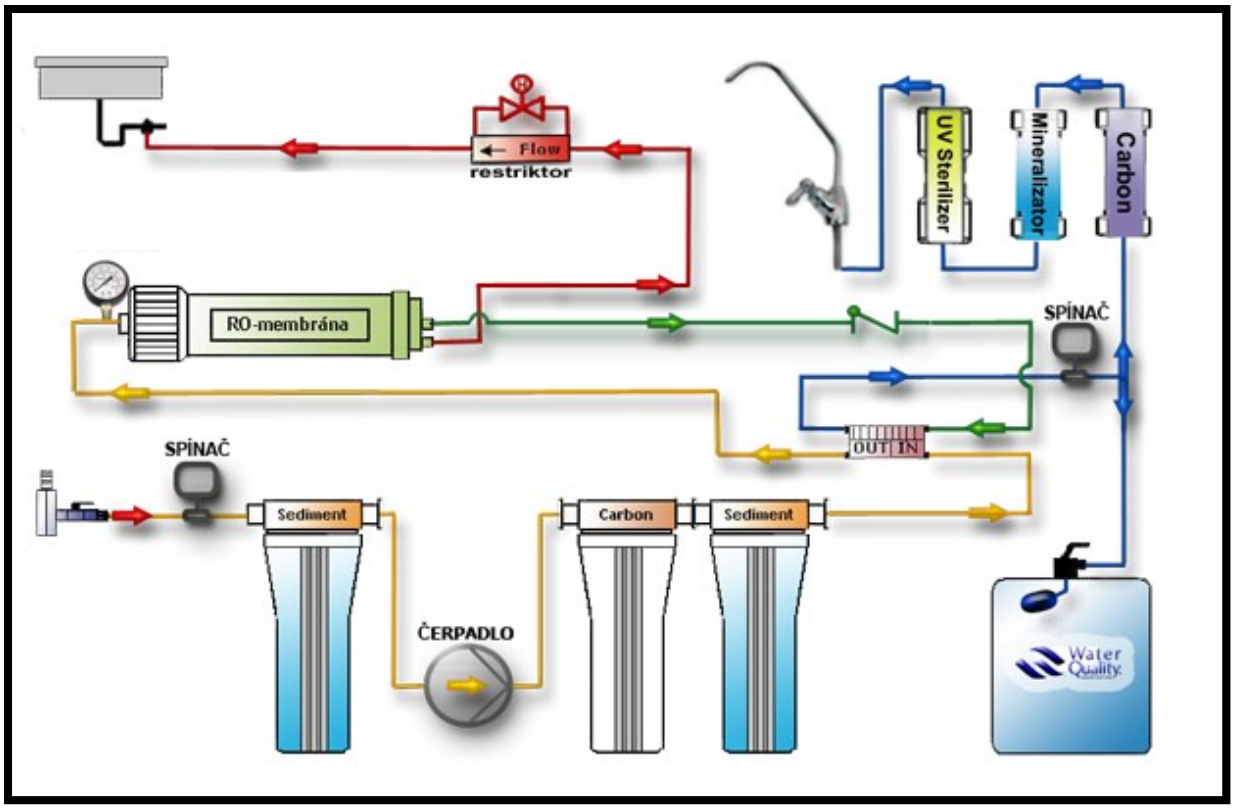

Fig. 11: A schematic illustration of the treatment apparatus used in laboratory experiments. Adapted from Reverzní osmózy (2017).

Before the start of water treatment using the reverse osmosis process, several preparation steps need to be done. At first, the water tank (with a maximum capacity of 1000 litres) is filled with inlet/tap water using a hose. For the determination of an adequate boron concentration in water tank, it is advised to calculate the mass of borax decahydrate (in grams) needed for a particular experiment from the proportion of molecular masses of boron and borax decahydrate multiplied by the volume of water in the water tank. While filling the water tank, the dissolution of borax decahydrate is carried out in multiple steps, each consisting of dissolution of few grams of borax decahydrate in hot tap water (with a temperature of ca 50-60°C) taking place in a bowl. Each dissolution step should last several minutes in order to achieve proper dissolution (i.e. there is no visible borax decahydrate powder afterwards). Once completed, the content is poured into the water tank and the dissolution steps are repeated until the entire calculated mass of dissolved borax decahydrate is poured into the water tank. It is vital to pour the entire content of dissolved borax decahydrate during filling of the water tank as to achieve optimal mixing of the newly formed solution of borax decahydrate in the water tank.

In order to make a representative sample of water to be treated using the proposed technology, it is necessary to add chemical compounds containing desired elements (notably As, B and others if these are not naturally occurring in the tap water) in line with their occurrence in the waters subjected to treatment at various sites in southern Peru. Each of these compounds must be carefully weighted prior to its addition into the resulting solution created in the water tank. The calculation of their concentrations to be added into the water tank solution is derived from the initial concentrations of particular elements/compounds in tap water, laboratory data from the analyses of particular water samples in Peru and their difference (all concentrations are stated in mg/l). Those elements/compounds, where the calculated difference is positive (i.e. the samples of Peruvian waters have a higher concentration of these elements/compounds than the tap water), must be added into the water tank solution using chemicals containing respective elements/compounds in the concentrations calculated according to the above mentioned procedure. It must be noted, however, that the concentrations of nitrate (NO_3^-) and chloride (Cl^-) anions could not be lowered in the water tank solution, given their occurrence in the tap water. The calculation procedure is illustrated in Table 3, where the chemicals to be added into the water tank solution are highlighted in pale red in the bottom part of this table.

Tab. 3: Calculation and concentrations/masses of particular elements/compounds to be added as to achieve a representative water tank solution.

Element/ion	Original concentration[mg/l]	Peruvian concentration [mg/l]	difference in concentrations [mg/l]	difference [mg] per 1000 l	Chemicals
NH_4^+	0,05		-0,05	-50	
Ca	1125	144	-981	-981000	
Cr	0,005		-0,005	-5	
NO_3^-	99,9	4,2	-95,7	-95700	
NO_2^-	0,05		-0,05	-50	
Fe	0,11	0,016	-0,094	-94	
F^-	0,09		-0,09	-90	
PO_4^{3-}	0,05		-0,05	-50	
HCO_3^-	31		-31	-31000	
Cl^-	12,6	0,04	-12,56	-12560	
K	13,9	14,6	0,7	700	
Mg	8,73	29,72	20,99	20990	
Mn	0,008	0,0003	-0,0077	-7,7	
Na	15,3	160	144,7	144700	46,87 g Na_2SO_4
SO_4^{2-}	58,7	366	307,3	307300	207,8 g Na_2SO_4
As		0,0583	0,0583	58,3	76,9 mg As_4O_6
B		5,425	5,425	5425	47,9 g of borax
pH	6,4	7,57			K(OH)
Conductivity	43,6 [mS/m]	133,5 [mS/m]			

Once the water tank is filled, it is necessary to provide the water flow from the tank to the pre-treatment filters using thin polyethylene (PE) hoses/tubing. Given that the water must overcome gravity during this process, the suction from the water tank and subsequent flow is driven by the deployment of a 12V lead-acid battery accumulator operating under the pressure range of 0.7 to 1.1 bar. The optimal pressure range is controlled by a pressure switch. Once the pressure exceeds 1.1 bar, the pressure switch shuts down both the suction of water from the water tank and its flow to the pre-treatment filters, thus effectively halting the entire treatment process. As to preserve functionality as well as longevity of the pressure switch, an expansion module must be added; otherwise the pressure switch would continuously turn on and/or off, respectively.

Before the water is subjected to its treatment on a membrane, it passes through three filters. The first filter contains sediment granules with thickness of 5 µm, the second one is composed of active carbon and the third filter with sediment thickness of 1 µm serves for the most precise purification before the treated water flows to the membrane. However, two major modifications can be determined during the water flow between the second and third filter:

a) direct passage of water from the second to the third filter, i.e. without using Katalox Light® in the treatment process

b) after being treated in the active carbon filter, the treated water flows to the Katalox Light® column for treatment and then it flows to the third filter with pore size 1 μm

Katalox Light® is a commercially available water treatment product manufactured by WatchWater GmbH from Germany. Its usage helps to increase pH of the treated water, which is of significant importance in terms of boron removal on a membrane. For laboratory experiments, a column containing 31 litres of Katalox Light® was utilised from June 2019 to November 2019. The flow profile of this column has an outer annulus of 20 cm and an inner annulus of 3 cm. Commencing late November 2019, a smaller column of Katalox Light® was used (with an identical composition, though the volume of its column is 5 litres instead of 31 litres in the version used previously). The flow profile of this column has an outer annulus of 8 cm and an inner annulus of 2 cm. The filling of Katalox Light® contains >80% of ZEOSORB® substance (this is composed of 100% klinoptilolite, a clay mineral belonging to the group of zeolites), 15% manganese (IV) oxide (MnO_2) acting as a catalyst and 4% calcium oxide (CaO).

Due to its very small atomic size, boron must be complexed into a larger molecule of $B(OH)_4^-$ (aq); this anion is formed under alkaline pH. The speciation of boron species upon pH and oxidation-reduction potential (Eh) is illustrated in Figure 5.

After the water is treated with the 1 μm sediment filter, it passes on the membrane for treatment. Two membranes were utilised in laboratory experiments – Vontron ULP1812-75 GPD (having been used in field operation in Peru since 2018) and KeenSen RO-1812-75 (only in one round of laboratory experiments conducted on March 3, 2020). The outflow from the membrane is then split into permeate and retentate phases, each distinguished by distinct colour of their respective PE hoses/tubing.

In total, three deliver-valves are installed – the first one is emplaced in front of the third filter after the water is subjected to the action of Katalox Light® (i.e. occurring only when Katalox Light® is applied in the treatment process), while the second deliver-valve regulates the permeate flow and the third one controls the retentate flow. In the case of the first

deliver-valve, it is strongly advised to maintain its outflow of water as low as possible so that the maximum possible amount of water is fed onto the membrane.

9.4. Methodology and sample collection

Key physical quantities necessary for comprehensive interpretation of laboratory experiments include electrical conductivity (EC; measured in µS/cm), pH and flow (in ml/min.). In optimal case, after successful boron removal in the reverse osmosis process, the resultant permeate phase (treated water) should have an alkaline pH at ca 9 - 9.5 prior to its remineralisation using calcite and/or dolomite. EC of the permeate phase should be very low (50 µS/cm at maximum), given that all salts present in the treated water are remediated on the membrane. Both pH and EC measurements were carried out using WTW 3430 multimeter with pH probe.

All samples subjected to the laboratory determination of boron removal efficiency were collected into plastic test tube bottles of 50 ml volume; each bottle contained 0.7 ml of 5M nitric acid. Its presence in the bottle is vital for the conservation of a sample; therefore, it is strongly advised not to rinse the test tube bottle prior to sample collection. For a proper interpretation of boron removal efficiencies, the collected samples represented (with labels marked according to respective pH values determined beyond the Katalox Light® column at the time of sample collection):

a) the pre-treated water tank solution prior to its treatment using Katalox Light®

b) the treated water after its passage from the Katalox Light® columns (either with a volume of 5 or 31 litres, respectively)

c) the permeate phase after the completion of RO process

The most suitable assessment of the proposed technology is expressed by its efficiency in boron removal. This efficiency is determined by an accredited laboratory (in this case ALS Czech Republic, s.r.o.) from the percentage difference between boron concentrations in water tank solution and permeate phase, respectively. As to prove the technology applicable in the field, boron concentration in the permeate phase (supply of drinking water) should not exceed 0.5 mg/l of boron (the maximum permissible level set by the WHO) or 1.5 mg/l

(according to the Peruvian legislation regulating the quality of drinking waters set by the Ministry of Health of Peru (Ministerio de Salud del Perú, 2011).

9.5. Types of laboratory experiments/measurements

Multiple rounds of laboratory experiments have been carried out from June 2019 to March 2020. Each round of laboratory testing was carried out under continuous supervision, not only in terms of data collection in pre-determined time steps, but with regards to the immediate resolution of potential disruptions in operation of the technology as well. Within the scope of this thesis, three major categories of laboratory experiments can be classified:

a) testing of the model water tank solution prepared in accordance with composition of the Peruvian waters and its treatment in a two-step procedure involving RO and Katalox Light®

b) testing of the model water tank solution prepared in accordance with composition of the Peruvian waters and its treatment by RO only

c) testing related to the backwash of a column containing Katalox Light® using tap water (not the water tank solution)

In all of the above-mentioned types of laboratory experiments, the retentate phase is drained into a large reservoir situated in the laboratory premises. Therefore, no leakage of boron-enriched wastewater into the municipal sewerage network occurs; wastewater is thus processed fully in accordance with both local and national regulations.

9.6. Results of field operation of the technology

Since the beginning of field operation of five water treatment plants at the aforementioned sites across the Department of Tacna in 2018, a comprehensive laboratory analysis was carried out for each site (Candarave, Coracorani, Chipe, Ilabaya and Tarata), providing a thorough description of quality and properties of local waters. The most crucial parameters for assessment of the technology involve its efficiencies in both arsenic and boron removal (in % of As and B removed, respectively), where the post-treatment

concentrations of As and B should comply with both Peruvian legislation as well as the WHO guidelines for drinking water. The concentrations of As and B both pre- and post-treatment as well as the % efficiency of the technology in As and B removal for each of the five investigated sites are presented in Table 4.

Tab. 4: Pre- and post-treatment concentrations of As and B at investigated sites and % efficiency of the technology in terms of As and B removal.

Site	**Candarave**		**Coracorani**		**Chipe**		**Ilabaya**		**Tarata**	
Elements [mg/l]	Input	Output	Input	Output	Input	Output	Input	Output	Input	Output
As	0.580	<0.010	1.16	<0.010	0.048	<0.010	0.061	<0.010	0.062	<0.010
B	4.91	3.89	3.95	3.57	4.62	3.52	4.63	3.64	0.294	0.269
% As removed		>98%		>99%		>79%		>84%		>93%
% B removed		21%		10%		24%		21%		9%

As seen from Tab. 4, the technology fully meets the required maximum permissible limits (according to both the WHO as well as the Peruvian legislation) for arsenic in drinking water at all five investigated sites (Candarave, Coracorani, Chipe, Ilabaya and Tarata). All five post-treatment (output) concentrations below 0.01 mg/l of As indicate significant viability of this technology for arsenic removal.

The contrasting chemical composition of waters within the five investigated sites does not seem to influence the As removal efficiency. In comparison to Candarave, Chipe and Ilabaya, where the concentration of chlorides is below the detection limit of 0.01 mg/l in all cases, the waters in Coracorani and Tarata have elevated concentrations of chlorides at 119 and 5.72 mg/l, respectively. Furthermore, the concentrations of sulphates, nitrates, bromine, sodium, calcium, sulphur as well as the value of EC are significantly (manifold) lower for the waters in Coracorani and Tarata, pointing out to a lower water buffering capacity of these waters when compared to the waters in Candarave, Chipe and Ilabaya. However, the lower water buffering capacity does not affect the performance of the technology in As removal as well. Neither increased concentrations of total organic carbon (TOC) nor those of dried dissolved solids at 105°C (which indicate weaker dissolution of salts in the waters of Coracorani and Tarata) cause any obstacles in As removal using the proposed technology. Nevertheless, continuous supervision of the field operation at all investigated sites is required in terms of observing any changes in physico-chemical as well as biological properties. In combination with approaching the end of membrane longevity, a significant increase

in concentrations of respective elements and TOC may lead to more rapid membrane fouling and the necessity to replace the membrane as soon as possible in order to preserve efficient As removal using this technology.

According to the results of comprehensive laboratory analyses for each of the five investigated sites, the highest efficiencies of boron removal were documented in Chipe (24%), Candarave and Ilabaya (both 21%). To the contrary, boron removal efficiencies of just 9% and 10% were recorded in Tarata and Coracorani, respectively. Except for Tarata, it must be stressed that none of the post-treatment concentrations of boron in drinking waters are in accordance with neither the WHO guidelines nor the Peruvian legislation for drinking water.

In the case of boron removal, pH values of pre-treatment waters in all five investigated sites range between 7.4–7.8. At this pH range, boron mostly occurs in the form of $[H_3BO_3]^0$ in waters. This form of B is unsuitable to be treated by RO only due to the very small atomic size of boron and no charge of this species. Therefore, boron must be complexed into a more favourable (anionic) form – $B(OH)_4^-(aq)$ - for its more efficient treatment using RO. However, the complexation of boron takes place at pH 9 or greater only. Hence, the deployment of a two-step treatment process consisting of RO with Katalox Light® is necessary.

The actual efficiency of the catalyst in terms of boron removal represents a subject of laboratory experiments within the scope of this thesis. It must be noted that even the manufacturer does not provide a comprehensive analysis on the performance of the catalyst in boron removal from waters with variable chemical composition. Therefore, there does not exist a relevant data set which our results could be compared to.

9.7. Results of laboratory experiments

9.7.1. Experiments using Vontron ULP1812-75 GPD membrane

The first round of laboratory experiments was carried out on June 27 and 28, 2019. After the period of winter inactivity, it was necessary to conduct a thorough backwash of the Katalox Light® column as to get rid of the stagnant water interacting with the filling of the catalyst. Otherwise, this stagnant water would flow into the RO system, affecting results of the treatment process, particularly in terms of pH values of the permeate phase.

The testing of RO with deployed Katalox Light® (a 31-litre column containing 25 litres of filling) after its backwash took place using tap water with a flow ranging between 430-570 ml/min. (an equivalent of 26-34 l/h) for 250 minutes. Inside the column of the catalyst, the filling has a height of 60 cm. The testing commenced at 10:15 with a measurement of reference values for input (tap water) and both permeate and retentate phases (see Table 5).

Tab. 5: Results of reference measurements from the testing of RO with Katalox Light® on June 27, 2019.

Point of measurement	Date	pH	Q [ml/min.]	EC [µS/cm]	P [bar]	Time
INPUT	27/06/2019	6.82		270		10:15
PERMEATE	27/06/2019	11.01	65	550	3.5	10:15
RETENTATE	27/06/2019	11.18	345	1070	3.5	10:15

In total, three measurements were carried out during the testing of RO after Katalox Light® backwash. These were conducted with a considerable time step, given that the short-step measurements would mark the effect of backwash of the catalyst with little distinction, i.e. the resultant pH values would differ minimally between each other. Results of these measurements are presented in Table 6.

Tab. 6: The results of RO testing after Katalox Light® backwash conducted on June 27, 2019.

Point of measurement	Time	pH	Q [ml/min.]	EC [µS/cm]	P [bar]
INPUT	12:15	6.45		270	
	12:30	6.45		250	
	14:25	6.49		270	
PERMEATE	12:15	7.11	69	30	6.5
PERMEATE	12:30	6.88	90	20	6.5
	14:25	6.1	84	30	6.9

Point of measurement	Time	pH	Q [ml/min.]	EC [µS/cm]	P [bar]
RETENTATE	12:15	7.12	360	350	6.5
	12:30	6.74	480	320	6.5
	14:25	6.84	415	330	6.9

The results shown in Tab. 6 prove that after two hours of continuous backwash, the pH values of both permeate and retentate phases drop significantly. However, the rate of lowering of pH values decreases in time, as can be seen from the measurements of permeate and retentate phases at 14:25. Thus, it can be assumed that a very long backwash of the catalyst is not very efficient; this is also supported by a marginal increase in pH values of the retentate phase seen from its measurement at 14:25.

After the backwash of Katalox Light® the previous day, the RO testing with deployed catalyst was carried out on June 28, 2019 using tap water. This testing aimed to prove the efficiency of Katalox Light® in terms of creating alkaline conditions necessary for a proper complexation of boron in the treatment process. The testing took place for 230 minutes, firstly with a time step of 30 minutes, later increased to 50 and 120 minutes, respectively. Results of this testing are provided in Table 7.

Tab. 7: The results of RO testing with deployed Katalox Light® using tap water conducted on June 28, 2019.

Point of measurement	Time	pH	Q [ml/min.]	EC [µS/cm]	P [bar]
INPUT	10:25	7.06		240	
PERMEATE	10:25	9.85	80	10	7.2
	10:55	10.66	88	70	7.2
PERMEATE	11:25	10.88	88	160	7.3
	12:16	10.96	86	180	7.3

Point of measurement	Time	pH	Q [ml/min.]	EC [µS/cm]	P [bar]
	14:15	10.92	86	185	7.4
RETENTATE	10:25	10.14	473	250	7.2
	10:55	10.6	467	345	7.2
	11:25	10.8	480	390	7.3
	12:16	10.84	485	420	7.3
	14:15	10.85	472	465	7.4

The results from Tab. 7 have proven that the catalyst represents an essential option for achieving significantly alkaline conditions necessary for boron complexation in the RO treatment process. Another round of experiments related to Katalox Light® backwash on July 1, 2019 yielded similar results to those in Tab. 7, thus supporting the suitability of the catalyst for further rounds of laboratory experiments with the model water tank solution prepared accordingly to the chemical composition of waters from investigated sites in Peru.

For the first time, the water tank solution was subjected to the designed two-step treatment process (RO + Katalox Light®) on July 4, 2019. The treatment process lasted for 210 minutes and at the end of this process, samples were collected from the input (water tank solution) and both permeate and retentate phases. The accredited laboratory ALS Czech Republic s.r.o. analysed these samples and determined the following concentrations (with +/- 10.0% measurement uncertainty in each case) of boron in respective samples:

- input (water tank solution): c(B) = 5.72 mg/l
- permeate phase: c(B) = 0.632 mg/l
- retentate phase: c(B) = 5.85 mg/l

From the calculation of boron removal efficiency, the combination of RO with Katalox Light® succeeded to remove 89% of boron. This resultant concentration of boron in the permeate phase

can be considered as very promising, satisfying the maximum permissible limit of boron at 1.5 mg/l in the Peruvian legislation for drinking water. Although, it must be noted that the pH values of both permeate and retentate phases were greater than 11, i.e. these are unsatisfactory for drinking water purposes and must be lowered. For this reason, the subsequent rounds of laboratory testing have focused on the possibility of lowering pH values of the permeate phase so that these will be in compliance with the WHO guidelines and the Peruvian legislation for drinking water, both determining the pH range of drinking water at 6.5 – 8.5 (WHO, 2007; Ministerio de Salud del Perú, 2011).

The next round of laboratory testing from October 7, 2019 showed similar observations to the previous measurements from the beginning of July 2019 with the permeate phase having a pH value ranging between 10.65 and 11.0. Therefore, it was decided to carry out a rapid backwash of the Katalox Light® column within the testing on October 9, 2019 under a flow of 400 litres per hour. The results of this backwash testing are illustrated in Figure 12.

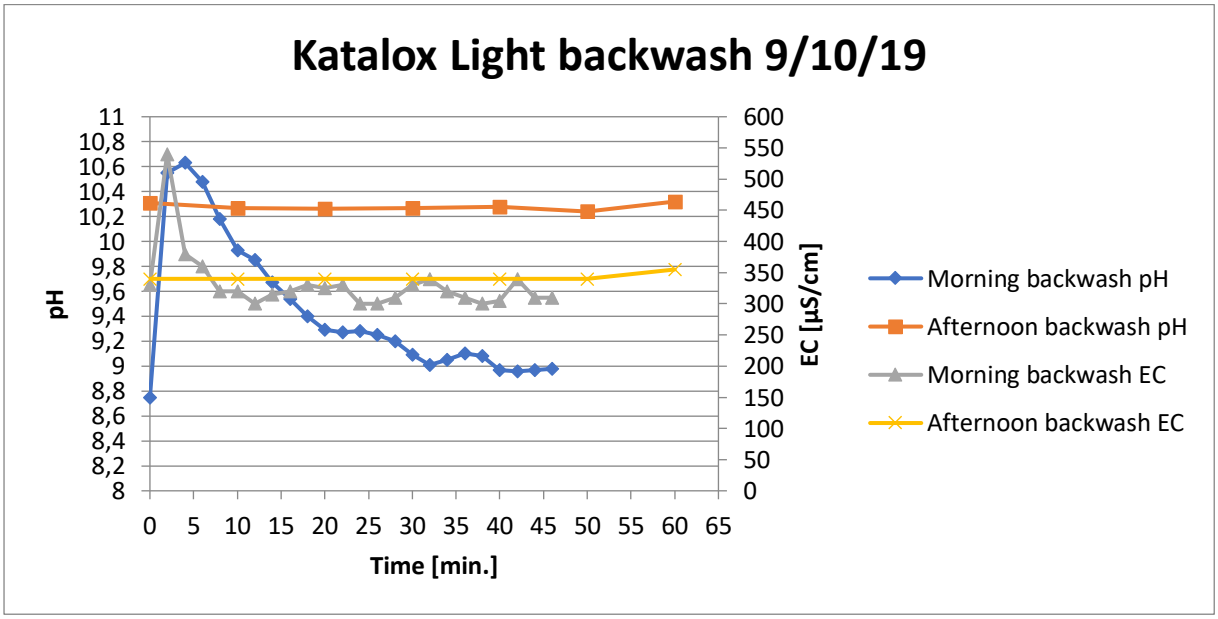

Fig. 12: A graphical illustration of the results of morning and afternoon stages of Katalox Light® backwash.

As can be seen from Fig. 12, the morning stage of Katalox Light® backwash showed a better performance in terms of lowering pH values of the permeate phase. The initial sharp increase in pH values is related to the flow of stagnant water from column of the catalyst. Since the 4th minute, pH values decrease considerably and reach pH 9 by the end of the morning stage

in the 46th minute. Similarly to pH, the values of EC firstly increase sharply, then start to fall and since the 10th minute, they fall within the interval of 320-340 µS/cm, which can be attributed to a measurement deviation/uncertainty of the measurement device.

On the other hand, the afternoon stage of Katalox Light® backwash show almost no change in both pH and EC values. This stage was carried out after the 240 minutes long testing of the RO + Katalox Light® treatment process; the associated results are presented in Figure 13.

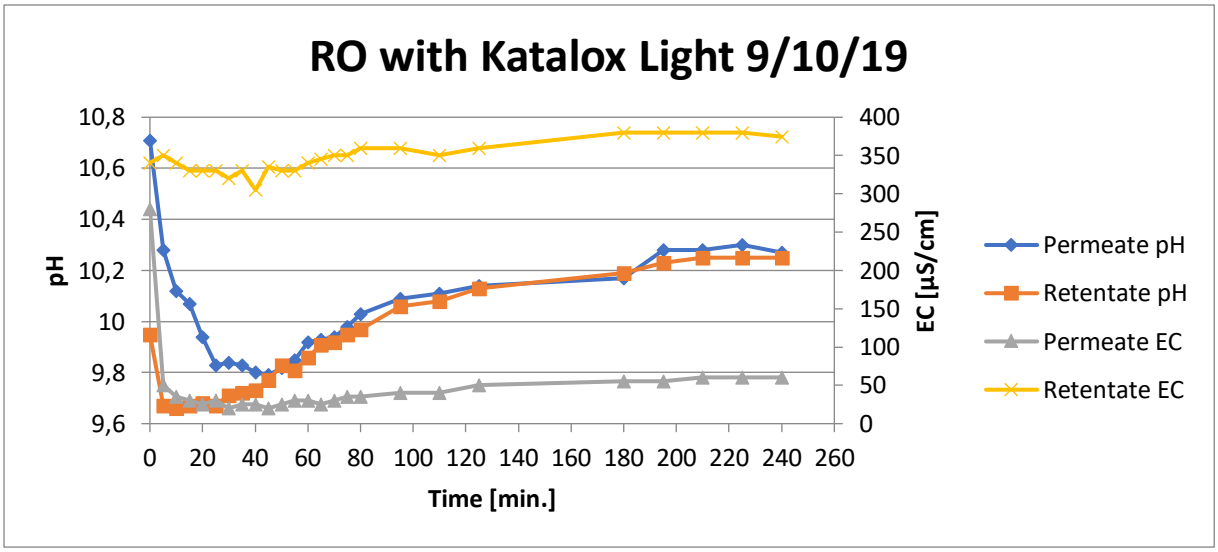

Fig. 13: A graphical illustration showing the results of laboratory testing of RO with Katalox Light® carried out on October 9, 2019.

The results shown in Fig. 13 firstly point out to a slump in both permeate pH and EC as well as retentate pH values, whereas retentate EC is far less influenced at the start of testing. Such a slump in all three quantities may be explained by the preserved effect of rapid backwash of the catalyst. Although, this effect is diminishing in time and from the 45th minute, the pH values of both permeate and retentate phases start to increase again. The values of permeate EC fall sharply at the beginning due to the outflow of stagnant water from the Katalox Light® column and later show a minimal increase only that could be attributed to the measurement deviation/uncertainty of the measurement device.

As an alternative, a one-step treatment process excluding the catalyst was carried out after the afternoon phase of backwash of the catalyst. With a measurement time step of 10 minutes, this test indicated a gradual decrease in pH values of the permeate phase (see Figure 14), though the values were recorded below pH 9.0 that is considered necessary for drinking water.

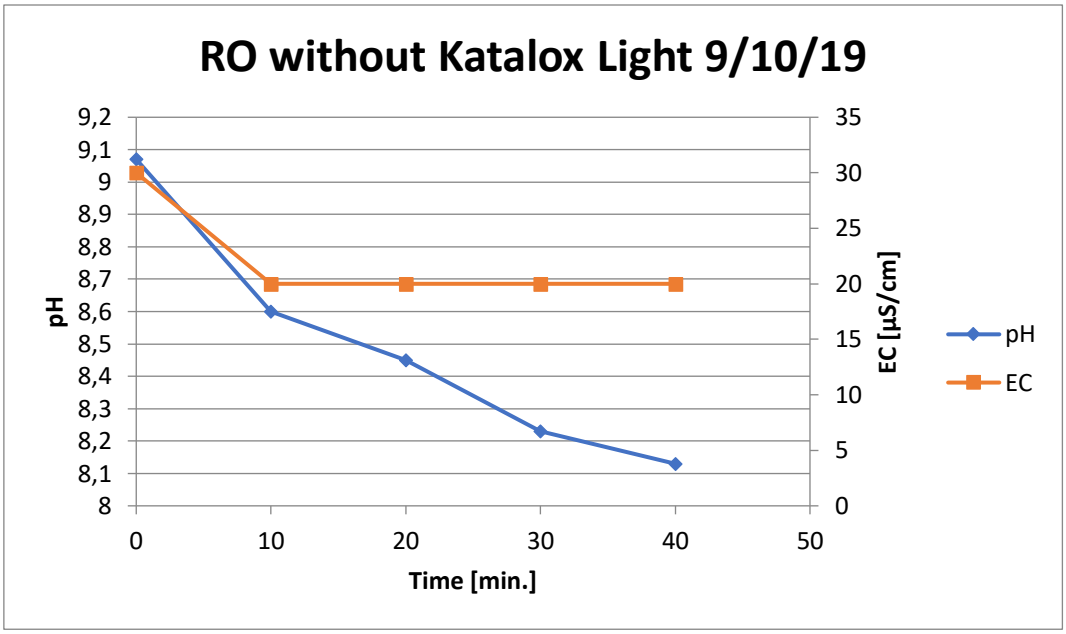

Fig. 14: A graphical illustration showing the results of a one-step treatment process using RO without Katalox Light® on October 9, 2019.

When summarising all the results of laboratory experiments from October 9, 2019, two important conclusions can be drawn:

a) Katalox Light® significantly increases pH of the permeate phase, regardless of the intensity and duration of its backwash

b) the effect of Katalox Light® backwash in the subsequent two-step treatment process combined with RO is very unstable (changing after 45-50 minutes at maximum)

Given that the RO itself could not keep sufficiently alkaline pH (>9) for proper boron complexation and on the other hand, application of the catalyst created highly alkaline conditions (reaching pH 11), it was necessary to come up with a method of preserving sufficient boron complexation and lowering pH of the permeate phase as such it will later be more suitable for drinking purposes when subjected to remineralisation. The choice fell on the purchase of a smaller Katalox Light® column with a filling volume of 5 litres, otherwise having an identical chemical composition to the previously used version of Katalox Light® column. The lower filling volume in this version of the catalyst was considered to be more appropriate for laboratory experiments, particularly in terms of better and faster backwash of its column as well as more moderate formation of alkaline conditions for boron complexation.

The first laboratory testing with deployed smaller column of the catalyst started on November 28, 2019. When operating without any alterations, the filling inside this column has a height of 36 cm. At first, experiments related to its backwash performance were carried out. As expected, the backwash effect occurred faster in the smaller column of Katalox Light® in comparison to its version with a larger column. The influence of the smaller Katalox Light® column backwash on the values of EC and pH is illustrated in Figure 15.

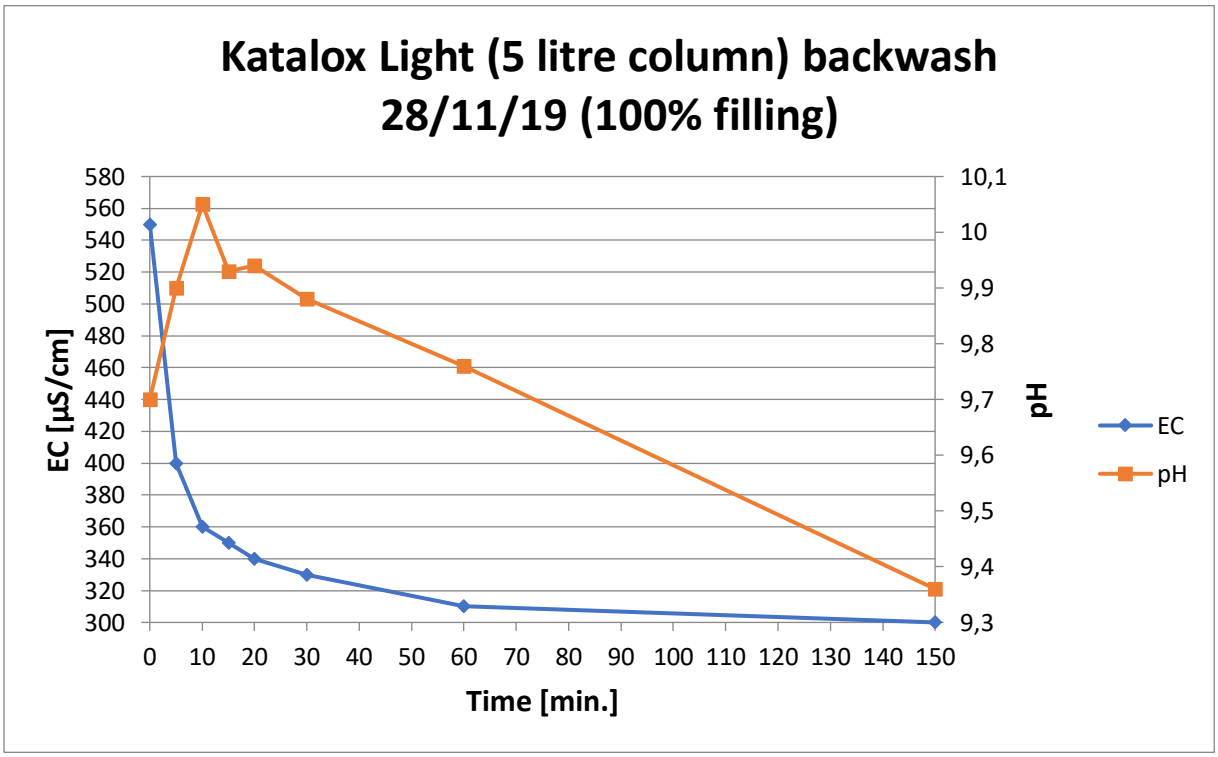

Fig. 15: A graphical illustration showing the influence of Katalox Light® (5 litre column) backwash on the values of EC and pH from the testing on November 28, 2019.

As seen from Fig. 15, the values of EC fell sharply in the very beginning of this testing while exhibiting further, albeit slower decrease of EC values. The values of pH initially rose from 9.7 to 10.0; this increase can be attributed to the initial breakthrough of water into the smaller Katalox Light® column, reflecting greater interaction of water with the filling and coating materials in the smaller column of the catalyst. Since the 25th minute, pH values also exhibit a gradual decrease, reaching values below pH 9.4 at the end of this testing.

Another round of Katalox Light® (5 litre column) backwash was carried out the next day prior to its first combination with RO. This backwash testing indicated similar trends in the values

of EC and pH to those observed the day before, as shown in Figure 16. The initially high values of EC and pH are related to the presence of stagnant water in the smaller Katalox Light® column.

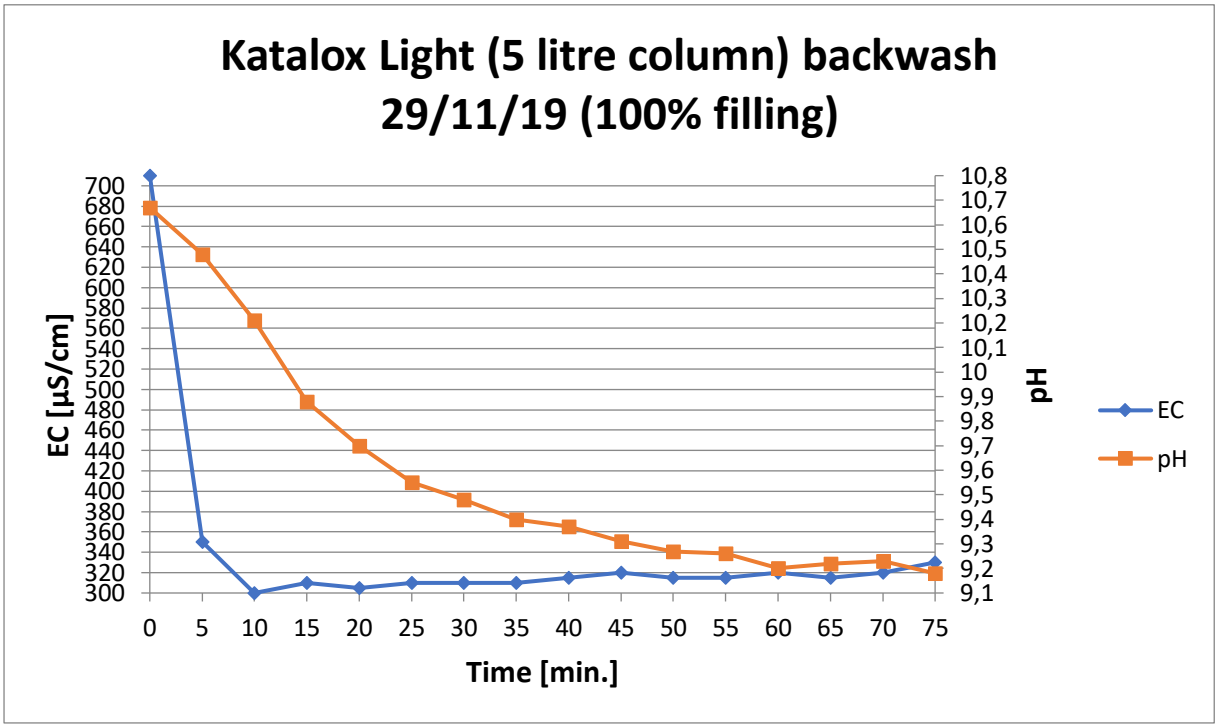

Fig. 16: A graphical illustration showing the influence of Katalox Light® (5 litre column) backwash on the values of EC and pH from the testing on November 29, 2019.

After the completion of this testing, it was decided to remove 2/3 of Katalox Light® (5 litre column) filling and to carry out experiments related to its performance under such modified conditions. In this setup, the filling inside the column has a height of 12 cm. The removal of filling of the catalyst was expected to lower pH, making the permeate phase more suitable for drinking water purposes. Moreover, if this assumption is proven correct, it may lead to a decrease in operation costs of the technology as lower amount of Katalox Light® filling will be needed in the treatment process.

The remaining 1/3 of the original volume of filling was firstly subjected to another backwash testing; its results are presented in Figure 17.

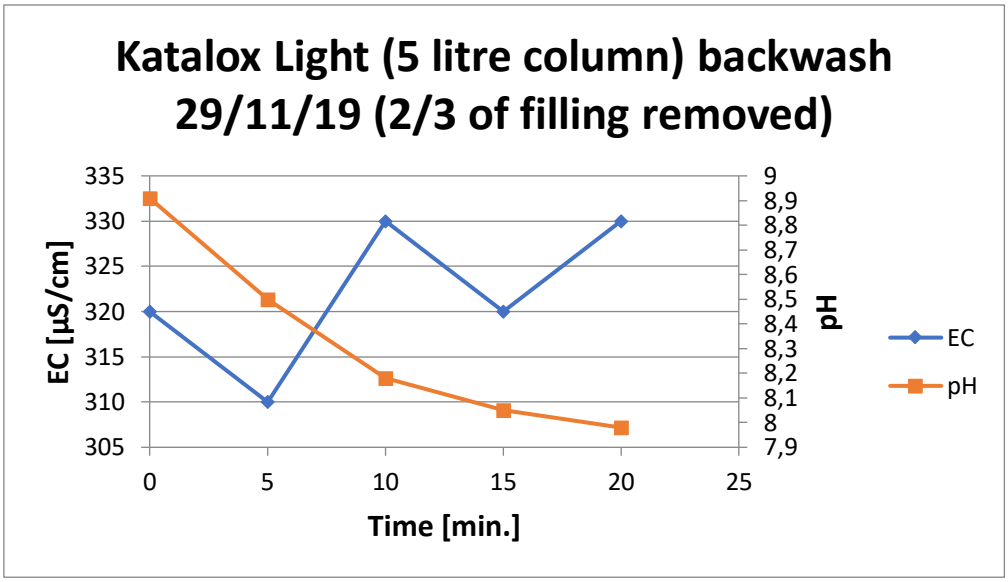

Fig. 17: A graphical illustration showing the influence of Katalox Light® (5 litre column) backwash (with 1/3 of the original volume of filling) on the values of EC and pH.

The results depicted in Fig. 17 show that pH values drop significantly below pH 9.0, progressively decreasing over the duration of testing and reaching values of pH even slightly below 8.0 by the end of the testing. The detected values of EC belong to a narrow interval of 310-330 µS/cm, which can be attributed to a measurement uncertainty of the measurement device.

After the completion of this backwash stage of the catalyst, the testing of RO with Katalox Light® began. As seen from Figure 18, the pH values of both permeate and retentate phases significantly decrease, even below pH 7.0 for the permeate phase. The values of EC for the permeate phase remain almost constant, though an initial increase in EC value of the retentate phase can be observed. It must be noted that such low pH values indicate that Katalox Light® has little to no influence on boron removal in the treatment process.

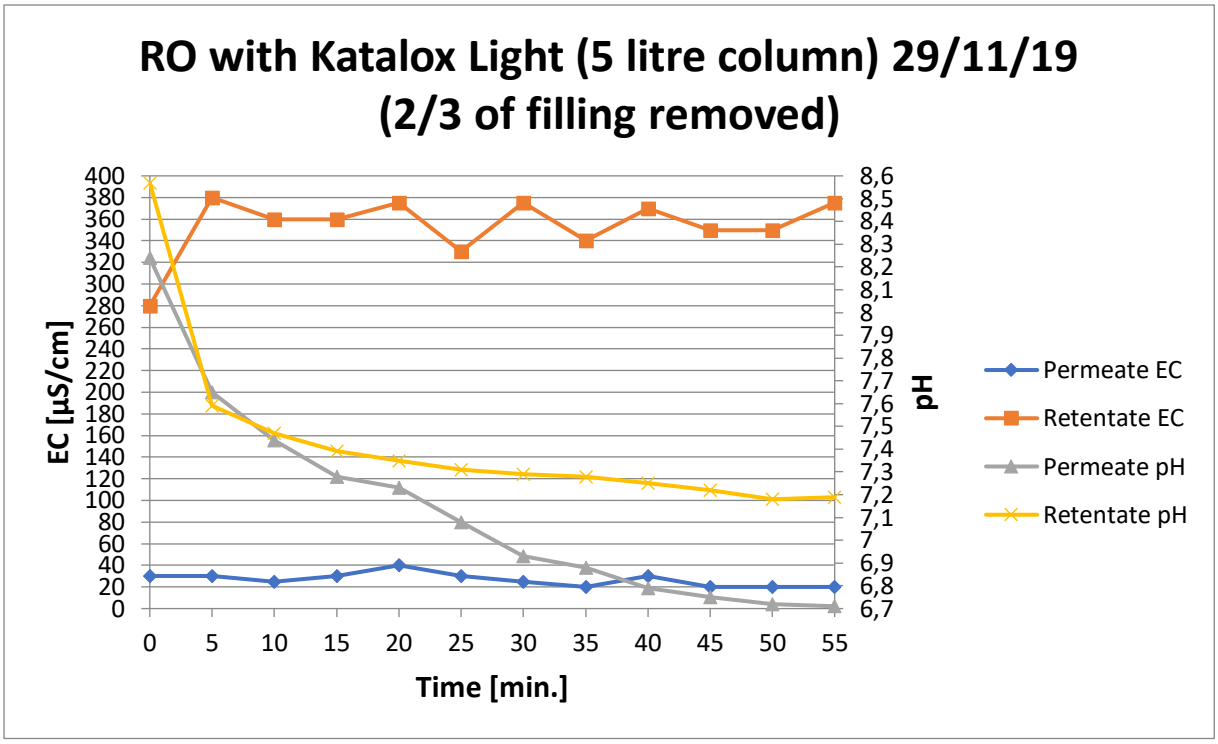

Fig. 18: A graphical illustration showing the results of a two-step treatment process of RO with Katalox Light® (5 litre column) carried out with 1/3 of the original volume of filling.

Before the initiation of another testing of RO with Katalox Light®, the amount of filling was slightly increased, reaching ½ of the original volume of filling with a height of 18 cm. Four points of measurement for this and later rounds of testing were determined. Point 1 was related to the tap water beyond the carbon block filter and before the interaction of water with the Katalox Light® column. Point 2 marked the outflow of water from the column of the catalyst prior to the entrance of water into the filter with 1 µm thick sediment. Points 3 and 4 represented permeate and retentate phases, respectively. For Points 1 and 2, the values of EC and pH were recorded in two measurements towards the end of the testing only; all results are summarised in Figure 19.

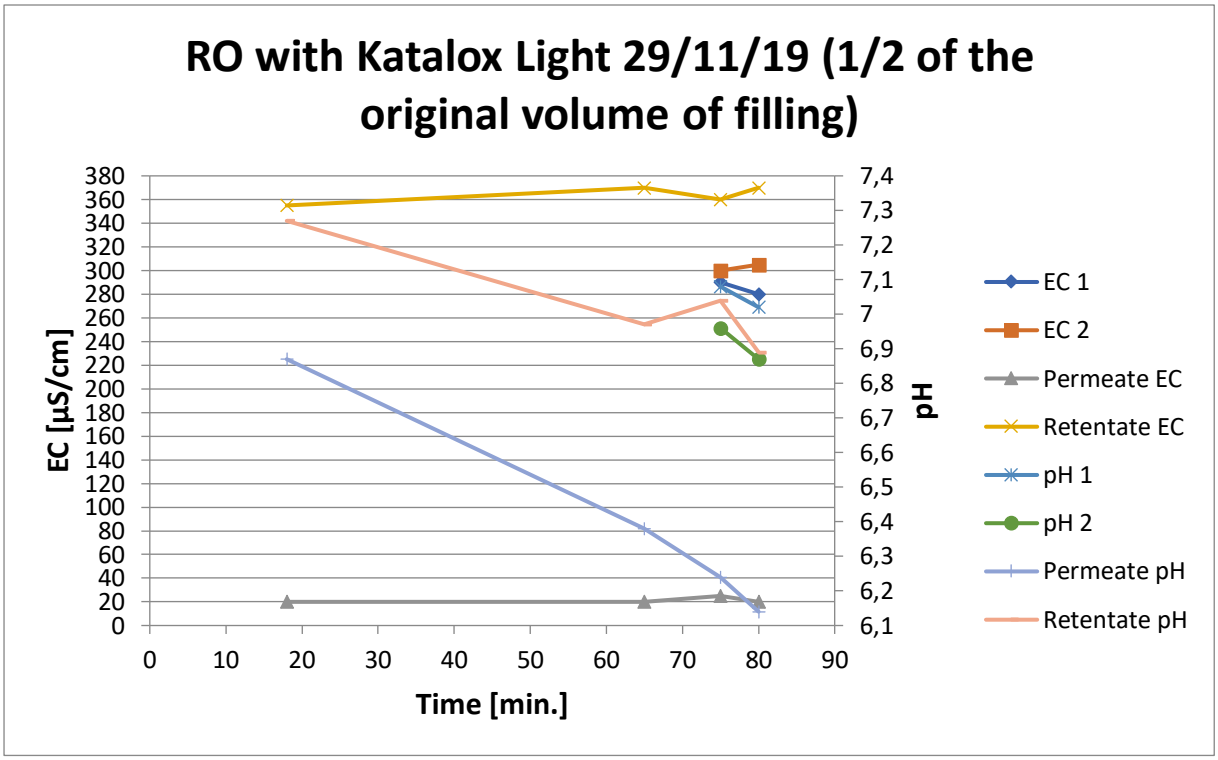

Fig. 19: A graphical illustration showing the results of a two-step treatment process of RO with Katalox Light® (5 litre column) carried out with 1/2 of the original volume of filling.

When comparing the results shown in Figures 18 and 19, the slight increase of volume of Katalox Light® filling did not increase pH closer to the alkaline conditions necessary for proper boron complexation. Therefore, it can be said that the modification of volume of Katalox Light® filling did not confirm the assumptions of achieving similar performance with lower operational costs stated prior to the beginning of these tests.

The next round of laboratory experiments on December 4, 2019 was related to a stress test assessing the performance of our technology in boron removal under excessive boron concentrations (borax decahydrate was weighed into the water tank solution as such its theoretical concentration more than 10 times exceeded the boron concentrations determined in the Peruvian waters). This round of testing took place for several hours and was divided into three sub-stages according to two dilution steps of intake water (further denoted as Dilution 1 and 2, respectively), each carried out in an approximate 1:1 ratio between the volume of water tank solution prior to dilution and the volume of tap water poured into the water tank in each dilution step. During this experiment, samples of input and the permeate phase were collected according to pH values at Point 2 (beyond the Katalox Light® column) of 9.5, 9.2, 9.0 and 8.85.

The values of pH and EC prior to the first dilution step in four points of measurement are presented in Figures 20 and 21, respectively.

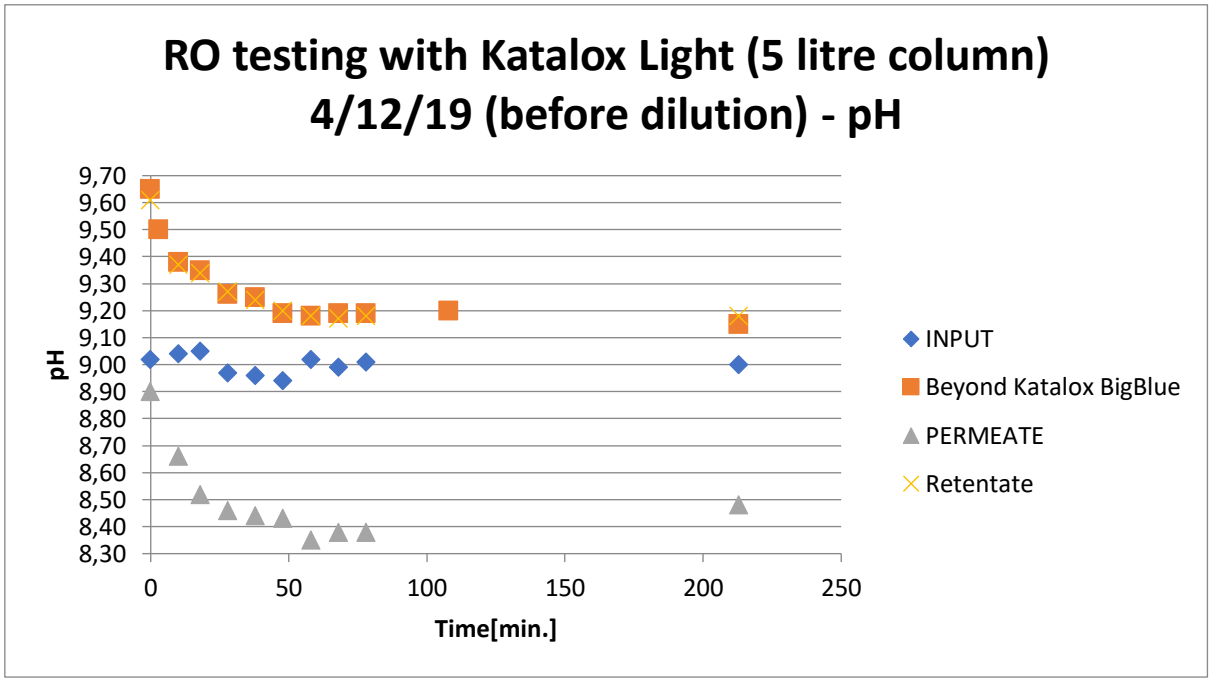

Fig. 20: A graphical illustration showing the values of pH as determined in a two-step treatment process of RO with Katalox Light® (5 litre column) on December 4, 2019.

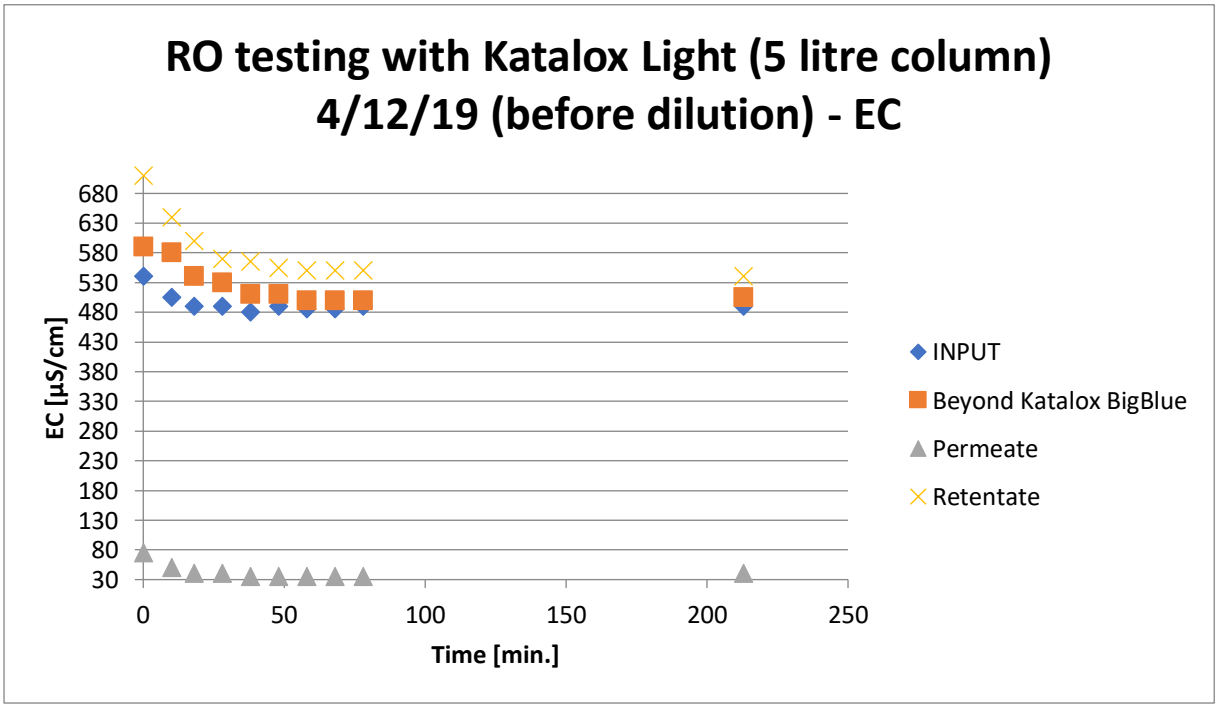

Fig. 21: A graphical illustration showing EC values as determined in a two-step treatment process of RO with Katalox Light® (5 litre column) on December 4, 2019.

Prior to Dilution 1, three samples were collected for the assessment of boron removal efficiency; these included the input at pH 9.5 and the permeate phases at pH values of 9.5 and 9.2, respectively (the pH values were marked according to those detected beyond the Katalox Light® column at Point 2). The boron concentrations in respective samples were found out to be the following according to the laboratory analysis by ALS Czech Republic s.r.o. (with ± 10.0% measurement uncertainty in each case):

- input (water tank solution): c(B) = 59.0 mg/l
- permeate 9.5: c(B) = 29.9 mg/l
- permeate 9.2: c(B) = 29.7 mg/l

From the above-mentioned boron concentrations, the two-step treatment process was successful to remove 49-50% of boron under the pH values of 9.5 and 9.2, respectively. Despite these results surely indicate the viability of this treatment process for boron removal, the boron removal efficiency rates were considered as insufficient for field operation, where these rates should reach more than 80%, but preferentially close to or more than 90% in order to satisfy both the WHO guidelines as well as the Peruvian legislation for drinking water.

Dilution 1 took place after three hours since the beginning of a stress test. This part of testing ran for 65 minutes with a measurement step of 5, later 10 and towards its end 15 minutes, respectively. The effect of Dilution 1 on the values of pH and EC is presented in Figures 22 and 23, respectively.

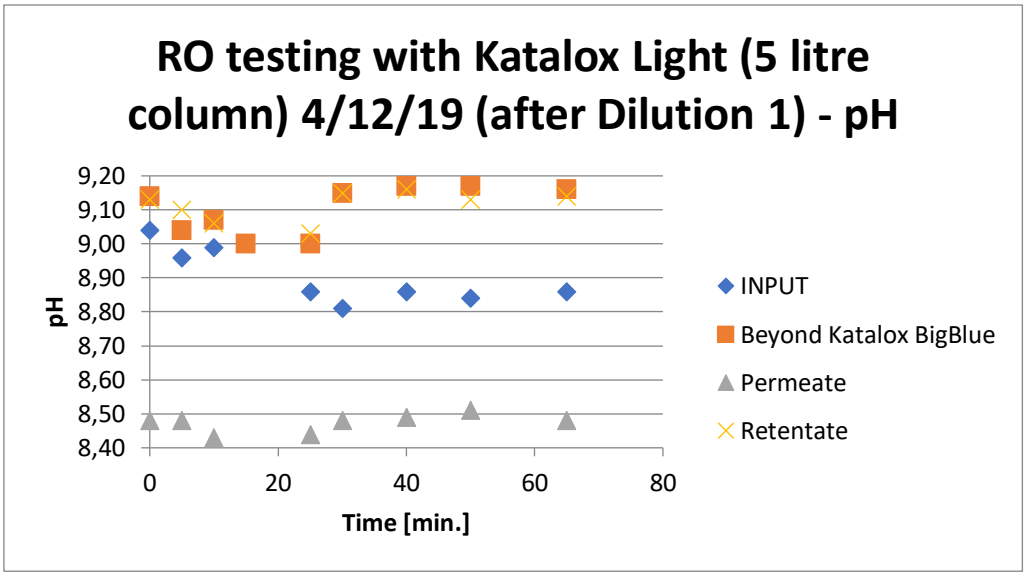

Fig. 22: A graphical illustration showing the values of pH as determined in a two-step treatment process of RO with Katalox Light® (5 litre column; after Dilution 1) conducted on December 4, 2019.

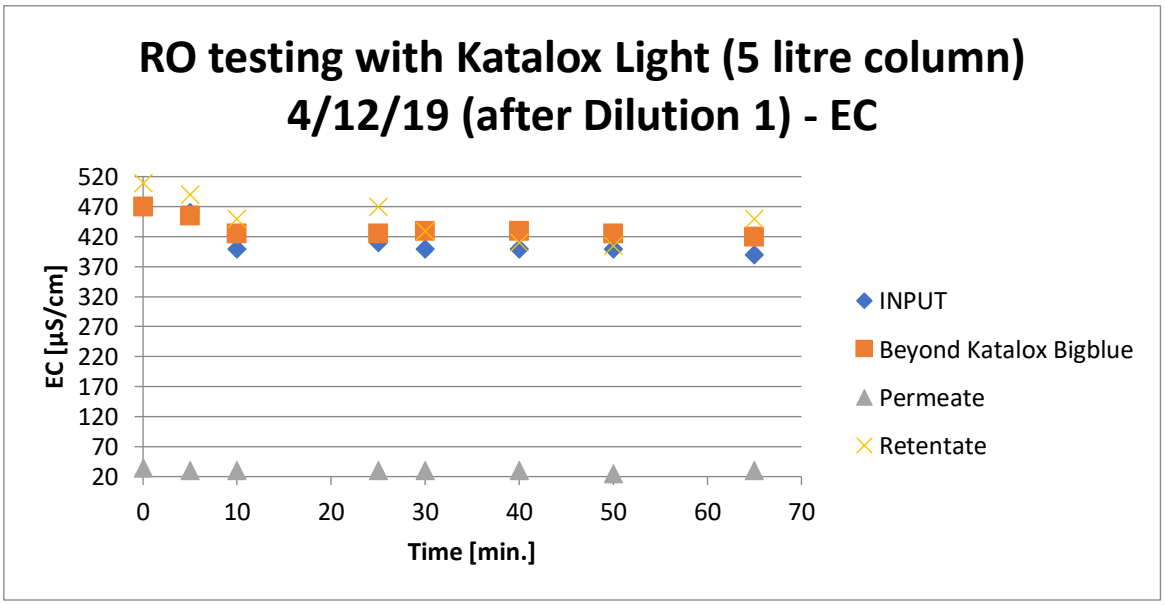

Fig. 23: A graphical illustration showing EC values as determined in a two-step treatment process of RO with Katalox Light® (5 litre column; after Dilution 1) conducted on December 4, 2019.

Two samples were collected for the assessment of boron removal efficiency – input and the permeate phase at pH 9.0. According to the results determined by ALS Czech Republic s.r.o.,

the following boron concentrations were determined as follows (with +/- 10.0% measurement uncertainty in each case):

- input (water tank solution): c(B) = 29.0 mg/l
- permeate 9.0: c(B) = 22.7 mg/l

After Dilution 1, the two-step treatment process of RO with Katalox Light® succeeded to remove 22% of boron. This value of boron removal efficiency highlights a huge slump of boron removal efficiency when just a minor decrease of pH (from 9.2 to 9.0) causes such a significant drop from 49-50% to 22% of removed boron.

Dilution 2 occurred after 270 minutes since the beginning of a stress test, while this last part of testing lasted for 90 minutes with an initial measurement step of 5 minutes, later prolonged to 10 minutes. Figures 24 and 25 show the influence of Dilution 2 on the values of pH and EC.

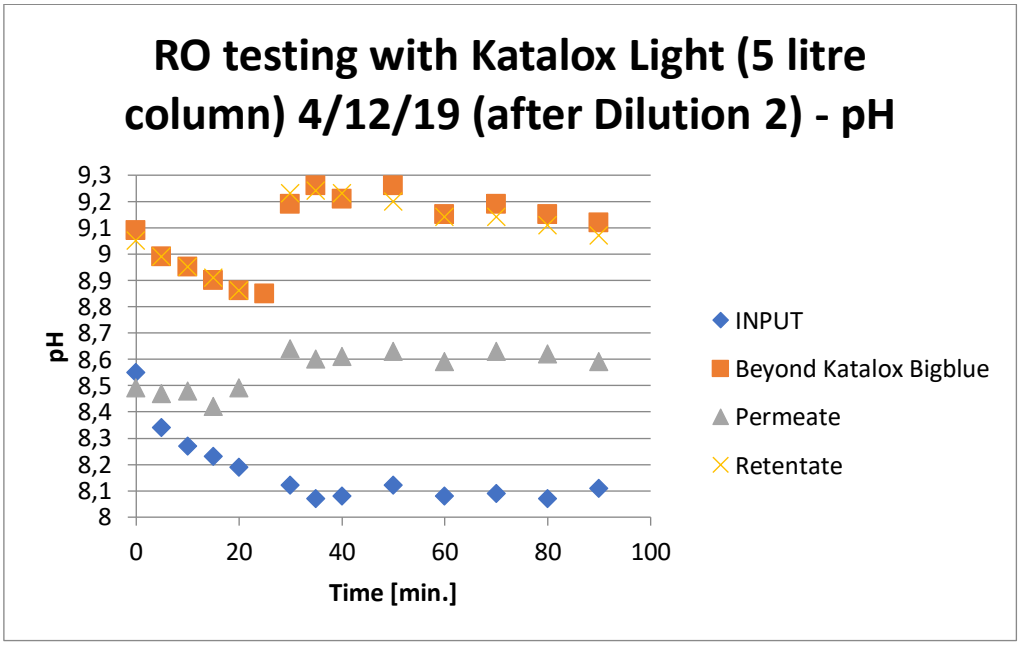

Fig. 24: A graphical illustration showing pH values as determined in a two-step treatment process of RO with Katalox Light® (5 litre column; after Dilution 2) conducted on December 4, 2019.

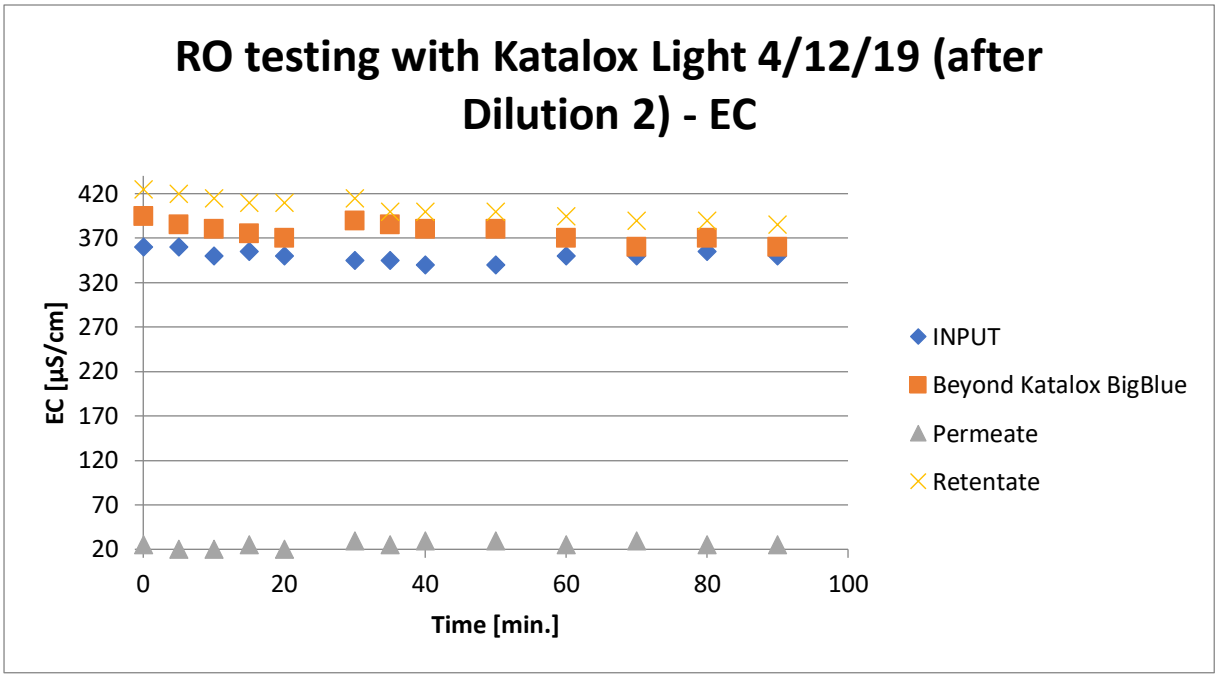

Fig. 25: A graphical illustration showing EC values as determined in a two-step treatment process of RO with Katalox Light® (5 litre column; after Dilution 2) conducted on December 4, 2019.

Two samples were collected for the assessment of boron removal efficiency – input and the permeate phase at pH 8.85. The comprehensive laboratory analysis of boron concentrations by ALS Czech Republic s.r.o. yielded the following concentrations of boron (with +/- 10.0% measurement uncertainty in each case):

- input (water tank solution): c(B) = 13.1 mg/l
- permeate 8.85: c(B) = 11.8 mg/l

According to the calculation of boron removal efficiency at pH 8.85, only 10% of boron was removed. Again, the drop in boron removal efficiency is disproportionally greater (from 22% to 10% in contrast to a marginal decrease in pH (from 9.0 to 8.85). These observations definitely highlight the importance of pH 9.0 as the threshold of proper boron complexation, although it is far more efficient at greater pH values (10-11), as documented by previous rounds of laboratory experiments.

9.7.2. Experiment using KeenSen RO 1812-75 membrane

After the winter break, it was decided to replace the Vontron ULP1812-75 GPD membrane with KeenSen RO 1812-75 membrane. This membrane has similar performance characteristics to the Vontron membrane and therefore, it was selected for laboratory experiments aiming to compare these two membranes when deployed in a two-step treatment process combined with Katalox Light® (5 litre column) carried out on March 3, 2020. Given that the decrease in volume of Katalox Light® filling proved detrimental for the overall boron rejection, this round of testing was conducted using 100% volume of Katalox Light® filling. The experiment lasted for 255 minutes and three samples were collected during its operation – input at pH 9.0 and the permeate phases at pH 9.0 and 8.8, respectively (all pH values stated according to those detected beyond the Katalox Light® column at Point 2 during the measurement). The results of this round of laboratory experiments are visualised in Figure 26.

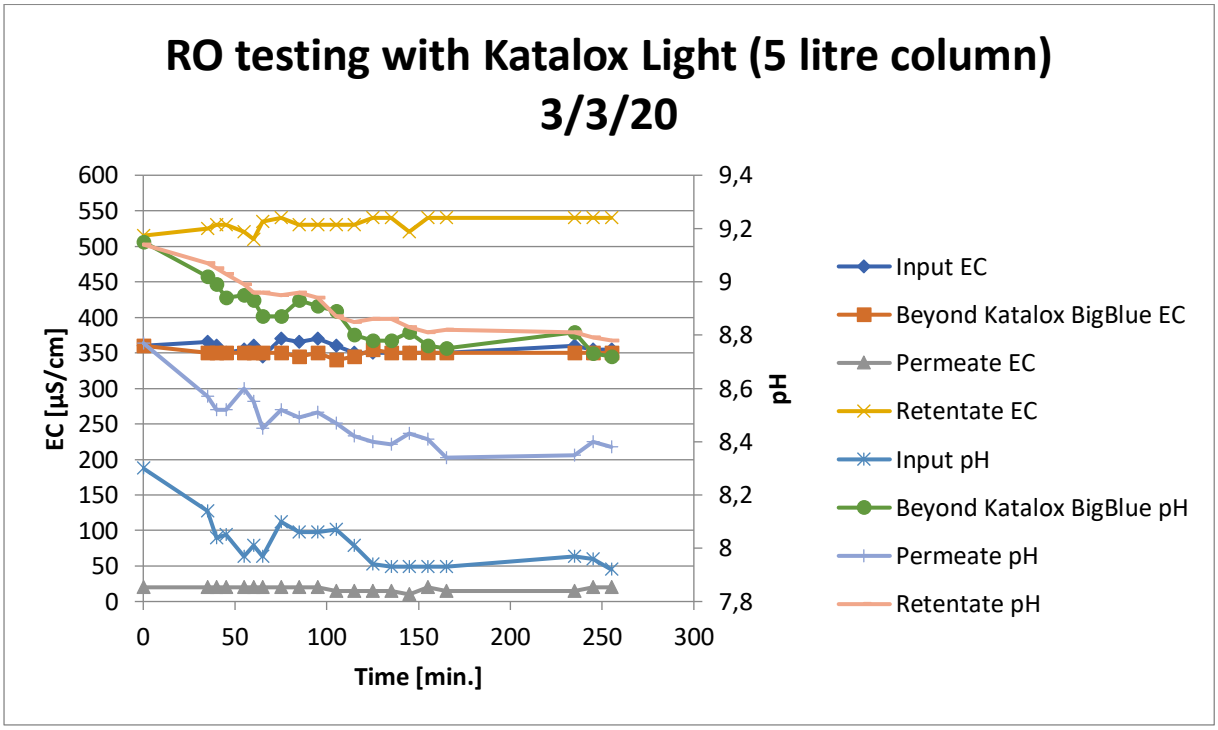

Fig. 26: A graphical illustration showing the results of EC and pH as determined in a two-step treatment process of RO with Katalox Light® (5 litre column) carried out on March 3, 2020.

A comprehensive laboratory analysis conducted by ALS Czech Republic s.r.o. detected the following concentrations of boron in respective samples:

- input (water tank solution): c(B) = 9.44 mg/l
- permeate 9.0: c(B) = 5.17 mg/l
- permeate 8.8: c(B) = 5.82 mg/l

From the calculation of boron rejection rates, 45% of boron was removed at pH 9.0 and just 38% of boron at pH 8.85. Such values of boron rejection rates definitely point out to the importance of keeping pH values at 9.0 or greater for boron complexation and better rejection as even with a minor decrease of pH below 9.0, the boron removal efficiency quickly decreases. Despite the fact that the KeenSen RO 1812-75 membrane achieved better rejection rates compared to the Vontron ULP 1812-75 GPD membrane (45% and 38% vs. 22% and 10% of boron at pH values of 9.0 and 8.85/8.8, respectively), this fact can be attributed to the long-term use of the Vontron membrane and possible degradation of its quality over time. For proper field operation, the boron rejection rates of newly deployed membranes should be far greater (reaching 80 or more %) at such initial concentrations of boron in treated waters.

10. DISCUSSION

The proper operation of a water treatment technology suitable for long-term remediation of arsenic and boron in a remote area like the Department of Tacna in southern Peru faces numerous challenges stemming from the local climatic conditions, poor infrastructure and engineering networks. However, Photon Water Technology s.r.o. was able to overcome these obstacles by proposing an environmentally sound treatment technology consisting of RO combined with Katalox Light®, whose efficiency has been subjected to multiple rounds of laboratory experiments related to the resolution of this master´s thesis. Given the uniqueness of this project and little to no available academic studies covering this issue in southern Peru, there are no relevant data sets which our results could be compared to.

During the field operation of this technology, which started in 2018, it has been observed that the chemical composition of natural waters does not significantly influence the performance of the technology in arsenic removal. Elevated concentrations of chlorides in natural waters of Coracorani and Tarata are related to the geogenic occurrence of salars, which are salt lakes created in an arid environment with very infrequent precipitation. Despite the occurrence of chlorides combined with lack of calcium, sodium and magnesium at these two sites, the technology was able to remove As in accordance with both the WHO guidelines as well as the Peruvian legislation for drinking water to post-treatment concentrations below 0.01 mg/l. Such a huge efficiency in As removal must be regarded as a significant achievement, protecting the health of the local population and greatly improving its standard of living.

In the cases of Candarave, Chipe and Ilabaya, the natural waters at these sites have a high buffering capacity allowing very good removal of As using RO only. Nevertheless, continuous supervision must be carried out at all investigated sites as to immediately react to any adverse changes in concentrations of respective elements and TOC, all of which may cause more rapid membrane fouling that results in shorter longevity of the membrane and the necessity of its replacement sooner than after 1 year of operation stated by the manufacturer.

The deployment of Katalox Light® is necessary for achieving alkaline conditions (greater than pH 9) needed for proper boron complexation into $B(OH)_4^-(aq)$; this species is better removed on the RO membrane. However, preserving the balance between maintaining sufficiently alkaline conditions and the resultant pH of the permeate phase (output drinking water) has been found out to be difficult. In a two-step treatment process with RO, the catalyst with

a filling volume of 31 litres increases the values of pH up to 11, which is too great for drinking water purposes (optimal pH range of drinking waters is determined at 6.5 – 8.5 by the WHO as well as the Peruvian legislation for drinking water). Furthermore, the usage of remineralisation filters at such high pH is more problematic in terms of providing a safe supply of drinking water.

The efficiency of boron removal expressed in post-treatment (permeate phase) concentrations of B [mg/l] is significantly dependent on pH, most notably above/below the pH 9.0, which is the threshold value for proper boron complexation. Two major factors significantly influence the performance of the proposed technology in boron removal; these include the longevity of the membrane currently in operation and boron concentration in untreated (intake) waters. During the course of laboratory experiments performed within the scope of this master´s thesis, a total of 7 samples were analysed for the efficiency in boron removal; the results are presented in Table 8.

Tab. 8: The results of boron removal efficiencies as determined in analysed samples by the ALS Czech Republic s.r.o. accredited laboratory.

Date	input c(B) [mg/l]	c(B) in permeate [mg/l]	pH	Efficiency in B removal (%)
04.07.2019	5,72	0,632	11,05	89
04.12.2019	59	29,9	9,50	49,5
04.12.2019	59	29,7	9,20	49,7
04.12.2019	29	22,7	9,00	22
04.12.2019	13,1	11,8	8,85	10
03.03.2020	9,44	5,17	9,00	45
03.03.2020	9,44	5,82	8,80	38

Table 8 shows that the highest recorded efficiency in boron removal was detected in the measurement on July 4, 2019, when 89% of boron was removed at pH 11.05. Moreover, this particular measurement had the lowest initial (pre-treatment) concentration of boron at 5.72 mg/l. During the stress test performed on December 4, 2019, the influence of pH on the post-treatment (permeate phase) concentrations of boron is clearly visible. Above pH 9.0 (at pH values of 9.5 and 9.2 respectively), the technology was capable of removing approximately 50% of boron. Moving to pH 9.0, the boron removal efficiency fell to 22%, while a further slump to 10% of removed boron was detected at pH 8.85 (a pH value below the threshold of proper boron complexation at pH 9.0). The effect of membrane longevity

is explained in two samples from the testing on March 3, 2020, when a new KeenSen RO 1812-75 membrane was used instead of the previously used Vontron ULP 1812-75 GPD membrane. Despite the initial boron concentration was lower in this case (at 9.44 mg/l instead of 29 and 13.1 mg/l in December 2019, respectively), the new KeenSen RO 1812-75 membrane removed 45% of boron at pH 9.0 and 38% of boron at pH 8.80; these values indicate its better performance at such pH values in comparison to the Vontron ULP 1812-75 GPD membrane previously used in multiple experiments.

Besides the creation of alkaline conditions for proper boron complexation, the importance of Katalox Light® in other aspects of boron removal is debatable. In the Katalox Light® column, ZEOSORB® is arranged in the form of specially processed angular microgranules that are capable of filtering particles with a size of 2-3 μm only thanks to their microporous surface. However, no sorption of boron in the complexed anionic form of $B(OH)_4^-(aq)$ occurs due to the overall negative surface charge of ZEOSORB®. Therefore, it can be assumed that the overall boron rejection rate is related to the performance of RO membrane and the only role of Katalox Light® is represented by the creation of alkaline conditions necessary for proper boron complexation.

11. CONCLUSION

The provision of safe drinking water supplies for humans is of the utmost importance anywhere around the globe and the Department of Tacna in southern Peru is no exception. This region, situated in a remote area with dry and cold climate having infrequent precipitation, is entirely reliant on the natural waters flowing from the Andean Cordillera as the only source of drinking water. Due to the ongoing intensive volcanic activity within the Central Volcanic Zone of the Andes, the natural waters have excessive concentrations of arsenic and boron; these are further exacerbated by the widespread mining activity in the area, which hosts numerous deposits of economically important commodities, most notably gold and copper. The arid mountainous environment hosts tens of salt lakes (salars), where deposits of borates can be found, and boron dissociates into the natural waters upon their contact with surface and/or underground water. During mining operation, the acidic mine waters flow onto the surface, significantly increasing the concentrations of arsenic in surface waters due to the dissolution of arsenopyrite; its occurrence is widespread in the immediate vicinity of gold deposits.

Since 2018, Photon Water Technology s.r.o. has been addressing the issue of improving water quality in five municipalities within the Department of Tacna (Candarave, Coracorani, Chipe, Ilabaya and Tarata). Due to the remoteness of the area, the proposed technology consisting of reverse osmosis with a commercial water treatment product Katalox Light® represents an environmentally sound and affordable option for this area with poor infrastructure and engineering networks. From the already conducted field operation, arsenic concentrations have been successfully lowered at all five investigated sites (Candarave, Coracorani, Chipe, Ilabaya and Tarata) below the maximum permissible limit of 10 µg/l determined by the World Health Organisation and the Peruvian legislation for drinking water. This fact must be regarded as a great achievement in terms of improving the health conditions and living standard of the local population.

In Coracorani and Tarata, the excessive concentrations of chlorides in local waters (related to the occurrence of salars in their vicinity) do not affect the performance of this technology in arsenic removal, though continuous supervision is required as to address any adverse changes (increases) in concentrations of respective elements and TOC. Both of these may lead to more rapid membrane fouling that could significantly decrease the performance of the technology in arsenic and boron removal.

Laboratory experiments have focused on the importance and performance of Katalox Light® commercial water treatment product in terms of boron removal. Prior to each testing of a two-step treatment process involving RO with Katalox Light®, the columns (with a volume of 5 and/or 31 litres, respectively) had to be backwashed in order to get rid of stagnant water inside their columns from the previous tests or to decrease the influence of original column filling on the values of pH and EC in the treatment process. The deployment of Katalox Light® (31 litre column) increased the pH of the permeate phase up to pH 11 and successfully removed 89% of boron in combination with RO using the Vontron ULP 1812-75 GPD membrane. However, such high pH is deemed unsuitable for drinking water purposes and even remineralisation filters (containing calcite or dolomite) face difficulties when used to provide a safe supply of drinking water. Moving to pH values closely above/below pH 9.0 (the threshold of proper boron complexation), the efficiency of boron removal considerably decreases. The measurements carried out by the ALS Czech Republic s.r.o. accredited laboratory found out that at pH 9.5 and 9.2, ca 50% of boron was removed, while only 22% and 10% of boron were removed at pH values of 9.0 and 8.85, respectively. In comparison to the Vontron ULP 1812-75 membrane, the utilisation of a new KeenSen RO 1812-75 membrane improved the boron rejections rates to 45% and 38% at pH values of 9.0 and 8.85, respectively. Those values are, unfortunately, not sufficient for long-term field operation.

When using Katalox Light® (5 litre column) in a two-step treatment process with RO, the boron removal rates were far lower, most notably due to borderline alkaline conditions (oscillating around pH 9) that are necessary for proper boron complexation. Although the removal of Katalox Light® (5 litre column) filling led to the decrease in pH values, they fell significantly below the pH of 9.0 and therefore, it can be assumed that the boron rejection rate in this case was not influenced by the action of Katalox Light® filling.

Other rounds of laboratory testing have been planned; these should have included the increase in water buffering capacity through the addition of calcium salts and/or bicarbonates (HCO_3^-) in order to lower pH values of the permeate phase. Other experiments have aimed to utilise a new water treatment product for the treatment of boron-contaminated waters called Trappsorb® combined with another treatment product Borontrapp®, both of which are manufactured by the same producer of Katalox Light®. Unfortunately, due to the outbreak of the COVID-19 pandemic, these rounds of laboratory experiments could not be conducted within the scope of this master´s thesis.

The research and laboratory experiments conducted within the scope of this master thesis confirm the viability of the proposed technology, especially in arsenic removal, as already documented from the results of field operation in Peru. In terms of boron removal, the proposed technology still was found to have some limitations, particularly in terms of achieving either very high pH (at 11.0), which is not suitable for drinking water purposes and very low boron rejection rates (ranging between 10-50% at pH range of 8.8 to 9.5). Nevertheless, the observations found during multiple rounds of laboratory experiments conducted so far have a key role for the preparation of future tests, which will aim to improve the performance of this technology in boron removal.

12. REFERENCES

Abejón, A., Garea, A. and Irabien, A. (2015). Arsenic removal from drinking water by reverse osmosis: Minimization of costs and energy consumption. *Separation and Purification Technology*, *144*, 46-53.

Aguilar, M.I., Saez, J., Llorens, M., Soler, A. and Ortuno, J.F. (2002). Nutrient removal and sludge production in the coagulation–flocculation process. *Water Res.*, *36*, 2910–2919.

Ahmad, A.L., Kusumastuti, A., Derek, C.J.C. and Ooi, B.S. (2011). Emulsion liquid membrane for heavy metal removal: An overview on emulsion stabilization and destabilization. *Chem. Eng. J., 171*, 870−882.

Aitcheson, S.J., Moorbath, S., Soler, P., Schneider, A., Soria-Escalante, E., Steele, G., Swainbank, I. and Wörner, G. (1995). Pb isotopes define basement domains of the Altiplano, central Andes. *Geology*, Vol. 23, p. 555-558.

Aiuppa, A., Avino, R., Brusca, L., Caliro, S., Chiodini, G., D'Alessandro, W., Favara, R., Federico, C., Ginevra, W., Inguaggiato, S., Longo, M., Pecoraino, G. and Valenza, M. (2006). Mineral control of arsenic content in thermal waters from volcano-hosted hydrothermal systems: insights from island of Ischia and Phlegrean Fields (Campanian Volcanic Province, Italy). *Chemical Geology*, *229*(4), 313-330.

Ajwani, P., Lokwani, L. and Sharma, U. (2012). Bulk Liquid Membrane Transport of Alkali Metal Cations Using Non-Cyclic Ionophores. *Proc. Natl. Acad. Sci., India Section A: Phys. Sci.*, *82*, 91–95.

Akin, I., Arslan, G., Tor, A., Cengeloglu, Y. and Ersoz, M. (2011). Removal of arsenate [As(V)] and arsenite [As(III)] from water by SWHR and BW-30 reverse osmosis. *Desalination*, *281*, 88–92.

Aksenova, T.D., Borisenkov, V.I. and Dorofeyeva, V.A. (1989). Stability of natural magnesium borates in marine brine at various stages of halogenesis. *Geochem. Internat., 26*, 31-39.

Alemán, A. and Ramos, V.A. (2000). Northern Andes. In Tectonic evolution of South America (Cordani, U.G.; Milani, E.J.; Thomaz Filho, A.; Campos, D.A.; editors). *International Geological Congress*, No. 31, p. 453-480. Río de Janeiro.

Allmendinger, R, Jordan, T, Kay, S.M. and Isacks, B. (1997). The evolution of the Altiplano-Puna plateau of the Central Andes. *Annual Reviews on Earth and Planetary Sciences*, Vol. 25, p. 139-174.

Al-Malack, M.H., Abuzaid, N.S. and El-Mubarak, A.H. (1999). Coagulation of polymeric wastewater discharged by a chemical factory. *Water Res.*, *33*, 521–529.

Al-Mutairi, N.Z., Hamoda, M.F. and Al-Ghusain, I. (2004). Coagulant selection and sludge conditioning in a slaughterhouse wastewater treatment plant. *Biores. Technol.*, *95*, 115–119.

An, B., Fu, Z., Xiong, Z., Zhao, D. and SenGupta, A.K. (2010). Synthesis and characterization of a new class of polymeric ligand exchangers for selective removal of arsenate from drinking water. *React. Funct. Polym*., *70*, 497–507.

Arellano-Yanguas, J. (2011). Aggravating the resource curse: decentralisation, mining and conflict in Peru. *The Journal of Development Studies*, *229*(4), 617-638.

Argust, P. (1998). Distribution of boron in the environment. *Biological trace element research*, *66*(1-3), 131-143.

Atencio, C.R., Vilca, J.A., Tejada Vásquez, E.H., Zegarra, R.N. and Zeballos, J.V. (2017). ANALISIS DE SITUACION DE SALUD. Región de Salud Tacna, 113 p.

Awual, M.R., Shenashen, M.A., Yaita, T., Shiwaku, H. and Jyo, A. (2012). Efficient arsenic (V) removal from water by ligand exchange fibrous adsorbent. *Water Res.*, *46*, 5541–5550.

Ayyildiz, H.F. and Kaya, H. (2004). Boron removal by ion exchange membranes. *Desalination*, *180*, 99-108.

Babu, R.R., Bhadrinarayana, N.S., Sheriffa Begum, K.M.M. and Anantharanam N. (2007). Treatment of tannery wastewater by electrocoagulation. *J. Environ. Sci.* (China), *19*(12), 1409-1415.

Bakirdere, S., Orenay, S., & Korkmaz, M. (2010). Effect of boron on human health. *The Open Mineral Processing Journal*, *3*(1).

Banerji, S.K. (1969). Boron adsorption on soils and biological sludges and its effects on endogenous respiration. *Purdue Univ Eng Ext Ser*.

Bansal, I.K. (1980). Boron recovery by reverse osmosis. *Industrial Wastes, 26*(6), 12–31.

Barreiro, B.A.; Clark, A.H. 1984. Lead isotopic evidence for evolutionary changes in magma-crust interaction, central Andes, Southern Perú. *Earth and Planetary Science Letters*, Vol. 69, p. 30-42.

Bebout, G.E., Ryan, J.G., Leeman, W.P. and Bebout, A.E. (1999). Fractionation of trace elements by subduction-zone metamorphism-effect of convergent-margin thermal evolution, *Earth Planet. Sci. Lett., 171*, 63 – 81.

Beck, H.E., Zimmermann, N.E., McVicar, T.R., Vergopolan, N., Berg, A., & Wood, E.F. (2018). Present and future Köppen-Geiger climate classification maps at 1-km resolution. *Scientific Data*, *5*(1). doi: 10.1038/sdata.2018.214

Beck, S., Zandt, G., Myers, S., Wallace, T., Silver, R. and Drake, L. (1996). Crustal-thickness variations in the central Andes. *Geology*, Vol. 24, p. 407-410.

Bedoya, G.T., Chavez, R.R., Lince, M.L., Garcia, E.P. and Zegarra, G.F. (2007). Zonificación Ecológica y Económica – Región Tacna. Estudio Geología y Geomorfología. Gobierno Regional de Tacna, 122 p.

Bey, S., Criscuoli, A., Figoli, A., Leopold, A., Simone, S., Benamor, M. and Drioli, E. (2010). Removal of As(V) by PVDF hollow fibers membrane contactors using Aliquat-336 as extractant. *Desalination*, *264*, 193–200.

Blahušiak, M. and Schlosser, Š. (2009). Simulation of the adsorption—microfiltration process for boron removal from RO permeate. *Desalination*, *241*, 156–166.

Blum, J.S., Bindi, A.B., Buzelli, J., Stolz, J.F. and Oremland, R.S. (1998). Bacillus arsenicosleenatis sp. nov., and Bacillus selenitireducens sp. nov.: two haloalkaliphiles from Mono Lake, California that respire oxyanions of selenium and arsenic. *Arch. Microbiol.*, *171*, 19–30.

Bottino, A., Capannelli, G. and Comite, A. (2002). Preparation and characterization of novel porous PVDF-ZrO_2 composite membranes. *Desalination*, *146*, 35–40.

Bowen, W.R. and Mukhtar, H. (1996). Characterization and prediction of separation performance of nanofiltration membranes. *J. Membr. Sci.*, *112*, 263–274.

Bowen, W.R., Mohammad, A.W. and Hilal, N. (1997). Characterization of nanofiltration membranes for predictive purposes—use of salts, uncharged solutes and atomic force microscopy. *J. Membr. Sci.*, *126*, 91–105.

Brady, J.E. and Humiston, G.E. (1978). *General chemistry: Principles and structure*. New York: John Wiley and Sons.

Brandhuber, P. and Amy, G. (1998). Alternative methods for membrane filtration of arsenic from drinking water. *Desalination*, *117*(1), 1-10.

Brinker, C.J. and Sherer, G.W. (1990). Sol–Gel Science: The Physics and Chemistry of Sol–Gel Processing. Academic Press, New York, 908 p.

Bryjak, M., Wolska, J., Soroko, I. and Kabay, N. (2009). Adsorption-membrane filtration process in boron removal from first stage seawater RO permeate. *Desalination*, *241*, 127–132.

Bundschuh, J., Litter, M. I., Parvez, F., Román-Ross, G., Nicolli, H. B., Jean, J.-S., Liu C.-W., López, D., Armienta, M.A., Guilherme, L.R.G., Cuevas, A. G., Cornejo, L., Cumbal, L. and Toujaguez R. (2012). One century of arsenic exposure in Latin America: a review of history and occurrence from 14 countries. *Science of the Total Environment*, *429*, 2-35.

Cengeloglu, Y., Kir, E. and Ersoz, M. (2002). Removal of fluoride from aqueous solution by using red mud. *Sep. Purif. Technol.*, *28*(1), 81-86.

Chang, F., Liu, W. and Wang, X. (2014). Comparison of polyamide nanofiltration and low pressure reverse osmosis membranes on As(III) rejection under various operational conditions. *Desalination*, *334*, 10–16.

Chen X., Chen, G.C. and Yue, P.L. (2000). Separation of pollutants from restaurant wastewater by electrocoagulation. *Separ. Purif. Technol.*, *19*, 65–76.

Chew, D., Magna, T., Kirkland, C., Miškovič, A., Cardona, A., Schaltegger, U. and Spikings, R. (2008). Detrital zircon fingerprint of the Proto-Andes: Evidences for a Neoproterozoic active margin? *Precambrian Res., 167*, 186–200.

Choong, T.S., Chuah, T.G., Robiah, Y., Koay, F.G. and Azni, I. (2007). Arsenic toxicity, health hazards and removal techniques from water: an overview. *Desalination*, *217*(1), 139-166.

Chung, J., Li, X. and Rittman, B.E. (2006). Bio-reduction of arsenate using a hydrogen-based membrane biofilm reactor. *Chemosphere, 65*, 24-34.

Comstock, D.L. (2009). Method of Treating Reverse Osmosis Membranes for Boron Rejection Enhancement. North Pacific Research, U.S.

Coursey, J.S., Schwab, D.J., Tsai, J.J. and Dragoset, R.A. (2015). *Atomic Weights and Isotopic Compositions (version 4.1.).* National Institute of Standards and Technology, Gaithersburg, MD. Retrieved from https://www.nist.gov/pml/atomic-weights-and-isotopic-compositions-relative-atomic-masses. Accessed on May 6, 2020.

Cox, J.A., Lundquist, G.L., Przyjazny, A. and Schmulbach, C.D. (1978). Leaching of boron from coal ash. *Env. Sci. Technol., 12*, 722-723.

Craw, D., Chappell, D., & Reay, A. (2000). Environmental mercury and arsenic sources in fossil hydrothermal systems, Northland, New Zealand. *Environmental Geology*, *39*(8), 875-887.

Criscuoli, A., Galizia, A. and Drioli, E. (2010). Arsenic Oxidation by Membrane Contactors. In *Water Treatment Technologies for the Removal of High-Toxicity Pollutants*; Springer: Dordrecht, Netherlands; NATO Science for Peace and Security Series C: Environmental Security, pp. 107–118.

Daikopoulos, C., Georgiou, Y., Bourlinos, A., Baikousi, M., Karakassides, M., Zboril, R., Steriotis, T. and Deligiannakis, Y. (2014). Arsenite remediation by an amine-rich graphitic carbon nitride synthesized by a novel low-temperature method. *Chem. Eng. J.*, *256*, 347–355.

Darwish, N.B., Kochkodan, V. and Hilal, N. (2015). Boron removal from water with fractionized Amberlite IRA743 resin. *Desalination*, *370*, 1-6.

Davidson, G.R., & Bassett, R.L. (1993). Application of boron isotopes for identifying contaminants such as fly ash leachate in groundwater. *Environmental science & technology*, *27*(1), 172-176.

Davidson, J., McMillan, N., Moorbath, S., Wörner, G. and López-Escobar, L. (1990). The Nevados de Payachata volcanic region (18°S/69°W, N. Chile) II. Evidence for widespread crustal involvement in Andean magmatism. *Contributions to Mineralogy and Petrology*, Vol. 105, p. 412-432.

Davidson, J.P. and de Silva, S.L. (1995). Late Cenozoic magmatism of the Bolivian Altiplano. *Contributions to Mineralogy and Petrology*, Vol. 119, p. 387-408.

Davidson, J.P., Harmon, R.S. and Wörner, G. (1991). The source of central Andean magmas: some considerations. In Andean Magmatism and Its tectonic Setting (Harmon, R.S.; Rapela, C.W.; editors). *Geological Society of America*, Special Publication, Vol. 265, p. 233-243.

Davies, R.L. and Etris, S.F. (1997). The development and functions of silver in water purification and disease control, *Catal. Today*, *36*, 107–114.

Davis, T.A. (2010). Donnan dialysis. Encyclopedia of Desalination and Water Resources (DESWARE), Vol. 2.

Dean, J.A., ed. (1987). *Lange's handbook of chemistry*. New York: McGraw-Hill.

Diarro Correo (2016). *"Captan extraño fenómeno en medio de las aguas del lago Titicaca (VIDEO)"*. Retrieved from: https://diariocorreo.pe/edicion/puno/captan-extrano-fenomeno-en-medio-de-las-aguas-del-lago-titicaca-video-719071/?ref=dcr. Accessed on February 23, 2020.

Dirección Regional de Salud Tacna (2012). Boletín Estadístico del Programa de Control de la Tuberculosis Oficina de Estadística e Informática.

Dirección Regional de Salud Tacna (2014). Analisis de Situación de Salud Tacna. 110 p.

Donia, A., Atia, A. and Mabrouk, D. (2011). Fast kinetic and efficient removal of As(V) from aqueous solution using anion exchange resins. *J. Hazard. Mater.*, *191*, 1–7.

Dowdle, P.R., Laverman, A.M. and Oremland, R.S. (1996). Bacterial reduction of arsenic(V) to arsenic(III) in anoxic sediments. *Appl. Environ. Microbiol*., *62*, 1664–1669.

Dutré, V., & Vandecasteele, C. (1995). Solidification/stabilisation of arsenic-containing waste: leach tests and behaviour of arsenic in the leachate. *Waste Management*, *15*(1), 55-62.

Dydo, P. and Turek, M. (2012). Boron transport and removal using ion-exchange membranes: A critical review. *Desalination*, *310*, 2-8.

Ellis, A.J. and Mahon, W.A.J. (1977). *Chemistry and Geothermal Systems*. Academic Press, University of Wisconsin – Madison, 392 p.

Evans, C. M., & Sparks, D. L. (1983). On the chemistry and mineralogy of boron in pure and in mixed systems: A review. *Communications in soil science and plant analysis*, *14*(9), 827-846.

European Centre for Ecotoxicology and Toxicology of Chemicals (1995). Reproductive and general toxicology of some inorganic borates and risk assessment for human beings. *Technical Report* 63, pp. 28-30.

Eckenfelder, W.W. (unknown date). Industrial Water Pollution Control. 2nd Edition McGraw-Hill Book Company.

Elimelech, M., Zhu, X., Childress, A.E., and Hong, S. (1997). Role of membrane surface morphology in colloidal fouling of cellulose acetate and composite aromatic polyamide reverse osmosis membranes. *J. Membr. Sci.*, No. 127, 101–109.

Fail, P.A., Chapin, R.E., Price, C.J., & Heindel, J.J. (1998). General, reproductive, developmental, and endocrine toxicity of boronated compounds. *Reproductive toxicology*, *12*(1), 1-18.

Fang, J. and Deng, B. (2014). Rejection and modeling of arsenate by nanofiltration: contributions of convection, diffusion and electromigration to arsenic transport. *J. Membr. Sci*., *453*, 42–51.

Feeley, T.C. and Davidson, J.P. (1994). Petrology of calc-alkaline lavas at Volcán Ollagüe and the origin of compositional diversity at Central Andean stratovolcanoes. *Journal of Petrology*, Vol. 35, p. 1295-1340.

Fernández Prado, J.M., Cáceres, D.M., Díaz, F.V., & Acosta, E.T. (2013). Agua, minería y comunidades campesinas en la región Tacna. *Ciencia & Desarrollo*, *15*, 73-80.

Figoli, A. (2010). Liquid Membrane in Gas Separations. In *Liquid Membranes: Principles and Applications in Chemical Separations and Wastewater Treatment*, Kislik, V.S., Ed.; Elsevier: Burlington, MA, USA; 327–356.

Figoli, A., Criscuoli, A., Hoinkis, J. and Drioli, E. (2011). Arsenic removal by traditional and innovative membrane technologies. In Proceedings of *4th International Conference on Metals and Related Substances in Drinking Water*, Kristianstad, Sweden, 13–15 October 2010; IWA PUBLISHING: London, UK, 2011; p. 129.

Figoli, A., Sager, W.F.C. and Mulder, M.H.V. (2001). Facilitated oxygen transport in liquid membranes: Review and new concepts. *J. Membr. Sci.*, *181*, 97–110.

Flora, S. J. (2015). Arsenic: chemistry, occurrence, and exposure. In *Handbook of arsenic toxicology* (pp. 1-49). Academic Press.

Francis, P.W. and Hawkesworth, C.J. (1994). Late Cenozoic rates of magmatic activity in the Central Andes and their relationships to continental crust formation and thickening. *Journal of the Geological Society of London*, Vol.151, p. 845-854.

Francis, P.W.; Gardeweg, M.; Ramirez, C.F. and Rothery, D.A. (1985). Catastrophic debris avalanche deposit of Socompa volcano, northern Chile. *Geology*, Vol. 13, p. 600-603.

Fu, F., Dionysiou, D.D. and Liu, H. (2014). The use of zero-valent iron for groundwater remediation and wastewater treatment: a review. *J. Hazard. Mater.*, *267*, 194–205.

Gansser, A. (1973). Facts and theories on the Andes. *Journal of the Geological Society of London,* Vol. 129, p. 93-131.

Giese, P., Scheuber, E., Schilling, F., Schmitz, M. and Wigger, P. (1999). Crustal thickening processes in the central Andes and the different natures of the Moho-discontinuity. *Journal of South American Earth Sciences*, Vol. 12, p. 201-220.

Goldberg, S., Forster, H. S., & Heick, E. L. (1993). Boron adsorption mechanisms on oxides, clay minerals, and soils inferred from ionic strength effects. *Soil Science Society of America Journal*, *57*(3), 704-708.

Gupta, U. C., Jame, Y. W., Campbell, C. A., Leyshon, A. J., & Nicholaichuk, W. (1985). Boron toxicity and deficiency: a review. *Canadian Journal of Soil Science*, *65*(3), 381-409.

Gill, J. B. (1981). *Orogenic Andesites and Plate Tectonics*. Springer-Verlag, New York, 390 p.

Garcés, I.M. (2000). Modelización geoquímica de soluciones concentradas: Aplicación al estudio de la evolución de algunos salares tipo chilenos [tesis doctoral]. Zaragoza, España: Universidad de Zaragoza; p. 225.

Garcés, I., & Chong, G. (1993). Minerales de boro de yacimientos chilenos: características, usos, mercados y aplicaciones. *Rev. Innovación*, *6*, 23-36.

Geffen, N., Semiat, R., Eisen, M.S., Balazs, Y., Katz, I. and Dosoretz, C.G. (2006). Boron removal from water by complexation to polyol compounds. *Journal of Membrane Science*, *286*, 45–51.

Georgiou, Y., Dimos, K., Beltsios, K., Karakassides, M.A. and Deligiannakis, Y. (2015). Hybrid [polysulfone–Zero Valent Iron] membranes: Synthesis, characterization and application for As^{III} remediation. *Chemical Engineering Journal*, *281*, 651-660.

Glueckstern, P. and Priel, M. (2003). Optimization of boron removal in old and new SWRO systems. *Desalination*, *156*, 219–228.

Greenlee, L.F., Lawler, D.F., Freeman, B.D., Marrot, B. and Moulin, P. (2009). Reverse osmosis desalination: water sources, technology and today's challenges. *Water Res.*, *43*(9), 2317–2348.

Harrington, J.M., Fendorf, S.E. and Rosenzweig, R.F. (1998). Biotic generation of arsenic(III) in metal(oid)-contaminated freshwater lake sediments. *Environ. Sci. Technol.*, No. 32, 2425–2430.

Hart, D., & Paucar-Caceres, A. (2014). Using Critical Systems Heuristics to Guide Second-Order Critique of Systemic Practice: Exploring the Environmental Impact of Mining Operations in Southern Peru. *Systems Research and Behavioral Science*, *31*(2), 197-214.

Hatcher, J.T., Bower, C.A., & Clark, M. (1967). Adsorption of boron by soils as influenced by hydroxy aluminum and surface area. *Soil Science*, *104*(6), 422-426.

Hawkesworth, C.J., Gallagher, K., Hergt, J.M. and McDermott, F. (1993). Mantle and slab contributions in arc magmas. *Ann. Rev. Earth Planet. Sci.*, *21*, 175 – 204.

Haynes, W.M., Bruno, T., & Lide, J. (2015). Properties of the elements and inorganic compounds. *CRC Handbook of Chemistry and Physics*, *95*, 145-152.

Helvacı, C. (2015). Geological features of Neogene basins hosting borate deposits: An overview of deposits and future forecast. *Turkey, Bull. Min. Res. Exp., 151*, 169- 215.

Helvacı, C. (2017). Borate Deposits: An overview and future forecast with regard to mineral deposits. *Bor Dergisi*, *2*(2), 59-70.

Hichour, M., Persin, F., Molénat, J., Sandeaux, J. and Gavach, C. (1999). Fluoride removal from diluted solutions by Donnan dialysis with anion-exchange membranes. *Desalination*, No. 122, 53–62.

Hickey-Vargas, R., Moreno, H., López Escobar, L. and Frey, F. (1989). Geochemical variations in Andean basaltic and silicic lavas from the Villarrica-Lanín volcanic chain (39.5°S): an evaluation of source heterogeneity, fractional crystallization and crustal assimilation. *Contributions to Mineralogy and Petrology*, Vol. 103, p. 361-386.

Hickey-Vargas, R., Sun, M., López-Escobar, L., Moreno, H., Reagan, M.K., Morris, J.D. and Ryan, J.G. (2002). Multiple subduction components in the mantle wedge: evidence from eruptive centers in the Central Southern volcanic zone, Chile. *Geology*, Vol. 30, p. 199-202.

Hickey-Vargas, R.L., Frey, F.A., Gerlach, D.C. and López-Escobar, L. (1986). Multiple sources for basaltic arc rocks from the Southern Volcanic Zone of the Andes (34°-41°S): Trace element and isotopic evidence for contributions from subducted oceanic crust, mantle and continental crust. *Journal Geophysical Research,* Vol. 91, No. 6, p. 5963-5983.

Hirano, S., Cui, X., Li, S., Kanno, S., Kobayashi, Y., Hayakawa, T., & Shraim, A. (2003). Difference in uptake and toxicity of trivalent and pentavalent inorganic arsenic in rat heart microvessel endothelial cells. *Archives of toxicology*, *77*(6), 305-312.

Hoeft, S.E., Kulp, T.R., Stolz, J.F., Hollibaugh, J.T. and Oremland, R.S. (2004). Dissimilatory arsenate reduction with sulfide as electron donor: experiments with mono lake water and isolation of strain MLMS-1, a chemoautotrophic arsenate respirer. *Appl. Environ. Microbiol.*, No. 70, 2741–2747.

Holleman, A.F. and Wiberg, E. (2001). *Inorganic chemistry*. New York: Academic Press.

Hollis, J.F., Keren, R. and Gal, M. (1988). Boron release and sorption by fly ash as affected by pH and particle size. *J. Environ. Qual.,* No. 17, 181-184.

Holt, P.K., Barton, G.W., Wark, M., & Mitchell, C.A. (2002). A quantitative comparison between chemical dosing and electrocoagulation. *Colloids and Surfaces A: Physicochemical and Engineering Aspects*, *211*(2-3), 233-248.

IARC Working Group on the Evaluation of Carcinogenic Risks to Humans, World Health Organization, & International Agency for Research on Cancer. (2004). *Some drinking-water disinfectants and contaminants, including arsenic* (Vol. 84). IARC.

Instituto Geográfico Nacional (1989). *Atlas del Perú*. Lima, Peru: Ministerio de Defensa.

Instituto Nacional de Estatica e Informática (2001). PERU: Compendio Estadístico 2001, 784 p.

Instituto Nacional de Estatica e Informática (2017). *POBLACIÓN DEL PERÚ TOTALIZÓ 31 MILLONES 237 MIL 385 PERSONAS AL 2017*. No. 108, June 2018, 3 p.

Instituto Nacional de Innovacion Agraria (INIA), Organización de las Naciones Unidas para la Alimentación y la Agricultura (FAO), ed. (2009). *PERU: SEGUNDO INFORME SOBRE EL ESTADO DE LOS RECURSOS FITOGENETICOS PARA LA ALIMENTACION Y LA AGRICULTURA.* Lima, Marzo 2009, p. 12.

Isa, M.H., Ezechi, E.H., Ahmed, Z., Magram, S.F. and Kitty, S.R.M. (2014). Boron removal by electrocoagulation and recovery. *Water Res.*, *51*, 113-123.

Isacks, B. (1988). Uplift of the Central Andes plateau and bending of the Bolivian Orocline. *Journal of Geophysical Research*, Vol. 93, p. 3211-3231.

Issa, N.B., Rajaković-Ognjanović, V.N., Marinković, A.D., & Rajaković, L.V. (2011). Separation and determination of arsenic species in water by selective exchange and hybrid resins. *Analytica chimica acta*, *706*(1), 191-198.

Jacob, C. (2007). Seawater desalination: boron removal by ion exchange technology. *Desalination*, *205*, 47–52.

Jaillard, E., Hérail, G., Monfret, T., Díaz-Martínez, E., Baby, P., Lavenu, A. and Dumont, J.F. (2000). Tectonic evolution of the Andes of Ecuador, Peru, Bolivia and northernmost Chile. *In* Tectonic evolution of South America (Cordani, U.G.; Milani, E.J.; Thomaz Filho, A.; Campos, D.A.; editors). *International Geological Congress*, No. 31, p. 481-559. Río de Janeiro.

James, D.E. (1984). Quantitative models for crustal contamination in the central and northern Andes. In Andean Magmatism: chemical and isotopic constraints. (Harmon, R.S.; Barreiro B.A., editors). *Shiva Geology Series, Shiva Publishing Limited,* p. 124-138. Natwich, UK.

James, D.E. and Sacks, I.S. (1999). Cenozoic formation of the Central Andes: A geophysical perspective. In Geology and Ore Deposits of the Central Andes (Skinner, B.J.; editor). *Society of Economic Geology*, Special Publication, No. 7, p. 1-26.

James, W.D., Graham. C.C., Glascock, M.D. and Hanna, A.-S.G. (1982). Water-leachable boron from coal ashes. *Env. Sci. Technol.*, *16*, 195-197.

Jones, D.R. (1995). In Environmental Aspects of Trace Elements in Coal, Kluwer Academic Publ. Dordrecht, pp. 221-255.

Jordan, T., Burns, W., Veiga, R., Pángano, F., Copeland, F., Kelley, S. and Mpodozis, C. (2001). Extensional basin formation in the southern Andes caused by increased convergence rate: a mid-Cenozoic trigger for the Andes. *Tectonics*, Vol. 20, No. 3, p. 308-324.

Jordan, T., Isacks, B., Allmendinger, R., Brewer, J., Ramos, V.A. and Ando, C.J. (1983). Andean tectonics related to geometry of the subducted Nazca Plate. *Geological Society of America, Bulletin*, Vol. 94, No. 3, p. 341-361.

Kabay, N., Güler, E. and Bryjak, M. (2010). Boron in seawater and methods for its separation — a review. *Desalination*, *261*, 212–217.

Kabay, N., Sarp, S., Yuksel, M., Arar, Ö. and Bryjak M. (2007). Removal of boron from seawater by selective ion exchange resins. *Reactive and Functional Polymers*, *67*(12), 1643–1650.

Kabay, N., Sarp, S., Yuksel, M., Kitis, M., Koseoğlu, H., Arar, Ö., Bryjak, M. and Semiat, R. (2008). Removal of boron from SWRO permeate by boron selective ion exchange resins containing N-methyl glucamine groups. *Desalination*, *223*(1-3), 49–56.

Kabay, N., Yilmaz, I., Bryjak, M. and Yuksel, M. (2006). Removal of boron from aqueous solutions by a hybrid ion exchange-membrane process. *Desalination*, *198*, 158–165.

Kanel, S.R., Manning, B. A., Charlet, L. and Choi, H. (2005). Removal of arsenic(III) from groundwater by nanoscale zero-valent iron. *Environmental Science Technology*, *39*(5), 1291-1298.

Kay, S.M., Mpodozis, C. and Coira, B. (1999). Neogene magmatism, tectonism and mineral deposits of the Central Andes (22°-33°S Latitude). In Geology and ore deposits of the Central Andes (Skinner, B.; editor). *Society of Economic Geology*, Special Publication 7, p. 27-59.

Kerrick, D.M. and Connolly, J.A.D. (2001). Metamorphic devolatilization of subducted oceanic metabasalt: Implications for seismicity, arc magmatism and volatile recycling. *Earth Planet. Sci. Lett., 189*, 19 – 29.

Khairul, I., Wang, Q.Q., Jiang, Y.H., Wang, C., & Naranmandura, H. (2017). Metabolism, toxicity and anticancer activities of arsenic compounds. *Oncotarget*, *8*(14), 23905.

Kikkinedes, E.S., Stoitsas, K.A. and Zaspalis, V.T. (2003). Correlation of structural and permeation properties in sol-gel-made nanoporous membranes. *Journal of Colloidal and Interface Science*, *259*(2), 322-330.

Kikkinedes, E.S., Stoitsas, K.A., Zaspalis, V.T. and Burganos, V.N. (2004). Simulation of structural and permeation properties of multi-layer ceramic membranes. *Journal of Membrane Science*, *243*(1-2), 133-141.

Kistler, R.B. and Helvacı, C. (1994). *Boron and Borates.* In: Industrial Minerals and Rocks, (Donald D. Carr editor) 6th Edition, Society of Mining, Metalurgy and Exploration, Inc., 171-186.

Kitano, Y., Okumura, M., & Idogaki, M. (1978). Coprecipitation of borate-boron with calcium carbonate. *Geochemical Journal*, *12*(3), 183-189.

Kley, J., Monaldi, C. and Salfity, J. (1999). Along-strike segmentation of the Andean foreland; causes and consequences. *Tectonophysics*, Vol. 301, p. 75-94.

Kocherginsky, N.M. and Yang, Q. (2007). Big Carrousel mechanism of copper removal from ammoniacal wastewater through supported liquid membrane. *Sep. Purif. Technol.*, *54*, 104–116.

Koparal, A.S. (2002). The removal of salinity from produced formation by conventional and electrochemical methods. *Fresen. Environ. Bull., 12A*(11), 1071–1077.

Korkmaz, M., Uzgören, E., Bakırdere, S., Aydın, F., & Ataman, O.Y. (2007). Effects of dietary boron on cervical cytopathology and on micronucleus frequency in exfoliated buccal cells. *Environmental Toxicology: An International Journal*, *22*(1), 17-25.

Kosutic, K., Furac, L., Sipos, L. and Kunst, S.B. (2005). Removal of arsenic and pesticides from drinking water by nanofiltration membranes. *Sep. Purif. Technol*., *42*, 137–144.

La República (2018). *"Puno: Tornado causó pánico en La Rinconada [VIDEO]"*. Retrieved from: https://larepublica.pe/sociedad/1241088-puno-tornado-causo-panico-rinconada/. Accessed on February 23, 2020.

Lackovic, J.A., Nikolaidis, N.P. and Dobbs, G.M. (2000). Inorganic arsenic removal by zero-valent iron. *Environmental Engineering Science*, *17*(1), 29-39.

Lapp, T.W. and Cooper, G.R. (1976). *Chemical technology and economics in environmental perspectives: Task II—Removal of boron from wastewater*. Kansas City, MO: Midwest Research Institute (for EPA Office of Toxic Substances).

Lee, K.C. and Rittmann, B.E. (2000). A novel hollow-fiber membrane biofilm reactor for autohydrogenotrophic denitrification of drinking water. *Water Sci. Technol*., *41*, 219–226.

Lindsay, J.M., Schmitt, A.K., Trumbull, R.B., de Silva, S.L., Siebel, W. and Emmermann, R. (2001). Magmatic evolution of the La Pacana Caldera system, central Andes, Chile: compositional variation of two cogenetic, large-volume felsic ignimbrites and implications for contrasting eruption mechanisms. *Journal of Petrology*, Vol. 42, p. 459-486.

Liu, A., Garcia-Dominguez, E., Rhine, E.D. and Young, L.Y. (2004). A novel arsenate respiring isolate that can utilize aromatic substrates. *FEMS Microbiol. Ecol*., *48*, 323–332.

Loewy, S.L., Connelly, J.N. and Dalziel, I.W.D. (2004). An orphaned basement block: The Arequipa-Antofalla Basement of the central Andean margin of South America. *Geological Society of America Bulletin*, Vol. 116, No. 1, pp. 171-187.

Lu, P. and Zhu, C. (2011). Arsenic Eh-pH diagrams at 25°C and 1 bar. *Environ Earth Sci*, *62*, 1673-1683.

Lucassen, F., Becchio, R., Kasemann, S., Franz, G., Trumbull, R., Wilke, H., Romer, R. and Dulski, F. (2001). Composition and density model of the continental crust at an active continental margin- the Central Andes between 21° and 27°S. *Tectonophysics*, Vol. 341, p. 195-223.

Macy, J.M., Nunan, K., Hagen, K.D., Dixon, D.R., Harbour, P.F., Cahill, M. and Sly, L.I. (1996). Chrysiogenes arsenatis gen. nov., sp. nov., a new arsenate-respiring bacterium isolated from gold mine wastewater. *Int. J. Syst. Bacteriol*., *46*, 1153–1157.

Manning, B.A. and Goldberg, S. (1997). Adsorption and stability of arsenic (III) at the clay mineral–water interface. *Environ. Sci. Technol.*, *31*, 2005–2011.

Manning, B.A., Fendorf, S.E. and Goldberg, S. (1998). Surface structures and stability of arsenic (III) on goethite: spectroscopic evidence for inner-sphere complexes. *Environ. Sci. Technol.*, *32*, 2383–2388.

Marino, T. and Figoli, A. (2015). Arsenic removal by liquid membranes. *Membranes*, *5*, 150-167.

Mass, M. J., Tennant, A., Roop, B. C., Cullen, W. R., Styblo, M., Thomas, D. J., & Kligerman, A. D. (2001). Methylated trivalent arsenic species are genotoxic. *Chemical research in toxicology*, *14*(4), 355-361.

Masuda, H. (2018). Arsenic cycling in the Earth's crust and hydrosphere: interaction between naturally occurring arsenic and human activities. *Progress in Earth and Planetary Science*, *5*(1), 68.

Melnik, L., Vysotskaja, O. and Kornilovich, B. (1999). Boron behavior during desalination of sea and underground water by electrodialysis. In: European Conference on Desalination and the Environment, Elsevier Science BV, Las Palmas, Spain, 1999.

Millas, I.G. (2020). Boron Industry, Sources, and Evaporitic Andean Deposits: Geochemical Characteristics and Evolution Paths of the Superficial Brines. In: *Recent Advances in Boron-containing Materials*. IntechOpen.

Miller, J.F. and Harris, N.B.W. (1989). Evolution of continental crust in the Central Andes; constraints from Nd isotope systematics. *Geology*, Vol. 17, No. 7, p. 615-617.

Mills, A., & Le Hunte, S. (1997). An overview of semiconductor photocatalysis. *Journal of photochemistry and photobiology A: Chemistry*, *108*(1), 1-35.

Mining Data Online (2020). *Major Mines & Projects: Pucamarca Mine*. Retrieved from: https://miningdataonline.com/property/3070/Pucamarca-Mine.aspx. Accessed on February 26, 2020.

Ministerio de Salud del Perú (2011). Reglamento de la calidad de Agua para Consumo Humano: D.S. No. 031-2010-SA / Ministerio de Salud. Dirección General de Salud Ambiental - Lima, 44 p.

Ministry of Agriculture and Irrigation of Peru (2015). *El clima*. Retrieved from: https://www.minagri.gob.pe/portal/53-sector-agrario/el-clima. Accessed on February 21, 2020.

Molina, O., Olivari, J. and Pietrobelli, C. (2016). *Global value chains in the Peruvian mining sector*. Inter-American Development Bank Technical Note 1114, 43 p.

Molinari, R., Argurio, P. and Poerio, T. (2009). Studies of various solid membrane supports to prepare stable sandwich liquid membranes and testing copper(II) removal from aqueous media. *Sep. Purif. Technol.*, No. 70, 166–172.

Morales-Simfors, N., Bundschuh, J., Herath, I., Inguaggiato, C., Caselli, A. T., Tapia, J., Choquehuayta, F.E.A., Armienta, M.A., Ormachea, M., Joseph, E. & López, D. L. (2020). Arsenic in Latin America: A critical overview on the geochemistry of arsenic originating from geothermal features and volcanic emissions for solving its environmental consequences. *Science of The Total Environment*, *716*, 135564.

Morris, J., Leeman, W. P. and Tera, F. (1990). The subducted component in island arc lavas: Constraints from Be isotopes and B/Be systematics, *Nature*, *344*, 31 – 36.

Munk, L. A., Boutt, D. F., Hynek, S. A., & Moran, B. J. (2018). Hydrogeochemical fluxes and processes contributing to the formation of lithium-enriched brines in a hyper-arid continental basin. *Chemical Geology*, *493*, 37-57.

Munk, L. A., Hynek, S. A., Bradley, D., Boutt, D., Labay, K., & Jochens, H. (2016). Lithium brines: A global perspective. *Reviews in Economic Geology*, *18*, 339-365.

Nadav, N., Priel, M. and Glueckstern, P. (2005). Boron removal from the permeate of a large SWRO plant in Eilat. *Desalination*, *185*, 121–129.

Nathan, Y., Dvorachek, M., Pelly, I. and Mimran, U. (1999). Characterization of coal fly ash from Israel. *Fuel*, *78*, 205-213.

National Research Council (NRC, 2001). Subcommittee to Update the 1999 Arsenic in Drinking Water Report. Arsenic in Drinking Water: 2001 Update. National Academy Press Washington DC.

Nerenberg, R., Rittmann, B.E. and Najm, I. (2002). Perchlorate reduction in a hydrogen-based membrane-biofilm reactor. *J. Am. Water Works Ass*., *94*, 103–114.

Ng, L.Y., Mohammad, A.W., Leo, C.P. and Hilal, N. (2013). Polymeric membranes incorporated with metal/metal oxide nanoparticles: a comprehensive review. *Desalination*, *308*, 15–33.

Nguyen, C.M., Bang, S., Cho, J. and Kim, K.-W. (2009). Performance and mechanism of arsenic removal from water by a nanofiltration membrane. *Desalination*, *245*, 82-94.

Nguyen, V.T., Vigneswaran. S., Ngo, H.H., Shon, H.K. and Kandasamy, J. (2009). Arsenic removal by a hybrid membrane filtration system. *Desalination*, *236*, 363-369.

Nickson, R.T., McArthur, J.M., Ravenscroft, P., Burgess, W.G., & Ahmed, K.M. (2000). Mechanism of arsenic release to groundwater, Bangladesh and West Bengal. *Applied Geochemistry*, *15*(4), 403-413.

Nordstrom, D.K. (2002). Worldwide occurrences of arsenic in ground water. *Science*, *296*, 2143 - 2145.

Nordstrom, D.K., & Archer, D.G. (2003). Arsenic thermodynamic data and environmental geochemistry. In *Arsenic in ground water* (pp. 1-25). Springer, Boston, MA.

O'Neil, M.A., Ishii, T., Albersheim, P. and Darvill, A.G. (2004). Rhamnogalacturonan II: structure and function of a borate cross-linked cell wall pectic polysaccharide. *Annual Review of Plant Biology*, *55*(1), 109–139.

Oehmen, A., Valerio, R., Llanos, J., Fradinho, J., Serra, S., Reis, M.A.M., Crespo, J.G. and Velizarov, S. (2011). Arsenic removal from drinking water through a hybrid ion exchange membrane – coagulation process. *Sep. Purif. Technol.*, *83*, 137–143.

Oh, J.I., Yamamoto, K., Kitawaki, H., Nakao, S., Sugawara, T., Rahman, M.M., and Rahman, M.H. (2000). Application of low-pressure nanofiltration coupled with a bicycle pump for the treatment of arsenic-contaminated groundwater. *Desalination*, *132*, 307–314.

Oremland, R.S., Blum, J.S., Culbertson, C.W., Visscher, P.T., Miller, L.G., Dowdle, P. and Strohmaier, F.E. (1994). Isolation, growth, and metabolism of an obligately anaerobic, selenate-respiring bacterium, strain SES-3. *Appl. Environ. Microbiol*., *60*, 3011–3019.

Ozol, A. A. (1977). Plate tectonics and the process of volcanogenic-sedimentary formation of boron. *Int. Geol. Rev., 20*, 692-698.

Pagana, A.E., Sklari, S.D., Kikkinedes, E.S. and Zaspalis, V.T. (2008). Microporous ceramic membrane technology for the removal of arsenic and chromium ions from contaminated water. *Microporous and Mesoporous Materials*, No. 110, 150-156.

Pardo-Casas, F. and Molnar, F. (1987). Relative motion of the Nazca (Farallon) and South American plates from Late Cretaceous time. *Tectonics*, Vol. 6, No. 3, p. 233-248.

Parks, J.L., & Edwards, M. (2005). Boron in the environment. *Critical Reviews in Environmental Science and Technology*, *35*(2), 81-114.

Peacock, S.M. (1996). Thermal and petrological structure of subduction zones (Overview). In *Subduction Top to Bottom, Geophys. Monogr. Ser.*, vol. 96, edited by G. E. Bebout, pp. 119 – 135, AGU, Washington, 1996.

Pearce, J.A. and Peate, D.W. (1995). Tectonic implications of the composition of volcanic arc magmas. *Annu. Rev. Earth Planet. Sci.*, *23*, 251 – 285.

Pessoa-Lopes, M., Crespo, J.G. and Velizarov, S. (2016). Arsenate removal from sulphate-containing water streams by an ion-exchange membrane process. *Separation and Purification Technology*, *166*, 125-134.

Petric, N., Martinac, V., M. Labor, M. and Mirosevic-Anzulovic, M. (1998). Isothermal and activated sintering of magnesium oxide from sea water. *Mater. Chem. Phys., 53*, 83-87.

Pfiffner, O.A., & Gonzalez, L. (2013). Mesozoic–Cenozoic evolution of the western margin of South America: Case study of the Peruvian Andes. *Geosciences*, *3*(2), 262-310.

Planer-Friedrich, B., Suess, E., Scheinost, A.C., & Wallschläger, D. (2010). Arsenic speciation in sulfidic waters: reconciling contradictory spectroscopic and chromatographic evidence. *Analytical chemistry*, *82*(24), 10228-10235.

Polat, H., Vengosh, A., Pankratov, I. and Polat, M. (2004). A new methodology for removal of boron from water by coal and fly ash. *Desalination*, *164*, 173-188.

Power, P.P. and Woods, W.G. (1997). The chemistry of boron and its speciation in plants. In: International Symposium on Boron in Soils and Plants (Boron97), Chiang Mai, Thailand, 1997.

Price, C.J., Marr, M.C., Myers, C.B., Seely, J.C., Heindel, J.J., & Schwetz, B.A. (1996). The developmental toxicity of boric acid in rabbits. *Fundamental and applied toxicology*, *34*(2), 176-187.

Ramos, V.A. (1999). Plate tectonic setting of the Andean Cordillera. *Episodes*, *22*, 183–190.

Ramos, V.A. (2008). The basement of the Central Andes: the Arequipa and related terranes. *Annu. Rev. Earth Planet. Sci.*, *36*, 289-324.

Ramos, V.A. (2009). Anatomy and global context of the Andes: Main geologic features and the Andean orogenic cycle. *Backbone of the Americas: shallow subduction, Plateau Uplift, and Ridge and Terrane collision*, *204*, 31-65.

Ravenscroft, P., Brammer H. and Richards, K. (2009). Arsenic Pollution: A Global Synthesis. RGS-IBG Book Series, Wiley-Blackwell: Chichester, UK, pp 498-500.

Redondo, J., Busch, M. and De Witte, J.-P. (2003). Boron removal from seawater using FILMTECTM high rejection SWRO membranes. *Desalination*, *156*, 229–238.

Reverzní osmózy (2017). Reverzní osmóza RO 106 M/P/UV (domácí systém). Retrieved from: http://www.reverzni-osmozy.cz/reverzni-osmoza-ro-106-manometr-pumpa-uv-filmtec-domaci-system-se-zasobnikem-p62. Accessed on August 12, 2020.

Rhoades, I.D., Krueger, B. and Reed, M.J. (1968). Laboratory determination of leachable soil boron. *Soil Sci. Sot. Am. J., 32*, 643-647.

Rhoades, J.D., Ingvalson, R.D., & Hatcher, J.T. (1970). Adsorption of boron by ferromagnesian minerals and magnesium hydroxide. *Soil Science Society of America Journal*, *34*(6), 938-941.

Risacher, F., & Fritz, B. (2009). Origin of salts and brine evolution of Bolivian and Chilean salars. *Aquatic Geochemistry*, *15*(1-2), 123-157.

Risacher, F., Alonso, H., & Salazar, C. (2003). The origin of brines and salts in Chilean salars: a hydrochemical review. *Earth-Science Reviews*, *63*(3-4), 249-293.

Rittmann, B.E., Nerenberg, R., Lee, K.C., Najm, I., Gillogly, T.E., Lehman, G.E. and Adham, S.S. (2004). Hydrogen-based hollow-fiber membrane biofilm reactor (MBfR) for removing oxidized contaminants. *Water Supply, 4*, 127–133.

Rosner, M., Erzinger, J., Franz, G., & Trumbull, R.B. (2003). Slab-derived boron isotope signatures in arc volcanic rocks from the Central Andes and evidence for boron isotope fractionation during progressive slab dehydration. *Geochemistry, Geophysics, Geosystems*, *4*(8).

Sasaki, K., Qiu, X., Miyawaki, J. Ideta, K., Takamori, H., Moriyama, S. and Hirajima, T. (2013). Contribution of boron-specific resins containing N-methylglucamine groups to immobilization of borate/boric acid in a permeable reactive barrier comprising agglomerated MgO. *Desalination*, *337*, 109-116.

Savage, K.S., Tingle, T.N., O'Day, P.A., Waychunas, G.A., & Bird, D.K. (2000). Arsenic speciation in pyrite and secondary weathering phases, Mother Lode gold district, Tuolumne County, California. *Applied Geochemistry*, *15*(8), 1219-1244.

Schmitt, A.K., de Silva, S.L., Trumbull, R.B. and Emmermann, R. (2001). Magma evolution in the Purico ignimbrite complex, Northern Chile: Evidence for zoning of a dacitic magma by injection of rhyolitic melts following mafic recharge. *Contributions to Mineralogy and Petrology*, Vol. 140, p. 680-700.

Schmitt, A.K., Lindsay, J.M., de Silva, S.L. and Trumbull, R.B. (2002). U-Pb zircon chronostratigraphy of early-Pliocene ignimbrites from La Pacana, north Chile: implications for the formation of stratified magma chambers. *Journal of Volcanology and Geothermal Research*, Vol. 120, p. 43-53.

Schmitz, M., Heinsohn, W.D. and Schilling, F.R. (1997). Seismic, gravity and petrologic evidence for partial melt beneath the thickened Central Andean crust (21-23°S). *Tectonophysics*, Vol. 270, p. 313-326.

Schmitz, M., Lessel, K., Giese, F., Wigger, F., Araneda, M., Bribach, J., Graeber, F., Grunewald, S., Haberland, C., Lüth, S., Röber, F., Ryberg, T. and Schulze, A. (1999). The crustal structure beneath the Central Andean forearc and magmatic arc as derived from seismic

studies - the PISCO 94 experiment in northern Chile (21°- 23°S). *Journal of South American Earth Sciences*, Vol. 12, p. 237-260.

Schneider, A. (1987). Eruptive processes, mineralization and isotopic evolution of the Los Frailes, Kari Kari region, Bolivia. *Revista Geológica de Chile*, *30*, p. 27-33.

Scott, M.J., & Morgan, J.J. (1995). Reactions at oxide surfaces. 1. Oxidation of As (III) by synthetic birnessite. *Environmental Science & Technology*, *29*(8), 1898-1905.

Seddique, A.A., Masuda, H., Mitamura, M., Shinoda, K., Yamanaka, T., Nakaya, S., & Ahmed, K.M. (2011). Mineralogy and geochemistry of shallow sediments of Sonargaon, Bangladesh and implications for arsenic dynamics: focusing on the role of organic matter. *Applied geochemistry*, *26*(4), 587-599.

Shackelton, M.R., Ries, A.C., Coward, M.P. and Cobbold, P.R. (1979). Structure, metamorphism and geochronology of the Arequipa Massif of coastal Peru. *J. Geol. Soc. Lond.*, *136*, 195–214.

Sheps-Pelleg, S. and Cohen, H. (2001). Workshop on Novel Products from Combustion Residues. Morella, Spain.

Shih, M.-C. (2005). An overview of arsenic removal by pressure-driven membrane processes. *Desalination*, No. 172, 85–97.

Simonnot, M.O., Castel, C., Nicolai, M., Rosin, C., Sardin, M. and Jauffret, H. (2000). Boron removal from drinking water with a boron selective resin: Is the treatment really selective? *Water Res., 34*(1), 109-116.

Singh, R., Singh, S., Parihar, P., Singh, V.P. and Prasad, S.M. (2015). Arsenic contamination, consequences and remediation techniques: A review. *Ecotoxicology and Environmental Safety*, *112*, 247-270.

Stern, C.R. (1988). Source region versus intra-crustal contamination in the petrogenesis of the Quaternary volcanic centers at the northern end (33-34° S) of the Southern Volcanic Zone. *In Congreso Geológico Chileno, No. 5, Actas*, Vol. 3, p. I29-I45. Santiago.

Stern, C.R. (2004). Active Andean volcanism: its geologic and tectonic setting. *Revista geológica de Chile*, *31*(2), 161-206.

Stern, C.R. and Kilian, R. (1996). Role of the subducted slab, mantle wedge and continental crust in the generation of adakites from the Andean Austral Volcanic Zone. *Contributions to Mineralogy and Petrology,* Vol. 123, p. 263-281.

Stern, C.R. and Skewes, M.A. (1995). Miocene to Present magmatic evolution at the northern end of the Andean Southern Volcanic Zone, Central Chile. *Revista Geológica de Chile*, Vol. 22, No. 2, p. 261-272.

Stern, C.R., Frey, F.A., Futa, K., Zartman, R.E., Peng, Z. and Kyser, T.K. (1990). Trace element and Sr, Nd, Pb and O isotopic composition of Pliocene and Quaternary alkali basalts of the Patagonian Plateau Lavas of southernmost South America. *Contributions to Mineralogy and Petrology*, Vol. 104, No. 3, p. 294-308.

Stern, C.R., Futa, K., Muehelnbachs, K., Dobbs, F.M., Muñoz, J., Godoy, E. and Charrier, R. (1984). Sr, Nd, Pb and O isotope composition of Late Cenozoic volcanics, northernmost SVZ (33-34°S). *In* Andean Magmatism: Chemical and Isotopic Constraints (Harmon, R.S.; Barriero, B.A., editors). *Shiva Geology Series, Shiva Publishing*, p. 96-105. Cheshire, UK.

Stolz, J.F. and Oremland, R.S. (1999). Bacterial respiration of arsenic and selenium. *FEMS Microbiol. Rev.*, *23*, 615–627.

Stolz, J.F., Ellis, D.J., Blum, J.S., Ahmann, D., Oremland, R.S. and Lovley, D.R. (1999). Sulfurospirillum barnesii sp. nov., Sulfurospirillum arsenophilus sp. nov., and the Sulfurospirillum clade in the Epsilon Proteobacteria. *Int. J. Syst. Bacteriol*., *49*, 1177–1180.

Styblo, M., Del Razo, L.M., Vega, L., Germolec, D.R., LeCluyse, E.L., Hamilton, G.A., Reed, W., Wang, C., Cullen, W.R. & Thomas, D.J. (2000). Comparative toxicity of trivalent and pentavalent inorganic and methylated arsenicals in rat and human cells. *Archives of toxicology*, *74*(6), 289-299.

Su, C., & Suarez, D.L. (1995). Coordination of adsorbed boron: A FTIR spectroscopic study. *Environmental science & technology*, *29*(2), 302-311.

Swenson, J., Beck, S. and Zandt, G. (2000). Crustal structure of the Altiplano from broadband regional waveform modeling: implications for the composition of thick continental crust. *Journal of Geophysical Research,* Vol. 105, No. B1, p. 607-621.

Taniguchi, M., Fusaoka, Y., Nishikawa, T. and Kurihara, M. (2004). Boron removal in RO seawater desalination. *Desalination*, *167*, 419-426.

Tassi, E.L., Pedron, F. and Barbafieri, M. (2011). Evaluating the Absorption of Boron by Plants – A Potential Tool to Remediate Contaminated Sediments from Cecina River Basin in Italy. *Water Air Soil Pollut.*, *216*, 275-287.

Tatsumi, Y., and Eggins, S. (1995). Subduction Zone Magmatism. *Frontiers in Earth Sciences*, Blackwell Sci., Malden, Mass.

The ANCORP Working Group (1999). Seismic reflection image revealing offset of Andean subduction-zone earthquake locations into the oceanic mantle. *Nature, 397*, 341 – 344.

Thorpe, R.S. (1984). The tectonic setting of active Andean volcanism. *In* Andean magmatism: Chemical and Isotopic Constraints (Harmon, R.S.; Barreiro, B.A.; editors). *Shiva Geological Series, Shiva Publications,* Nantwich, U.K., p. 4-8.

Tosdal, R.M. (1996). The Amazon-Laurentian connection as viewed from the Middle Proterozoic rocks in the Central Andes, western Peru and Northern Chile. *Tectonics*, Vol. 15, p. 827-842.

Tosdal, R.M., Farrar, E. and Clark, A.H. (1984). K-Ar geochronology of the late Cenozoic volcanic rocks of the Cordillera Occidental, southernmost Peru. *Journal of Volcanology and Geothermal Research*, Vol. 10, Issues 1-3, p.157-173.

Trumbull, R.B., Wittenbrink, R., Hahne, K., Emmermann, R., Büsch, W. and Gerstenberger, H. (1999). Evidence of Late Miocene to Recent contamination of arc andesites by crustal melts in the Chilean Andes (25°-26°S) and its geodynamic implications. *Journal of South American Earth Sciences*, Vol. 12, p. 135-155.

Tu, K.L., Nghiem, L.D. and Chivas, A.R. (2010). Boron removal by reverse osmosis membranes in seawater desalination applications. *Sep. Purif. Technol.*, *75*, 87-101.

US EPA (2016). Arsenic compounds. Retrieved from:

https://www.epa.gov/sites/production/files/2016-09/documents/arsenic-compounds.pdf. Accessed on June 30, 2020.

Uddin, M.T., Mozumder, M.S.I., Islam, M.A., Deowan, S.A. and Hoinkis, J. (2007). Nanofiltration membrane process for the removal of arsenic from drinking water. *Chem. Eng. Technol.*, *30*(9), 1248–1254.

Urbano, B.F., Rivas, B.L., Martinez, F. and Alexandratos, S.D. (2012). Water-insoluble polymer-clay nanocomposite ion exchange resin based on N-methyl-Dglucamine ligand groups for arsenic removal. *React. Funct. Polym*., *72*, 642–649.

US EPA (2000a). Technologies and Costs for Removal of Arsenic from Drinking Water.

US EPA (2000b). Arsenic Removal from Drinking Water by Ion Exchange and Activated Alumina Plants. EPA/600/R-00/088, Cincinnati, Ohio.

Valyashko, M.G. (1970). Genesis and exploration of borate deposits related to marine salt deposits. *Internat. Geol. Rev., 12*, 711-719.

Van Geen, A., Rose, J., Thoral, S., Garnier, J.M., Zheng, Y., & Bottero, J.Y. (2004). Decoupling of As and Fe release to Bangladesh groundwater under reducing conditions. Part II: Evidence from sediment incubations. *Geochimica et Cosmochimica Acta*, *68*(17), 3475-3486.

Van Geen, A., Zheng, Y., Cheng, Z., Aziz, Z., Horneman, A., Dhar, R.K., Mailloux, B., Stute, M., Weinman, B., Goodbred, S., Seddique, A.A., Hoque, M.A. & Ahmed, K.M. (2006). A transect of groundwater and sediment properties in Araihazar, Bangladesh: Further evidence of decoupling between As and Fe mobilization. *Chemical Geology*, *228*(1-3), 85-96.

Vasudevan, S., Lakshmi, J. and Sozhan, G. (2012). Electrochemically assisted coagulation for the removal of boron from water using zinc anode. *Desalination, 310*, 122-129.

Velizarov, S. (2013). Transport of arsenate through anion-exchange membranes in Donnan dialysis. *J. Membr. Sci.*, *425–426*, 243–250.

Vengosh, A., Starinsky, A., Kolodny, Y., & Chivas, A.R. (1994). Boron isotope geochemistry of thermal springs from the northern Rift Valley, Israel. *Journal of Hydrology*, *162*(1-2), 155-169.

Victor, P., Oncken, O. and Glodny, J. (2004). Uplift of the western Altiplano plateau: Evidence from the Precordillera between 20° and 21°S (northern Chile). *Tectonics*, Vol. 23, No. 4, TC4004 10.1029/2003TC001519.

Vidal, J.P. (1981). *Geografía del Perú: Las Ocho Regiones Naturales del Perú.* Lima: Editorial Universo, 256 p.

Waggott, A. (1969). An investigation of the potential problem of increasing boron concentrations in rivers and water courses. *Water Research*, *3*(10), 749-765.

Wang, Y., Li, P., Guo, Q., Jiang, Z., & Liu, M. (2018). Environmental biogeochemistry of high arsenic geothermal fluids. *Applied Geochemistry*, *97*, 81-92.

Warren, J.K. (2016). Non-potash salts: Borates, Na-sulphates, Na-carbonate, lithium salts, gypsum, halite and zolites. In: *Evaporites* (pp. 1187-1302). Springer, Cham.

Watanabe, T. (1964). Geochemical cycle and concentration of boron in the earth's crust. V.I. Verdenskii Inst. Geochim. and *Anal. Chem. U.S.S.R. 2*, 167-177.

Water for Peru (2020). Applications. Retrieved from:

http://www.waterforperu.com/applications/. Accessed on July 28, 2020.

Water Technology (unknown date). Ashkelon Seawater Reverse Osmosis (SWRO) Plant, Israel. Retrieved from https://www.water-technology.net/projects/israel/. Accessed on November 25, 2018.

Wided, B., Khawla, M., Eya, B.K. and Béchir, H. (2014). Evaluation of boron removal by coagulation-flocculation and electrocoagulation. *International Journal of Engineering Research & Technology*, *3(*2), 2923-2928.

Williams, M. (2001). Arsenic in mine waters: an international study. *Environmental Geology*, *40*(3), 267-278.

Wong, J.M. (1984). Boron control in power plant reclaimed water for potable reuse. *Environ. Prog., (United States)*, *3*(1), 5-11.

World Health Organisation (1998). Boron: 8.1.1. Short term toxicity and poisoning incidents. Enviromental health criteria 204: Geneva, Switzerland: World Health Organization. Retrieved from: http://www.inchem.org/documents/ehc/ehc/ehc204.htm. Accessed on June 6, 2020.

World Health Organisation (2006). Guideline for drinking-water quality [electronic resource]: incorporating first addendum. Vol. 1, Recommendations. -3rd ed. WHO Press, Geneva, Switzerland, ISBN 92 4 154696 4. pp.515

World Health Organisation (2007). pH in drinking water. Revised background document for development of WHO *Guidelines for Drinking-water Quality*. Retrieved from: https://www.who.int/water_sanitation_health/dwq/chemicals/ph_revised_2007_clean_version.pdf. Accessed on June 27, 2020.

World Health Organisation (2009). Boron in drinking water: background document for development of WHO guidelines for drinking-water quality. World Health Organization. Retrieved from: https://apps.who.int/iris/handle/10665/70170. Accessed on June 6, 2020.

Wörner, G., Moorbath, S. and Harmon, R.S. (1992). Andean Cenozoic volcanic centers reflect basement isotopic domains. *Geology*, Vol. 20, p. 1103-1106.

Wörner, G., Moorbath, S., Entenmann, J., Davidson, J.D. and López-Escobar, L. (1994). Large geochemical variations along the Andean Arc of northern Chile (17.5-22°S). *In* Tectonics of the Southern Central Andes. Structure and evolution of an active continental margin (Reutter, K.J.; Scheuber, E.; Wigger, P.J.; editors). *Springer-Berlin*, p. 77-91.

Yan, L., Li, Y.S., Xiang, C.B. and Xianda, S. (2006). Effect of nano-sized Al_2O_3-particle addition on PVDF ultrafiltration membrane performance. *J. Membr. Sci., 276*, 162–167.

Yan, X.P., Kerrich, R., & Hendry, M.J. (2000). Distribution of arsenic (III), arsenic (V) and total inorganic arsenic in porewaters from a thick till and clay-rich aquitard sequence, Saskatchewan, Canada. *Geochimica et Cosmochimica Acta*, *64*(15), 2637-2648.

Yildiz, Y.Ş., Koparal, A.S., İrdemez, Ş., & Keskinler, B. (2007). Electrocoagulation of synthetically prepared waters containing high concentration of NOM using iron cast electrodes. *Journal of hazardous materials*, *139*(2), 373-380.

Yilmaz, A.E., Boncukcuoğlu, R. and Kocakerim, M.M. (2007). A quantitative comparison between electrocoagulation and chemical coagulation for boron removal from boron-containing solution. *J. Hazard. Mater.*, *149*, 475-481.

Yilmaz-Ipek, I., Kabay, N. and Özdural, A.R. (2011). Non-equilibrium sorption modeling for boron removal from geothermal water using sorption–microfiltration hybrid method. *Chem. Eng. Proc.: Proc. Inten.*, *50*, 599–607.

Yokoyama, T., Takahashi, Y., & Tarutani, T. (1993). Simultaneous determination of arsenic and arsenious acids in geothermal water. *Chemical geology*, *103*(1-4), 103-111.

Zaspalis, V.T., Pagana, A.E. and Sklari, S.D. (2007). Arsenic removal from contaminated water by iron oxide sorbents and porous ceramic membranes. *Desalination*, *217*(1-3), 167-180.

Zhao, L., Fei, D., Dang, Y., Zhou, X. and Xiao, J. (2010). Studies on the extraction of chromium(III) by emulsion liquid membrane. *J. Hazard. Mater.*, *178*, 130–135.

İrdemez, Ş., Demircioğlu, N., & Yildiz, Y.Ş. (2006). The effects of pH on phosphate removal from wastewater by electrocoagulation with iron plate electrodes. *Journal of Hazardous Materials*, *137*(2), 1231-1235.

Öğütveren, Ü.B., & Koparal, S. (1997). Electrocoagulation for oil-water emulsion treatment. *Journal of Environmental Science & Health Part A*, *32*(9-10), 2507-2520.

Şayli, B.S. (2001). Assessment of fertility and infertility in boron-exposed Turkish subpopulations. *Biological trace element research*, *81*(3), 255.